WADC TECHNICAL REPORT 55-86, Part 2

# FATIGUE CRACK DETECTION METHODS

## PART 2

## REVIEW OF EXPERIMENTAL DATA ON THE INITIATION AND PROPAGATION OF FATIGUE CRACKS IN TEST SPECIMENS

L. J. DEMER
UNIVERSITY OF MINNESOTA

JUNE 1955

Materials Laboratory
Contract No. AF 33(038)-20840
Project No. 7360
Task No. 73604

Wright Air Development Center
Air Research and Development Command
United States Air Force
Wright-Patterson Air Force Base, Ohio

Part of This Work Was Sponsored By
Office of Naval Research
Under Contract N8-ONR-66207

# FOREWORD

This report was prepared by the University of Minnesota, under USAF Contract No. AF33(038)-20840 on work done during the period January through March 1955. Part of this work was sponsored by the Office of Naval Research under Contract N8-ONR-66207. The USAF Contract was initiated under Project No. 7360, "Materials Analysis and Evaluation Techniques", Task No. 73604, "Fatigue Properties of Structural Materials", formerly RDO No. 614-16, and was administered under the direction of the Materials Laboratory, Directorate of Research, Wright Air Development Center, with Mr. W. J. Trapp acting as project engineer.

Appreciation is due A. A. Blatherwick, of the University of Minnesota for reviewing the manuscript and offering helpful suggestions.

## ABSTRACT

Current fatigue literature contains numerous references to a few recent studies in which fatigue cracks have been detected very early in the specimen life. This paper attempts to clarify such isolated observations by making a detailed review of the available experimental data in relation to crack initiation and growth in laboratory fatigue test specimens. The data are analyzed considering the nature of the test material, the character of the specimen, the stress level of the test, and the manner of testing. Conclusions are reached in regard to the effect of these factors on the percentage of fracture cycles at which fatigue cracks are detected. The formula of A. K. Head for the actual growth of fatigue cracks is reviewed and its agreement with experimental results is discussed.


## PUBLICATION REVIEW

This report has been reviewed and is approved.

FOR THE COMMANDER:

M. R. WHITMORE
Technical Director
Materials Laboratory
Director of Research

# TABLE OF CONTENTS



## LIST OF TABLES

# LIST OF FIGURES

## Unnotched Specimens



## Notched Specimens



## Comparison Plots, Crack and Fracture Data

# SECTION I. INTRODUCTION

This report is the second of a series dealing with the general subject of fatigue cracking. A previous publication, Demer (55), 1/ dealt with the various fatigue crack detection methods available for use particularly with laboratory fatigue specimens. This present paper reviews much of the experimental data which have been reported to date on the initiation and propagation of fatigue cracks in test specimens. Subsequent papers will be concerned with other aspects of the subject of fatigue.

## 1.1 Background

Over fifty years ago Ewing and Humfrey (02) described the progress of fatigue fracture in rotating beam tests of specimens of Swedish iron in these words:

> "The course of the breakdown was as follows: -- The first examination, made after a few reversals of stress, showed slip-lines on some of the crystals, on many of them if the stress was comparatively great, but on only a few if the stress did not much exceed the lower limit named above (of 9 tons per sq. inch). At this early stage the slip-lines were quite similar in appearance to those which are seen when a simple tensile stress exceeding the elastic limit is applied. Viewed under vertical illumination they appeared as fine dark lines. After more reversals of stress additional slip-lines appeared, which had not been visible in the first instance, but the most conspicuous feature was that those which were visible before became far more distinct and showed a tendency to broaden. After many reversals they changed into comparatively wide bands with rather hazily defined edges, losing entirely the fine and sharp character which slip-lines present when they first appear. As the number of reversals increased this process of broadening continued, and some parts of the surface became almost covered with the dark markings made up of groups of broadening lines. When this stage was reached it was found that some of the crystals had cracked. The cracks occurred along broadened slip-bands; in some instances they were first seen on a single crystal, but soon they joined up from crystal to crystal, until finally a long continuous crack was developed across the surface of the specimen. When this happened a few more reversals brought about fracture."

After half a century during which many investigators performed an extremely large number of tests it can be said that the general picture of the fatigue process is still the same. The discussions of Forsyth (51, 54), Head (53), Dolan (53), and others attest to this. Thus the fatigue process in most ductile metals is now pictured as consisting usually of three stages during which the following phenomena occur:

Stage 1. The material undergoes bulk deformation and work hardening. Slip subsequently occurs accompanied by some disorientation and fragmentation of the crystals.

Stage 2. The slip lines thicken and intensify into slip bands which are usually in the direction of greatest shear stress. When this process has proceeded to a limit it results in the final rupture of the crystal lattice and the appearance or initiation of submicroscopic cracks.

Stage 3. During this stage, the submicroscopic cracks coalesce to form visible spreading cracks resulting ultimately in the complete fracture of the specimen.

---

1/ Parenthetical numerals indicate publication date of reference, viz (55)=1955.

During recent years considerable attention has been directed toward obtaining detailed knowledge of the changes taking place during the fatigue process especially in the stages prior to actual cracking. Utilizing X-ray techniques as well as optical and electron microscopy and interferometry, many interesting and important facts concerning the structural changes involved are being uncovered. For details refer to the previously mentioned references.

## 1.2 Present Investigation

This study is concerned not with the detailed changes taking place in, but rather with the length of the various stages of the fatigue process and, more particularly, with the length of the third stage which involves the growth of the fatigue crack or cracks to the point of complete rupture of the specimen. This aspect of the problem has received some attention in previous investigations, but the picture is still clouded by contradictory observations and conclusions. Some investigators view the second or intermediate stage, in which the slip lines intensify and proceed to final rupture of the lattice and initiation of a fatigue crack, as forming the major part of the life of a specimen. Others are of the opinion that the first two stages are short and that the major part of the specimen involves the growth of the fatigue cracks to final rupture of the specimen or part. Actually it may be that there are certain conditions under which each of the above cases may be true.

There has been much tendency to generalize from isolated bits of information, thus leading perhaps to erroneous conclusions. For example, Love (52) in work on ingot iron employing an electron microscope reported cracks of 2-3 microns in length at approximately 0.1 per cent of the fatigue life. This does not mean, however, that in all materials and at all stress levels, fatigue cracks exist so early in the specimen life. Lessells and Jacques (50) and Fenner, Owen, and Philips (51) have reported finding fatigue cracks at stress levels far below the fatigue limit in steels. But this is no proof that for all materials and in all specimen forms, fatigue cracks exist at these stress levels, since both of these investigations employed specimens of extremely high stress concentration and, in addition, the results were also possibly affected by other factors. Yet so many of the recent papers dealing with fatigue cite references such as those given above, along with others equally specialized, to support observations obtained under totally different conditions.

The purpose of this study was, therefore, to collect most of the existing published data in regard to the length of the cracking stage in fatigue tests of laboratory specimens, and data relating to the rate of crack propagation, to critically examine and evaluate these, to make certain generalities, and to draw any reasonable conclusions possible from the analysis.

## 1.3 Related Factors

There are a number of factors which should be taken into consideration when investigating the point of fatigue crack initiation and the subsequent crack propagation, or when evaluating results of such studies. A listing of such factors is given in Table I. These will be discussed briefly at this point. Their relationship to the experimental data presented in this review will be analyzed later.

The term "crack initiation" has been used in various instances throughout fatigue literature to designate all variations between the earliest rupture of atomic bonds detectable by the most powerful techniques of electron microscopy to the formation of a macroscopic discontinuity of a given arbitrary length on the specimen surface. In any discussion of fatigue crack initiation, therefore, it is important to keep in mind the magnitude of the existing defect, the presence of which has been arbitrarily chosen as the start of a fatigue crack.

Definition of the condition constituting fatigue "failure" may be of considerable importance in determining the length of the third stage of fatigue. There has been little uniformity in the past in reporting the number of cycles to failure in fatigue tests. Occasionally it is taken as the number of cycles to form a "detectable" crack. This vague term is much dependent on the sensitivity of the detection method employed. Sometimes "failure" refers to the development of a crack of a given arbitrary length. Again, it is defined as a crack of sufficient magnitude to result in an increase in amplitude or a decrease in frequency such that a stopping mechanism on the testing machine may be actuated. In many cases too, the number of cycles to complete fracture of the specimen is the criterion of failure. Comparison of the results of various times or cycles to failure in fatigue tests requires knowledge of the condition defined as failure.

The end of the second and the beginning of the third stage in the fatigue process is marked by the final rupture of the crystal lattice and the appearance or initiation of very minute cracks. The actual number of cycles to this point in a given fatigue test is distinctly dependent, therefore, on the sensitivity of the method employed for the detection of such cracks. Demer (55) discusses the various methods available for crack detection in laboratory fatigue test specimens.

The length of the various stages in the fatigue process may be greatly affected by the material under test. For example, the number of operative slip systems, 48 for body-centered cubic, 12 for face-centered cubic, and 3 for hexagonal crystal structures might well be expected to affect the cracking characteristics of a material. The state of purity, number of phases present, grain size, homogeneity of structure, and thermal treatment are other factors which are important in such a study.

The specimen form is of major importance in crack initiation for it is a determining element in the state of stress concentration and other factors which may affect both crack initiation and growth. For example, the cracking characteristics of smooth and notched specimens of the same material are considerably different. The specimen size determines the stress gradient in certain types of fatigue tests and is therefore important in crack growth. The surface finish of the specimen and accompanying stress condition of the surface layer where fatigue cracks generally initiate may exert a major effect on the point of crack initiation in fatigue tests.

The mode of fatigue stressing employed, that is, whether alternating axial tension-compression, reversed flexure, rotating bending, reversed torsion, or a combined stress test, has an effect on fatigue cracking since it determines the state of stress and the stress gradient at the surface and in the body of the test specimen. Furthermore, the rate of crack propagation in a test specimen would obviously not be expected to be the same for a material tested under either constant maximum stress or constant maximum strain amplitude conditions as for one tested under conditions of constant maximum load or moment.

It has been observed that the appearance of the deformation marks on the surface of a fatigue specimen is rather pronouncedly different for frequencies above a certain critical value. This could cause a frequency dependence in crack initiation. In addition, internal damping and insufficient heat dissipation might result in a temperature rise in the specimen affecting both crack initiation and growth.

The actual test temperature can be expected to exert an effect not only on the initiation of cracking through its effect on the physical properties of the material, but also on crack growth especially at the higher temperature levels through possible corrosive action at the tip of the crack.

# SECTION II. EXPERIMENTAL DATA CONCERNING THE EARLY DETECTION OF FATIGUE CRACKS

## 2.1 Manner of Presenting Data

It was thought desirable to separate the experimental observations of previous investigators into two divisions -- those in which smooth contour or generously filleted specimens were used and those in which specimens of rather high stress concentration were employed. Here will be given in chronological order for each division, the results of some investigations concerned with the subject of crack initiation in fatigue test specimens. This compilation is intended to be representative but not necessarily exhaustive.

The problem of comparing crack initiation data for different materials is complicated by the absence of a readily available basis for measurement. For example, pure nickel and pure magnesium differ quite widely in their static and fatigue strengths. If similar specimens of these two materials were tested at a given stress level above the long time fatigue strength of magnesium, fatigue cracks would initiate and grow to rupture of the specimen long before fatigue cracks appeared, if they did so at all, in the nickel specimen tested at the same stress. One method of comparison which makes allowance for different levels of material strength is comparison at similar ratios of test stress to fatigue limit or fatigue strength at an arbitrarily selected number of cycles. Presentation of the data in this review will be made on this basis.

For the sake of uniformity and ease of comparison of the various sets of data, two graphical presentations are given in each case where sufficient experimental results are available. One type of graph presents the fatigue stress amplitude as a function of the number of imposed stress cycles. Instead of using an absolute stress scale, the ordinate is the ratio of the test stress to the fatigue strength of the type of specimen, that is $S/S_{fs}$. For the torsional fatigue tests reported here the strain ratio $\gamma/\gamma_{fs}$ is alternately used. In cases where the material in a given specimen form possesses a distinct fatigue limit that value is used for the fatigue strength. In most of the other cases the stress value used is that for a fatigue strength of $2 \times 10^7$ cycles. Where any deviation from this value is made the choice is so indicated. In these graphs, the data for each specimen or the representative data for a group of specimens at a given stress level are indicated by the symbol (——|). The start of the horizontal line shows the number of cycles at which a fatigue crack was detected, that is $N_c$, and the vertical line indicates the number of cycles at fracture, or $N_f$. Thus the horizontal line represents the period in which detectable cracking is occurring.

A true perspective of the relative length of the cracking stage at different stress levels is rather difficult to obtain from mere examination of the length of the line representing the cracking stage on the usual S-N plot because of the logarithmic scale employed for the cycles scale in the graphs. Thus, although the crack line (——|) shown in the graphs may be shorter at the lower stress levels, it can represent many times the number of cycles which a line of equivalent length represents at a high stress level but small number of cycles. For a better comparison of the actual length of the crack stage at different stress levels, perhaps the actual number of cycles between the first evidence of cracking and fracture should be compared. These values for $(N_f - N_c)$ have been plotted and designated by the symbol (x) on many of the graphs presented. The variation of these data will be discussed later.

A second type of graph used in reporting the experimental results shows the stress ratio $S/S_{fs}$, or the strain ratio $\gamma/\gamma_{fs}$, as a function of the crack-fracture cycle ratio $N_c/N_f$. It is intended that this also will show the differences in cracking behavior at various stress levels.

## 2.2 Data for Unnotched Specimens

Laute and Sachs (28) working with nickel studied the effect of annealing fatigue specimens subjected to various percentages of their fatigue life at a given stress. For an unnotched specimen tested in direct stress at a magnitude resulting in a life of about 750,000 cycles, they found that beyond one-sixth of the total number of cycles to fracture no recovery takes place. It might be supposed that this signifies the presence of cracks beyond that period.

deForest (36) studied crack initiation in cold rolled SAE 1020 steel rotating beam specimens. He detected cracks by means of a wet magnetic particle method and reported the number of cycles for the development of a crack of 0.10 inch in length in 5/8 inch diameter specimens, and also the number of cycles for fracture. His data are shown in Fig. 1. The percentage of fracture life at which cracks were detected is in the range of approximately 70-90 per cent. Discussion of the number of cycles between cracking and failure will be deferred to a later section.

Bollenrath and Bungardt (38) tested carbon steel streamlined wires heat treated to 230,000 psi tensile strength. They also detected cracks by a magnetic method. Their data are not given is such form as to be readily reproducible according to the method adopted here. However, they indicated the inability to detect cracks until shortly before failure in the unnotched speciments tested.

Hempel (39) investigated the initiation and propagation of fatigue cracks rather thoroughly. He reviewed the literature on the subject to that date and noted that numerous contradictions and obscurities remained which required intensive and careful investigation. He carried out tests on two carbon steels, one of 0.05 per cent carbon and the other of 0.58 per cent carbon, in rotating bending and employed a wet magnetic method for fatigue crack detection. Concerning the sensitivity of the crack detection method, it appeared that the Magnaflux method does not indicate initial cracking but only detects cracks of a certain minimum length. The actual presence of cracks and their magnitude, and progress across the section were observed from the appearance of the fracture of specimens tested for a portion of their fracture life in fatigue and then pulled apart in a tension machine.

Hempel studied smooth test pieces and also specimens with a transverse hole. The specimens were subjected to alternating bending stress in which the bending moment remained equal along the whole length of the specimen. His results for a carbon steel of 0.05 per cent carbon are shown in Fig. 2 for smooth solid specimens. Hempel made a comparison of his results and those of other investigators. He concluded that when stressed in rotating bending and with constant bending moment applied; a fatigue crack initiates in solid test pieces almost independently of the test piece diameter and of the material, after 70-90 per cent of the number of reversals to fracture. He observes, however, that comparison of the data indicates an effect of the type of stress.

Ferguson (44) notes that in his earlier work on the fatigue of lead alloys used in cable sheathing he was able to detect the formation of fatigue cracks at an early stage in the test by removing fatigue specimens from the fatigue working machine and stretching them slightly (not over 5 per cent) in a tensile testing machine. No data are given for which a curve can be plotted here, but Ferguson observes that in many instances the relative number of cycles for complete fatigue tests could be predicted from specimens run only about 10 per cent of their normal fatigue life. In the earlier study, strip specimens with preformed curved sections were subjected to considerable bending by subjecting the ends to deflection of constant amplitude. The tests are described in Ferguson and Bouton (45).

Bennett (46) studied the damaging effect of fatigue stressing on SAE X4130 steel using unnotched specimens in rotating bending fatigue machines. He employed a stroboscopic viewing device for observing the cracks while running the machine and an apparatus for counting and measuring fatigue cracks, the latter being external to the fatigue machines. Data on the initiation of cracking are shown in Fig. 3. Crack growth curves were obtained by taking microscope readings of the arc length of cracks at various numbers of cycles and extrapolating the plotted data. Bennett tested many specimens both to determine the start of cracking at various stress levels and to determine the fracture curve. The data show appreciable scatter in the number of cycles for first cracking. In Fig. 3 the experimental points are not given. Only representative curves are drawn for cracking and fracture. These data for S versus N show considerably smaller slope when plotted on the stress ratio basis than do those of most other investigators. The reason for this is not apparent.

Bennett and Baker (5) studied the effects of prior static and dynamic stresses on the fatigue strength of aluminum alloys using Krouse sheet bending fatigue testing machines. In work similar in pattern to that on X4130, by Bennett (46), the determination of the point at which cracks started in unnotched sheet specimens necessitated stopping the test when a small crack had formed. To accomplish this, fracture wires, after Foster (47), were employed with the wire carrying the operating current to a relay controlling the test motor. Some difficulty was experienced, however, due to the wires breaking before a crack had started. This was overcome by cementing the wire in a location on the specimen where the strain was not so great. Measurements were made at intervals till fracture using a microscope. Crack growth curves were extrapolated back to a 0.01 crack length ratio (ratio of crack length to width of test piece) and this was arbitrarily taken as the start of the crack. The resulting accuracy was considered adequate in view of the fact that the number of cycles from cracking to fracture was small in comparison to the number of cycles required to start the crack. Some of their results are shown in Fig. 4.

Duce (50) performed fatigue tests in alternating torsion under substantially constant maximum strain conditions on a variety of pure metals and alloys. The pure metals were iron, nickel, copper, aluminum, and magnesium. In addition to these, tests were made on a free-cutting mild steel and on a series of carbon steels of graded carbon content. The results of Duce's experiments have only appeared in thesis form to date. Because of their importance to this discussion they will be described in some detail.

The tests were made on a Chevenard Micro-machine using specimens with a straight cylindrical test section approximately 10 mm in length and 1.52 mm in diameter and with generous fillets on the ends. The machine permitted recording of the couple-twist diagram or hysteresis loop and thus it was possible to follow the changes in $\Delta E$, the damping energy absorbed per cycle, and in tan $\beta$, the slope of the line joining the two ends of the loop with respect to the axis of strain. This slope is directly proportional to an 'apparent' or 'secant' modulus of rigidity.

Duce also made rather detailed metallographic studies using electropolishing techniques and both optical and electron microscopy to follow the course of the fatigue process at a given location on the specimen surface throughout entire fatigue tests. From the results of the curves of $\Delta E$ and tan $\beta$ plotted versus the number of cycles, and the photomicrographs obtained at various points in the fatigue tests Duce divided the fatigue process into three stages, as has also been done by several other investigators. He found Stage I to be evidently one of rapid strain hardening, attended by the general formation of slip lines whether the strain amplitude be above, at, or just below the fatigue limit. Stage II was found to be generally the longest part of the test. Duce found this stage characterized by little change in $\Delta E$ and tan $\beta$, or any other property including X-ray diagrams. The one outstanding characteristic of this stage, he reported, is the development of the regions of intense slip bands in certain directions (except perhaps in the case

of magnesium) and the accompanying phenomena. The process is followed later in the stage by some form of deterioration of the grains either at isolated spots or more generally over the whole surface of the metal depending on the strain amplitude. The deformation during Stage II, because it is highly localized, causes very little strain hardening of the metal as a whole and this may be more than compensated (usually) by a breakdown of the crystals at the points of weakness, a process which leads eventually to a fatigue crack.

Duce reports Stage III to be undoubtedly a stage of crack propagation leading to final fracture. From metallographic examination of a few specimens of each material and by taking photomicrographs at various points in the specimen life, Duce was able to determine that the beginning of cracking was generally associated with the start of the third stage in the fatigue process. He does not report the number of cycles to initiation of cracking for each specimen used in obtaining the fatigue strength of the various materials, but shows the $\Delta E$ and tan $\beta$ versus N graphs for each. The approximate number of cycles at the beginning of the third stage, as indicated by the changes in these measured values, was read from Duce's graphs for each specimen by the author of this review. Other graphs were then prepared similar to those for the data of other investigators presented here except that the ratio of shearing strain of the test to the shearing strain at an arbitrarily selected fatigue strain was used instead of the corresponding stress ratio. This was done because of the manner of presentation of the original data in Duce's paper. The resulting graphs are shown in Fig. 6 for the pure metals nickel, copper, aluminum, and magnesium. Due to limitations of the testing machine and the low strength of some of the materials, it was not possible to obtain fatigue data for a large number of cycles and the fatigue strain at a smaller number of cycles is used as a basis for the graphs. In making any comparison between the results of Duce and those of other investigators reported in this review, it must be noted that these tests were performed in torsion and under substantially constant maximum strain conditions.

The data shown in Fig. 6 for commercially pure nickel indicate a cracking stage of rather short duration except at very high strain amplitude. Because of the linear scale for number of cycles employed by Duce it is difficult to determine the length of the first stage from his graphs. He does not report any numerical values. For one specimen examined metallographically at a strain ratio of 1.6, however, the first stage lasted until approximately 20,000 cycles or some 7 per cent of the fracture life. The last stage began at close to 80 per cent at this strain level. Of the pure metals tested by Duce, the face centered cubic metal nickel showed perhaps the shortest cracking stage.

The data for the high conductivity copper indicate a cracking stage of 60 to 85 per cent of the fracture life at the strain levels used. However, no specimen fractured at greater than $6.3 \times 10^6$ cycles. Thus no really high cycle data are available. For a specimen tested at a shear strain ratio of 1.8, the first stage had a length of approximately 20,000 cycles or 4 per cent of the fracture life, with the third stage beginning at about 80 per cent of the total cycles for fracture. It was not practicable to attempt to obtain from Duce's graphs other data in regard to the length of the first stage.

The fatigue data for aluminum were not extended much beyond $2 \times 10^5$ cycles because of testing machine limitations. In addition Duce found it impossible to take a series of photomicrographs of the deformation visible at various stages during a fatigue test on this material due to the fact that the annealed aluminum specimens were so soft that it was impossible to take the specimens out and reinsert them in the machine several times without damage. Therefore an examination of the fatigue process was made on a series of identically treated specimens tested at the same strain amplitude. A series was tested at an amplitude resulting in a net life of approximately 100,000 cycles. They were electropolished before testing to permit examination by electron microscope procedures. After polishing they were etched to remove the surface film formed during polishing which can interfere with the development of slip lines. Duce found this

interference to be quite marked, for example, an unetched specimen after 1000 cycles showed no slip lines while an etched specimen showed a considerable number.

Examinations were carried out both with the light microscope and electron microscope techniques to provide a remarkable series of photo-micrographs of the fatigue process in aluminum. They showed slip lines after only 27 cycles (fracture life, 100,000 cycles) and slip bands in a photomicrograph taken at 1000 cycles. Other changes in the process are clearly indicated. Cracking was noted after some 80,000 cycles at this strain amplitude. Fig. 6 shows the beginning of cracking to vary from 55 to 90 per cent of the fracture life over the range of strain employed.

Magnesium was the only hexagonal metal tested by Duce. Data for the tests in the replotted form are shown in Fig. 6. Metallographic examination was conducted on one specimen tested at a strain amplitude ratio of 1.65. Faint slip lines were visible in a few grains after 1000 cycles in the specimen which failed at 70,000 cycles. For another specimen tested at the same strain amplitude, the cracking stages began at approximately 15,000 cycles and the specimen fractured after 100,000 cycles. As Fig. 6 shows, there is a tendency for early cracking in this metal. The values obtained were from 15 to 80 per cent of total fracture life at the strain levels used in the tests. Duce found magnesium very prone to developing many crack centers over the surface of the specimen. He further observed the marked intercrystalline nature of the fatigue cracks as opposed to the generally intracrystalline deformation and fracture with a transcrystalline path as he found with the face-centered cubic metals.

Duce also performed some tests on iron and some plain carbon steels and used a variety of heat treatments. The results for any one condition are not complete enough to reproduce the type of data shown for the other pure metals. The effects of inclusions, carbon content, and heat treatment were all examined. He concluded that iron and steel show certain differences when compared with other pure metals in their fatigue behavior. The major difference exhibited by them is in the first stage of the fatigue test, where the changes in $\Delta E$ and tan $\beta$ are in general opposite in direction to those found for nickel, copper, aluminum, and magnesium. He showed also that these changes could be reversed in certain cases by suitable heat treatment of the iron. He found in many cases that cracks developed at a very early point in the specimen life. He was uncertain whether the typical behavior of iron and steel was due to the mechanism of deformation of the body-centered cubic lattice or to the presence of interstitial carbon (or nitrogen) even in minute amounts.

Duce also tested an inclusion-bearing free-cutting steel. The types of tests performed were similar to those on nickel, copper, etc., described above. The production of visible deformation in the free-cutting steel was shown to be very small. No slip lines were visible, although small regions of localized deformation were produced in later stages of the test near the cracks and perpendicular to them. With the inclusions elongated longitudinally Duce found that longitudinal cracks developed at a very early point in the life of a specimen. For example, in a specimen which was tested at a strain amplitude causing fracture in 390,000 cycles, cracks were observed to have formed already at 5,000 cycles. These small longitudinal cracks either connected the inclusions or emanated from them. It appeared that all the cracks originated in an inclusion.

Duce ran a few tests with wrought iron specimens in which the inclusions were elongated in a longitudinal direction, and for others in a transverse direction, with respect to the specimen axis. In the latter case no longitudinal cracks were formed but the fatigue life and limit were considerably reduced. Apparently in this case, the inclusions assist considerably in the formation of a circumferential crack which then propagates very rapidly. Results similar to this were also obtained with some pure iron containing inclusions initially tested by Duce. It is not possible to determine from his data the

approximate point of first cracking in the tests on the inclusion bearing materials because of the very early occurrence of cracking and the linear scale which Duce employed in plotting his data.

Sinclair and Dolan (51) used periodical reheating to the recrystallization temperature as a means of removing the effects of work hardening developed by repeated stressing in fatigue tests. They employed rotating beam machines in their study of unnotched specimens of annealed 70-30 cartridge brass. A group of specimens was given a recrystallization heat treatment at intervals of 20 per cent of the mean fatigue life of a control group of specimens not given intermediate treatments. It appeared that the recrystallization treatment at 20 per cent intervals had no appreciable effect on the fatigue life. The authors concluded that disruption of atomic bonds is initiated in local regions during a relatively early stage of cyclic stressing. This might be interpreted here to mean that microcrack initiation occurred earlier than 20 per cent of the fracture life at the stress level used (approximately 120 per cent of the fatigue strength at $2 \times 10^7$ cycles).

Love (52) studied the structural changes in iron caused by plastic and repeated stressing. Tests were run on unnotched specimens that were prestrained in tension or compression as well as on specimens not prestrained. The existence of very small (2-3 microns long) discontinuities interpreted as cracks, identified by the shadows cast by portions of electron micrograph replicas which had been withdrawn from a separation in the metal surface, were found in the early stages of fatigue at both the grain boundaries and along the intracrystalline slip bands. In general, these cracks began to appear after 100 to 1000 cycles at 40,000 psi stress level and after 1000 to 10,000 cycles at the 30,000 stress level. These data are shown in Fig. 7 for specimens not statically strained before testing. The dashed portion of the line indicates that initial cracking occurs somewhere in this region.

A study of slipping in the crystalline structure of the surface of the specimens was made by Love with the aid of a light microscope. Plots were made of perfunctory estimates of the percentage of area which exhibited slip by a disturbance of the electropolished surface. Extrapolation of the curves to zero slip indicates the existence of a delay interval at both levels of fatigue stress during which no slip was visible. As read from Love's data for specimens not previously strained, the delay intervals appear to be about 900 cycles at the higher stress and 9000 cycles at the lower stress. Love points out that the existence of a delay interval does not necessarily mean that no structural change has occurred during the early cyclic stressing. but suggests that the first changes which occur are probably of a submicroscopic nature (e.g. dislocation formation and movement).

Examining Love's data it is seen that hereports cracks observed in electron micrographs at approximately 0.1 per cent of the fatigue life or 100 cycles at the higher stress level, but the optical microscope data show the beginning of slip at approximately 900 cycles of stress. Similarly he indicates the start of cracking between 1000 and 10,000 cycles at the 30,000 psi level and shows the beginning of slip as observed by the optical microscope at approximately 9,000 cycles. This apparent contradiction is probably due to the differences in resolving power of the electron and optical microscopes. This would account for the fact that Love indicates both slip and cracking with the more powerful microscope long before the first indication of slip under the optical microscope.

Bennett and Weinberg (54) determined the notch sensitivity in fatigue for three aluminum alloys using rotating beam machines and three methods of crack detection: a deflection method, a vibration-responsive device, and microscope inspection method. They obtained the data on unnotched specimens shown in Fig. 5. These data were plotted from median values for the number of cycles to fracture and median values of the number of cycles for the start of cracking as reported in the original paper. As in an earlier study by Bennett (46), crack initiation was obtained by extrapolating crack growth curves. It was checked by extending some specimens under axial tension. The data for 7075-T6

alloy showed considerable scatter and could not be extended much beyond $10^6$ cycles of stress. Therefore the data shown for this alloy were computed on the basis of a fatigue strength of $2 \times 10^6$ cycles instead of the usual $2 \times 10^7$ value. The work of Bennett and Weinberg presents results obtained using very careful techniques of relatively high power. Furthermore, the statistical determinations made give evidence of the scatter that can be expected in such data even with careful investigations.

A very interesting study in which were employed the most powerful techniques presently available for the detection of fatigue cracking is that of Hunter and Fricke (54). They employed chemical polishing of the specimens and electron microscope methods in addition to plastic replica plus optical microscope techniques to follow the formation and progress of fatigue cracks in aluminum and in aluminum alloys from very early in the fatigue life to final, complete fracture. They observed that when an aluminum specimen is subjected to fatigue stressing, its surface undergoes a continuous sequence of submicroscopic and microscopic changes. These progressive changes include the development of submicroscopic slip bands within individual grains, the formation of extremely fine cracks within individual grains, the joining of cracks across grain boundaries to form major cracks, and the extension of these major cracks until sudden complete tensile failure of the material occurs. It is very interesting that this sequence of events observed with the present day highly sensitive technique is so similar to the course of fatigue breakdown in Swedish iron described by Ewing and Humfrey (02) over fifty years ago.

Hunter and Fricke show that points denoting the cycles required to produce these several stages of progressive change at various stress levels fall on smooth curves which bear a relationship to each other and to the familiar S-N curve denoting final failure. No numerical data are given in this report but curves are presented for specimens of various materials. Values were read from these curves of Hunter and Fricke and the data were replotted according to the method used with the other data in this review. The study included sheet bending tests of 1050-O aluminum (99.5 per cent purity) sheet, Alclad 2024-T3 sheet, 2024-T3 sheet, and rotating beam tests of 7075-T6 rod. Not all of the progressive changes outlined in the preceding paragraph were detected in all of the materials. Hunter and Fricke report that with materials of relatively low strength most of the changes observed prior to failure consist of slip stages with but little evidence of the steps involving cracking. On the other hand, with aluminum alloys of relatively high strength, these authors report that the earlier stages of change were difficult or impossible to detect. Most of the change observed during the fatigue life consists of cracking and crack extension. They believe, however, that all stages actually occur in all materials.

The results obtained with 1050-O sheet are given in Fig. 8. In this relatively soft material the various slip stages were evident but Hunter and Fricke report that very little cracking was apparent before final failure. Slip was observed very early in the test. The percentages of fracture cycles at each level are indicated in the number adjacent to the corresponding slip points. Another curve is shown for slip saturation. After this point, at each stress level, the authors report that a small amount of additional deformation occurred, some large cracks formed, and finally the specimen failed.

The data of Hunter and Fricke for Alclad 2024-T3 sheet are also shown in Fig. 8. This is a composite material with the much weaker aluminum material coating the alloy base. Curves are shown for first slip in the coating, for first crack by the replica and optical microscope method, for crack joining, for first crack by the penetrant method, and for final fracture. Again, first slipping occurred at a very early stage in the fatigue process, earlier even than for the pure aluminum sheet (on a fracture life basis) because the supporting effect of the core provided a longer fatigue life. The sensitivity difference between the detection of first cracking by the replica and by the penetrant methods is great and is clearly shown on this graph.

The authors report that the changes observed during the fatigue life of 2024-T3 and 7075-T6 alloys are similar. Because of their strength and the relatively small amount of slip that can occur without cracking, the slip stages are seldom seen with these alloys. They indicate that with these alloys there is also less tendency for general crack formation, and as a result, most of the period between formation of the first crack and ultimate failure is occupied by crack extension. Fig 9 shows the data for the 2024-T3 sheet specimens. First crack lines obtained by the replica and penetrant methods are both shown. The first crack lines are seen to join the fracture line at the long life end of the curves. Data for the rotating beam tests on 7075-T6 rod are given in Fig. 10 with the first crack indication by the replica technique occuring at values between 20 and 50 per cent of the fracture life. These values for first cracking are lower in general than those reported by Bennett and Weinberg for similar tests on the same material. Hunter and Fricke's investigation was not of the statistical type so far as is known. The points on the curves show surprisingly little scatter when compared with other investigations.

## 2.3 Data for Notched Specimens

Early data on the initiation of cracks in fatigue specimens were obtained by Moore (27) who tested rotating cantilever beam specimens cut from heat treated railroad car axles. The specimens contained a fillet for which the theoretical stress concentration factor was approximately 1.95 determined by using the results of Timoshenko and Dietz (25) and 1.45 by the curves of Peterson (53). Moore employed the oil-whiting and low (10X) power optical microscope methods of crack detection. Data from his report are plotted in Fig. 11. Graphs are shown for steel A(0.46 per cent carbon) and for steel B (0.62 per cent carbon). These are plotted from the data of Moore's paper according to the usual manner for this review. These data indicate that at the higher stresses a greater percentage of elapsed life of the specimen has occurred at the initiation of cracking than for stresses just above the fatigue limit. The results are not strictly in accordance with those of most later investigators which usually indicate the reverse effect.

In reporting fatigue tests on notched specimens of annealed 0.15 to 0.20 per cent carbon steel Davidenkow and Schewandin (31) state that cracks could be detected at the base of the notch at about 50 per cent of the life of the test piece. No further information from this study on cracking was available to the writer of this review.

Peterson (36) obtained data relating to crack growth in grooved specimens of normalized 0.45 per cent carbon steel. Values of the number of cycles to the beginning of cracking in these rotating bending, constant load tests were approximated here by extrapolating his crack growth curves. Values for number of cycles to fatigue fracture and the approximate fatigue strength are given in this reference. Peterson's data are shown in Fig. 12 plotted in the usual form.

Bennett (46), in his studies of damage in SAE X4130 steel, determined the number of cycles to the start of cracking and to fracture in cylindrical specimens with a circumferential groove. Tests were conducted in the conventional manner to fracture on a group of notched specimens to determine the fatigue limit. The median life of groups of specimens tested at four stress levels was used in this work. In the tests to determine $N_c$, or the number of cycles to form a crack of a definite size, at least 10 specimens were tested at each stress level and the median of each group was used as the representative value at that stress. Crack formation was detected by a deflection method. The deflection is a function of the size of the crack and the criterion chosen for $N_c$ was the number of cycles to produce a deflection of 0.005 mm corresponding to a crack area of about 12 per cent of the original cross section. The fatigue limit of the notched specimens was obtained from the results of several tests in the vicinity of that stress. The data from this study by Bennett are given in Fig. 13 for the values relating to cracking. Bennett

observed that within the stress range used in this study, the proportion of the total life for a crack to grow to the point of specimen rupture varies from as much as 50 to as little as 10 per cent. With the material used in this investigation, the ratio of the crack growth stage to the total life of the specimen was larger at stresses considerably above the fatigue limit than at stresses close to the fatigue limit.

Foster (47) used a fracture wire technique and found the method succesful in indicating the initiation of cracks in both fatigue specimens and actual parts. He reports that fatigue cracks so small as to require a microscope for observation were detected in this manner. The indications of his experimental data are that a larger percentage of total life remains after the crack initiates at the high end of the fatigue S-N curve than at the lower end. Data from his tests on Alclad 2024-T sheet in the form of flat strip specimens with a perforated hole in the center and tested in reversed bending are shown in Fig. 17.

MacGregor and Grossman (48) conducted a series of experiments in which the effects of different numbers of prior cycles of fatigue stress on the brittle transition temperature and on the brittle fracture strength were determined for SAE 1020 steel. Notched fatigue specimens were fractured at the appropriate transition temperature in a special slow-bend testing machine at controlled strain rates after being subjected to various numbers of cycles of fatigue at one of several stress levels. It was found that as the number of cycles at a given stress level (both above and below the endurance limit) increased, the brittle transition temperature increased through a broad range of temperatures, and the brittle fracture strength decreased greatly. Comparison of the results with the damage line for this material (obtained by other investigators) indicated that the usual damage line method of determining damage was not as sensitive as the slow-bend brittle transition temperature test since it does not show damage at the lower number of cycles at lower stresses as the latter does. The authors observed that an incipient and growing fatigue crack could account for all of the effects found in these tests. They also observed that after a certain number of cycles of prior fatigue stressing, a dark annulus begins to appear around the periphery of the fracture in the bend test. They noted that the same dark ring appears at a stress level considerably below the endurance limit. Reductions in fracture stress and increases in the brittle transition temperature were found at considerably less than one per cent of the life-to-failure at a given stress level. MacGregor and Grossman concluded (perhaps in error) that the annulus is merely a reflection of the mechanism of crack propagation during the slow bend tests and is not an indication of a spreading fatigue crack. They considered that the principal cause of the increase in transition temperature and of the decrease in brittle fracture strength produced by an increase in number of prior cycles at a given stress level is due to strain hardening and strain aging.

Jaffe, Reed, and Mann (49) studied discontinuous crack propagation in metals. In the course of their work they sought the occurrence of microcracks in metals near the path of brittle fractures. Microcracks were found in the rotating beam fatigue specimens of an alloy steel only near the path of final, complete, sudden fracture. This occurred where little or no evidence of deformation was observed and never in the "battered" area where progressive fracture presumable took place over many cycles. In one of their examinations no microcracks could be found (at a magnification of 500 X) below the notch in an unfractured specimen fatigued for 40,880,000 cycles in rotating bending at a stress of 87.5 per cent of the notched fatigue strength. They did not obtain other data suitable for reproduction in this study. The theoretical stress concentration factor for the specimen used in these tests on an alloy steel was not determinable from the data given in their report.

Lessells and Jacques (50) also conducted an investigation on the effect of fatigue on transition temperature of ship steels. A combination fatigue-impact specimen was designed and used. The test section of this specimen was cylindrical with a circumferential notch and could be tested in impact by sawing off the tapered ends necessary

for holding in the rotating beam fatigue machines used. The material was 0.18 per cent carbon (steel B) and 0.21 per cent carbon (steel W), semi-killed, hot-rolled, shipbuilding steel. Both unnotched and notched specimens were tested with the fatigue strength reduction factor being approximately 1.2 at $10^7$ cycles for steel B. The theoretical stress concentration factor for the notch was approximately 4.3 after Neuber (46). The notch was cut in the notched specimens in a single operation with a lathe tool. Notched specimens tested in fatigue for a given percentage of life at a given stress were then tested in an impact machine. These specimens when fractured showed a dark band about 0.02 inch wide on the fracture surface adjacent to the base of the notch. Similar bands were reported previously by MacGregor and Grossman (48). Lessells and Jacques attempted to prove that the bands were the result of fatigue cracks by testing unfractured specimens by means of Magnaflux, Zyglo, and penetrating dyes. All these were unsuccessful. Presumably the Magnaflux test failed because of the disturbing effect of the notch itself. The dyes would penetrate the crack but not in sufficient quantity to produce discoloration at the bottom after cleaning. A destructive sectioning method was finally employed and it was found that the cracks were readily located after sectioning the specimens longitudinally through the base of the notch, polishing, etching, and viewing in a microscope. Cracks were located down to a few ten thousandths of an inch in length (radially). Crack lengths were measured by use of an optical microscope.

Lessells and Jacques found that fatigue cracks were developing at the base of the notch both above and below the endurance limit. The lowest nominal stress at which a fatigue crack was found was 11,500 psi, about 45 per cent of the endurance limit of the notched bars for one of the steels. Russell and Welcker (36) earlier showed damage data for various materials using notched and unnotched specimens, but the damage regions in all cases were above the endurance limit. Their criterion of damage, of course, was the inability of a specimen to run indefinitely at its original endurance limit.

Lessells and Jacques showed "damage" also below the endurance limit although it is of a different nature. In Fig. 14 graphs are presented for some of the data from two of their materials showing the notched fatigue curve for fracture and data representing the number of cycles to the detection of a crack of a given small depth. At stresses slightly above the endurance limit for the 0.18% C. steel, the data indicate that cracks of 0.001 inch in depth were detected at less than one per cent of the number of cycles to fracture. The data shown here were replotted from values read from Figs. 11 and 14 showing crack growth data in the paper of Lessells and Jacques.

In regard to specimen preparation, the specimens of material B were used with the notch formed by turning with a contour tool. The authors mention, however, that machining of the notch left small circumferential ridges at the root of the notch with steel W and occasionally would tear small particles out of the bottom of the notch. Specimens with no tears were used. The minute ridges were lapped off using No. 30 bare copper wire and 440 grit lapping compound. Specimens of steel B were not so polished.

Fenner, Owen, and Phillips (51) conducted an investigation on the fatigue strength of mild steel under direct tension-compression stress with large, notched test pieces containing a very sharp V-groove. The theoretical stress concentration factor for the specimen form was estimated by the authors as near 20, but it appears to be approximately 14.0 by the results of Neuber (46) and 12.5 by the curves of Peterson (53). The notches were made by machining with a sharp cutting tool and great care was taken during the machining operation to avoid excessive cold working of the material. In these tests a small mean tension load (less than 1/2 ton) was applied to each test, to reduce hammering between the ends of the broken test pieces while the machine was shutting down. This procedure was adopted in the tests mentioned later, though for convenience the stresses are quoted as alternating stresses ($\pm$ half the applied range of stress).

During determination of the S-N curve for the notched specimens (fatigue strength approximately 4.5 tons per square inch), it became evident to these investigators that the test pieces were cracked at a very early stage in the test, though the endurance to fracture might be as high as 10 million cycles. They performed some experiments to determine the point in the specimen life at which a crack began. They used a portable magnetic crack detector on test pieces under test. They give no further description of the detection device. By the time the full stress values had been applied, in starting tests both at stress ratios of 1.6 and 1.1 times the fatigue strength, they observed crack indications. These occurred as early as 20,000 cycles after the start of the test. At the lower stress this represents a crack detected at 0.07 per cent of the specimen life.

Another specimen was continuously inspected for cracks while slowly increasing the stress from zero. At the first crack indication the nominal stress range was observed to be about 38 per cent of the fatigue strength and the number of cycles of stress at that time was about 20,000. The piece was then subjected to $25 \times 10^6$ cycles at this stress was later sectioned and examined microscopically. A crack was found to be present. A second specimen was subjected to the same stress range for only $5 \times 10^4$ cycles and then sectioned and examined. A crack was also found in this test piece. Another specimen subjected to $10^8$ cycles at this stress contained a small crack upon microscopic examination after sectioning.

Since it was thought possible that the formation of cracks had been caused or hastened by internal stress introduced in the machining operation, Fenner, et al. conducted tests similar to the above on specimens stress relieved after machining. Three of these were subjected to about $10^7$ cycles at stress ranges of 38, 45, and 53 per cent of the fatigue strength at $2 \times 10^7$ cycles. Subsequent microscopic examinations showed that one certainly contained a crack and another possibly contained a shallow crack. The depth of the cracks in the specimens examined microscopically in this study varied from an estimated 0.0005 to 0.0030 inches. The observed cracks were transcrystalline and did not develop uniformly around the circumference. In some cases it was necessary to examine a number of sections to locate a crack. In Fig. 15 of this report are presented some of the experimental results of the investigation of Fenner et al. A key to the various symbols used is included with the graph. This study is noteworthy for having indicated cracks so early in the lives of specimens tested at such low stress levels.

MacGregor and Grossman (52) conducted an investigation to determine the effects of cyclic loading on the mechanical behavior of 2024-T4 and 7075-T6 aluminum alloys and SAE 4130 steel. Unnotched, U-notched and V-notched specimens of the three materials were subjected to various numbers of prior fatigue cycles in rotating bending both above and below the fatigue limits. Special slow-bend tests at constant deflection rates and temperatures were employed to show the effects of prior cycles of fatigue stressing on the transition temperature to brittle fracture for SAE 4130 steel and on the energy absorption capacity of the aluminum alloys.

The authors had previously observed a change in the transition temperature of SAE 1020 steel due to fatigue and attributed it to strain hardening and strain aging. Later Lessells and Jacques using a different approach in testing technique, demonstrated the presence of small cracks in specimens subjected to prior fatigue cycles both above and below the notched endurance limit on two similar low-carbon steels. It was considered that the increases in transition temperature shown by these steels could be accounted for by the origin and growth of the small cracks.

In the newer study MacGregor and Grossman intended to discover if this change in transition temperature and the formation of cracks below the fatigue limit was a peculiarity of mild steel or whether the phenomenon occurred in other metals as well. Micrographic studies were made to observe and measure crack formation and propagation

and other additional tests were performed. Longitudinal sectioning of fatigue specimens to detect the formation of cracks yielded erratic results because the circumferential cracks which originated at the root of the notch and penetrated radially inward were not necessarily symmetrical about the axis of rotation of the specimen. As an alternate procedure in tests above the fatigue strength they photographed the stressed and subsequently fractured specimens. These showed the two clearly distinguishable areas mentioned previously, an outer ring due to the slowly penetrating cumulative "cracks" and an inner "core" from the portion which suddenly fractured. Crack growth data were also obtained by these investigators from measurements made on fractured specimens.

In preparation of their notched specimens, MacGregor and Grossman used contour lathe tools for forming the notches. The specimens were then finished with number 0 emery paper exclusive of the notch and that was polished in each case with a fine emery thread to provide axially running scratches. Some results of crack initiation data from this investigation are shown in Fig. 16. The fracture data indicated in these graphs were read from the figures presented in the paper of MacGregor and Grossman. Those authors do not present specific data, however, on the number of cycles to initial cracking. Photomicrographs of longitudinal sections made on specimens tested to a fraction of their fatigue life at various stress levels are shown and photographs of the fractures of cracked specimens from the slow bend tests are presented. In addition a graph is given for one type of notch showing average radial crack depth versus number of test cycles for the three materials at a stress level resulting in equal fatigue lives for the various specimens. The number of cycles to first cracking was estimated from these data by the writer of this review and were used in the construction of Fig. 16. The dashed portions in the crack lines indicate the region of uncertainty for start of cracking. Data are presented for the start of cracking at one stress level only, for three materials in each of two specimens forms.

MacGregor and Grossman state clearly in their report that with their techniques of sectioning for crack detection, the three metals tested did not show any cracks when stressed below their notched endurance limits. Tests were made on specimens previously stressed at various fractions of the notched endurance limits and carried to $50 \times 10^6$ cycles without any evidence of cracks. This behavior then was apparently different from that shown by the two carbon steels previously tested by Lessells and Jacques (50). However, MacGregor and Grossman point out that it is possible that a more refined technique might reveal minute cracks even for this range.

Demer and Lazan (53) obtained crack data for notched specimens of N-155 alloy, a heat-resistant material. The tests were conducted at room and two elevated temperatures. They employed rotating cantilever beam machines and used a deflection method in their detection of cracking. The deflection method was checked in the room temperature tests by sectioning and microscope examination. It was found that the percentage of fatigue life between the detection of a crack and failure is relatively greater at room than at the elevated temperatures. At all three temperatures this value increased with stress. Curves for the results of these tests are shown in Fig. 20. The notched specimens for the tests were prepared by first turning to an oversize value by means of a lathe tool and then grinding to size with a contoured grinding wheel with a number of light cuts.

Bennett and Weinberg (54) determined the initiation of cracking in three aluminum alloys for two types of notched specimens in rotating beam tests. In addition to the results of tests on these alloys in unnotched form given in Fig. 5, they also used 1/16 inch radius and 0.025 inch radius filleted specimens in each material. Their results for 2024-T4, 6061-T6, and 7075-T6 are presented in Fig. 18 and 19. As mentioned previously in connection with unnotched specimens, they employed three methods of crack detection and obtained rate of crack growth curves which they extrapolated back to initial values. The data presented in Figs. 18 and 19 are statistical values both for cracking and

fracture obtained by testing several specimens for each test condition. The filleted specimens for this study were prepared by first turning and then polishing the fillets with a rotating wire over which was carried 302 emery in a mixture of glycerine and water. The polishing wire was supported on a pivoted jig to assure uniform pressure.

## SECTION III. DISCUSSION OF EXPERIMENTAL DATA ON CRACK INITIATION AND GROWTH

The number of cycles of fatigue stressing required for the complete fracture of a test specimen at a given stress level depends upon the ease with which fatigue cracks are initiated in the material and the rate of propagation thereafter. A mere statement of the number of cycles to failure at a given stress level makes no differentiation between these two features of the fracture process. The data presented in Figs. 1 through 20 provide some information in regard to both features. The effect of various factors listed in Table I on crack initiation will be discussed in some detail. In so far as possible, the effect of arbitrariness in the definitions of crack initiation and failure were eliminated from the following comparisons. Presentation and discussion of direct experimental data on the rate of growth of fatigue cracks will be deferred to the next section of the report.

### 3.1 Detection Method Employed

The number of cycles at the first observation of cracking in a given test obviously depends on the sensitivity of the detection method employed. There have been few investigations, however, where the sensitivities of various methods of detection have been compared in tests on a given material. Even in the instances where comparisons were made, only a few types of detection methods were used. In any event, the electron microscope and the replica-optical microscope and medium power optical microscope methods appear to be superior in sensitivity to the other methods, see Demer (55). In this connection it should be pointed out that the surface finish of the fatigue specimen is a very important factor in the early detection of fatigue cracks for very smooth finishes facilitate early observance of the indication of cracking.

The data of Hunter and Fricke (54) in Fig. 9 give one instance of a comparison of the replica and the dye-penetrant methods. Another comparison of methods is available in the results of Hunter and Fricke, and Bennett and Weinberg (54) who tested the same material, 7075-T6 aluminum alloy in rod form in rotating bending with constant moment. For their work, Bennett and Weinberg used mechanical polishing of the specimens and employed deflection techniques and optical microscope crack detection methods, as contrasted with Hunter and Fricke who employed chemical polishing and plastic replica-optical microscope methods of crack detection. Bennett and Weinberg used statistical procedures and their values reported are median values. Evidently those for the other investigation were not obtained statistically. The graph of Fig. 21, which compares the data for these tests emphasizes the difference, not only in crack initiation data, but also fracture values which can be obtained even in present day investigations on the same material tested supposedly in the same manner. The data shown in Fig. 5 were used in this graph, and the data of Fig. 10 were replotted on the basis of a fatigue strength at $2 \times 10^6$ cycles for inclusion here. In connection with these results it should be pointed out that the material tested is one in which rather severe variability has been encountered on occasion in past fatigue studies. However, this would not appear to explain the reason for the large discrepancy in the values of $N_c/N_f$ at the various stress levels. The tendency toward lower values of this ratio for the lower stress levels shown by the data of Bennett and Weinberg was not displayed by the notched specimens of the same material (see Fig. 19) which they tested and is not thought to be the true behavior of this material.

In certain other investigations in which cracks have been reported at a very low percentage of fracture life it is probable that other factors in addition to the sensitivity of detection method have been important. Among those which may exert appreciable effect are the specimen form, stress level, surface finish, and nature of the material being tested. These and other factors will now be discussed.

## 3.2 Test Material

Table I lists a number of characteristics of the test material which probably affect fatigue crack initiation and growth. In many cases there are insufficient data available to support conclusions in regard to the effect of each of these factors. However, it appears of value to make certain comparisons and record several observations in regard to crack initiation and growth in polycrystalline materials.

Experimental data are presented in this review for pure metals of various crystal structures. In Fig. 6 are given crack and fracture data of Duce (50) for the face-centered cubic metals, nickel, copper, and aluminum, and the hexagonal metal, magnesium, obtained in reversed torsion. In Fig. 7 are shown data of Love (52) for iron of body-centered cubic structure obtained in reversed bending. Summary plots of these data are shown in Fig. 22. Graphs are presented with smooth curves for the crack and fracture data, for the crack to fracture cycle ratio $(N_c/N_f)$, and for the number of cycles between cracking and fracture $(N_f-N_c)$. Duce's data for aluminum could not be included in this graph because the fatigue tests were carried only to a relatively small number of cycles. However, on the same basis, a curve for aluminum would be close to and probably exceed the steepness of the curve for copper. The data for the other metals are on the basis of fatigue strength values at $10^7$ cycles. Two cracking lines are shown for iron in Fig. 22a. Love observed that the cracks initiated somewhere in the enclosed range.

The data of Fig. 22a indicate that the cracks initiate earliest in iron, then in magnesium, and then in nickel and copper, at a given stress or strain ratio level. On the basis of $N_c/N_f$, the materials fall in the same order, that is, cracking was found at an extremely small percentage of fracture life for iron, at a greater value for magnesium, and for still greater values for the FCC metals nickel and copper. The graph showing the number of cycles between cracking and fracture is also interesting. Copper exhibits the greatest relative resistance to crack initiation and also has generally the greatest number of cycles between cracking and fracture, and a high $N_c/N_f$ ratio. The former is not readily obvious from Fig. 22a. Nickel generally exhibits the smallest number of cycles between cracking and fracture except at very high strain ratio levels.

In Duce's discussion of the appearance of the various specimens in stage three of the fatigue process, he observes that magnesium is very prone toward developing many crack centers over the surface of the specimen. Such a large amount of subsidiary cracking was also found by Crussard (47) in experiments on zinc. Duce observed that the aluminum was remarkably free from subsidiary cracks of any kind. However, he noted that with the nickel specimens there were very few subsidiary cracks except possibly near the main fracture itself, but with copper the specimen surfaces tended to exhibit subsidiary cracks quite generally. This is evidence of the formation of many crack centers. It might be expected that in Fig. 22a, the curves for copper would fall between magnesium and nickel because of these considerations, but such is not the case.

Both Duce (50) and Love (52) have given crack data on pure iron, but not under similar conditions since Love tested under reversed bending while Duce employed reversed torsion. Duce found cracking at an extremely early point in the fatigue life of some specimens and somewhat later in others, but always earlier than for the other pure metals. He was uncertain, as mentioned previously whether this behavior was typical of this material with a BCC structure or due to the presence of interstitial carbon (or nitrogen) in minute amounts. Love (52) also found this very early cracking in iron of somewhat lesser purity. His data are shown in Fig. 22 with other data.

Duce found the cubic metals showing mainly intracrystalline deformation and fracture on a transcrystalline path. He observed that magnesium shows intercrystalline deformation and breaks with an intercrystalline fracture. Love, in the commercially pure iron, observed slipping and indications of cracking both within the grains and in the intercrystalline structure. No record is presented of his having followed the fatigue process through to fracture by following the spreading the fatigue cracks by less powerful means than the electron microscope.

Love found that round surface inclusions had little effect on the general structural changes occurring during the fatigue of ingot iron. Duce studied elongated inclusion bearing steels and found that with the inclusions properly oriented (longitudinally), cracks developed during the torsion tests at a very early point in the life of the specimen. It appeared that all of the cracks originated in an inclusion. Thus inclusions may or may not have an effect on early cracking depending on the curcumstances of shape *and orientation*.

Duce (50), Sinclair and Dolan (50), and Karry and Dolan (52) have studied the effect of grain size on fatigue properties of metals, but there appears to be little information on the effect of grain size on crack initiation.

It is interesting to compare the results of the two studies on pure aluminum reviewed here. The data of Duce obtained in reversed torsion, constant maximum strain, are shown in Fig. 6, and those of Hunter and Fricke (54) are in Fig. 8 from reversed bending, constant maximum deflection tests. The latter investigators observed slipping and slip saturation at very low percentages of the fracture life in unnotched specimens, but show no curve for crack initiation as they do with the other *materials* which they tested. They state that the slipping so roughened the surface that it was difficult to tell when cracking actually began. It seems strange that cracks could initiate and grow to the point of complete rupture of the specimen without being easily detectable at least at a relatively small magnitude even in a specimen with a surface severely roughened by slip. Duce found the annealed aluminum specimens so soft as to make it impossible to remove them from the machine for examination and reinsert them in the machine several times without damage, but studied crack initiation is a series of identically treated specimens. His tan $\beta$ and $\Delta E$ curves show changes interpreted as due to cracking at percentages of fractre life between 50 and 90 per cent. It is unfortunate that Hunter and Fricke did not obtain crack initiation data to compare with these.

None of the original data presented are useful for comparing crack initiation results for a pure metal and higher strength alloys tested under exactly similar conditions. deForest (36) and Hempel (39), however, studied the behavior of steels with different carbon contents under rotating bending conditions and both employed the Magnaflux method of crack detection. Figure 23 shows comparison plots of these data. For comparison purposes only, the data of Love (52) on ingot iron obtained on sheet material in reversed bending and employing electron microscope techniques for detection are also shown in these graphs. It is possible that dissimilar testing conditions in the studies may have exerted a large effect on these results. This should be kept in mind when the following observations are made from the graphs. The tendency toward crack initiation appears to increase and cracks are detectable at a lower percentage of fracture life with decreasing carbon content. The data for number of cycles between cracking and fracture show no regular relationship to carbon content, but this may have been a result of the different detection techniques employed.

Crack initiation data for three aluminum alloys obtained under the same testing conditions are shown in Fig. 24 for unnotched specimens. These data are from Bennett and Weinberg (54). The data for 2024-T4 and 6061-T6 shown in Fig. 5 were replotted on the basis of the fatigue strength at $2 \times 10^6$ cycles in order to be comparable with the data for 7075-T6. Although the fatigue strengths of 2024-T4 and 6061-T6 are

rather widely divergent (32,000 psi, and 23,000 psi, respectively, at $2 \times 10^6$ cycles), nevertheless their data are very comparable when compared on the stress ratio basis. Those for 7075-T6, however, appear to be characteristically different from the other two alloys in spite of the fact that the fatigue strength is almost identical with that for 6061-T6 at $2 \times 10^6$ cycles. The trend in the $N_c/N_f$ ratio for 7075-T6 may be due to scatter. It would be expected to approach 100 per cent with a decrease in stress level to conform with the behavior of other materials. This material has been found in other investigations also to be rather inhomogeneous.

### 3.3 Specimen Form

The experiments of Bennett and Weinberg (54), discussed previously, provide crack initiation data on three aluminum alloys in three specimen forms, namely unnotched or large radius single fillet specimens and two types of notches. It is interesting to examine the effect of specimen form in each of the three materials. Faired curves of their data for median values of cycles to cracking and cycles to failure, as given in their paper are shown in Fig. 25. In this graph the ordinate is maximum rotating bending stress. This graph is presented to show the crack and fracture results when plotted in the usual S-N manner. In Figs. 26 through 28, however, the data of Figs. 5, 8, and 19 are shown in summary on a stress ratio based as faired curves so that the effect of specimen form on the crack data of each of the materials may be observed.

Several behavior tendencies may be noted in the graphs of Figs. 26 through 28. On this stress ratio basis of comparison, the crack and fracture curves for a given material fall in a certain scatter band regardless of form. This may be seen in Figs. 26a, 27a, and 28a. The band is narrowest in the cases of 2024-T4 and 7075-T6. On the stress ratio basis it is seen that cracks may be detected at a lower percentage of cycles to fracture as the stress concentration factor increases. This tendency is very clear except for the data of 7075-T6. In general, the specimen form of highest stress concentration provides the largest number of cycles between first cracking and actual fracture when compared on the stress ratio basis, indicating a comparatively slower rate of growth as the stress concentration factor increases. Again this trend in 7075-T6 is somewhat obscured. When comparing the number of cycles between cracking and fracture for different specimen forms in a given material on a nominal stress basis, however, it is observed that the smoother specimen forms, those with the smaller stress concentration, display the slower average rate of crack growth. This is indicated by the $N_f$-$N_c$ data for 2024-T4 shown in Fig. 29.

It is interesting to note that the crack initiation data of MacGregor and Grossman (52) for 2024-T4 in rotating bending shown in Fig. 16 also fall in the same scatter band as for the data of Bennett and Weinberg (54) on the same material as shown in Fig. 26. The agreement in the case of the 7075-T6 alloy is not as good. Other comparisons of data on the same material shown in this review, such as that of Bennett (46) and MacGregor and Grossman (52) on X4130 steel show reasonable agreement, but it is difficult to ascertain the effect of different crack detection methods employed and other test conditions. For these reasons the comparisons are not shown here.

### 3.4 Specimen Size

The experimental data for cracking and fracture reviewed in this paper have all been obtained under the conditions of alternating bending or reversed torsion. Numerous investigators in the past have observed an increase in fatigue strength under these conditions for a given material as the specimen size was diminished. Several older theories in regard to this effect and also to stress gradient effects are discussed, and a new theory is explained by Vitovec (53). He attributes the size and stress gradient effects to the influences of the free surface of the specimen on the strength of the surface grains.

Unfortunately there are little experimental data disclosing the effect of size of specimen on crack initiation and crack growth. In general, each investigation was concerned with but one size of specimen. In an early work, Moore (27) tested specimens of two sizes, 1 in. and 0.3 in. in diameter giving general observations regarding the number of cycles between cracking and failure. One specimen form, however, contained a large radius single fillet and the other had a rather sharp fillet. There does not appear to be sufficient data to substantiate any conclusions in regard to the effect of specimen size on crack initiation or growth in fatigue specimens.

## 3.5 Specimen Finish

deForest (36) has reported work showing the effect of surface finish on crack development in a 0.20 per cent carbon steel. As described previously in reference to his work, rotating beam testing machines were employed and Magnaflux crack detection methods were used. Data are given for the number of cycles required to develop a crack 0.10 in. long in 5/8 in. diameter test bars with various surface finishes. Tests were made on the material with the as-rolled surface, with coarse circumferential scratches made by polishing with No. 0 emery paper, and with longitudinal scratches produced by rubbing with coarse emery cloth. The specimens with the rolled surface were tested in the as-received condition. The other specimens were annealed prior to testing. Results of these tests have been plotted in various forms in Fig. 30.

A typical S-N plot of the data for $N_c$, the number of cycles to develop a crack 0.10 in. long, and for $N_f$, the number of cycles to failure, are shown in Fig. 30a. The cycle scale has been enlarged for separation of the curves. It may be observed that the finish with the coarse circumferential scratches caused the earliest initiation of a fatigue crack at a given stress level. Even the fine circumferential polish resulted in earlier initiation than the coarse longitudinal scratches. The cold rolled finish provided the longest fatigue life at a given stress level presumably not only because of the smoothness of the finish, but also because of the residual compressive stresses. The plotted points on the left of Fig. 30a show the values of $(N_f-N_c)$. It was noted in deForest's paper that the rate of growth of cracks in bars with different surfaces is dependent only on stress level since the values of $(N_f-N_c)$ for the different finishes on the annealed bars are practically the same. It is evident at the stress levels of 50 and 45 kips, however, that the average rate of growth in the cold-rolled bar is considerably slower than for the annealed condition (see the diamond shaped points in Fig. 30a). This indicates an effect of residual surface stress.

It is interesting also in this case to compare the crack data on the basis of the ratio of test stress to fatigue strength as with other data previously discussed in this review. Fig. 30b shows that the data for $N_c$ all fall in a narrow scatter band regardless of finish or treatment. It should be recalled that there was also this tendency in the crack initiation data of Bennett and Weinberg (54) for all specimens of a given aluminum alloy *regardless* of specimen form, see Figs. 26a, 27a, and 28a. The $N_c/N_f$ ratios are plotted for the various specimens in Fig. 30c. The finish which tended toward development of the earliest crack in the annealed specimens also displayed cracking at a lower percentage of the fatigue life on a stress ratio basis. This is due to the fact that, as shown by Fig. 30d, those specimens also had relatively the greater number of cycles between cracking and fracture. This is not contradictory to the $N_f-N_c$ data of Fig. 30a when it is remembered that a given value of stress ratio corresponds to a higher stress in a material of higher fatigue strength than in one of lower fatigue strength. Assuming that the specimens with the circumferential finish possessed higher actual stress in the surface due to stress concentration effects, it is noted that this trend in the graph of Fig. 30d is the same as that noted for the aluminum alloys of different specimen form, as for example in Fig. 26c.

The data of deForest (36) also give some evidence of the effect of residual stresses on crack initiation data. The residual stresses were presumably compressive in nature from the cold rolling. Examination of the data for the as-rolled condition shows that on the stress-ratio basis the $N_c$ values fall in the scatter band for the annealed material but that the $N_f$-$N_c$ values are smaller at the higher ratios and far greater at the lower ratios. Presumably then, the residual stress affects the crack growth more than the crack initiation for this basis of comparison. The number of cycles for crack growth in the as-rolled specimens was also much greater at the lower stresses when compared on the basis of the same nominal stress, as shown in Fig. 30a. Scatter and insufficient data prevent conclusions regarding the relative behavior at the higher nominal stresses.

3.6 Stress Level

The data of most investigators, except the early data of Moore (27), indicate that in both unnotched and notched specimens tested above the fatigue limit or long time fatigue strength, cracks are detectable at a smaller percentage of the total number of cycles to fracture the greater the magnitude of test stress. The actual number of cycles between fracture and cracking, however, is greater at the lower stresses. Moore reached the opposite conclusion in regard to the percentage of fatigue life remaining when cracks were observed, but his results are not in accord with those of later studies.

Various investigators have noted that for tests run at a series of stress levels, lines drawn through points on the S-N plane indicating the beginning of cracking often form a smooth curve displaced from the fracture curve at the higher stresses but becoming asymptotic to it at levels in the neighborhood of the fatigue limit or long time fatigue strength. The curves of Bennett (46), see Fig. 3, are often referred to in discussing this observation. When the studies of Lessell's and Jacques (50), and Fenner, Owen, and Phillips (51) were reported, showing cracked specimens at stresses even less than 50 per cent of the long time fatigue strength, questions arose whether the latter behavior was indeed common to all materials for all specimens and had earlier escaped detection, or only encountered with notched specimens, or was merely the result of other special factors and not the usual behavior of materials. Review of prior work in an attempt to answer these questions is desirable.

The results of deForest (36), Hempel (39), and Bennett (46), Figs. 1, 2, and 3 on unnotched steel specimens which exhibit a definite fatigue limit, indicate that the crack curve meets the fracture curve at the fatigue limit. Duce (50) also provides some evidence that Stage 1 (a stage prior to cracking ) is the only one in the fatigue process in steels to occur beneath the fatigue limit. In his tests on steels the data showed that after a few million cycles beneath the fatigue limit, both $\Delta E$ and tan $\beta$ tended toward steady values indicating no development of Stages II or III, the precrack and cracking stages, in the fatigue process.

For the aluminum alloys and the materials which do not display a distinct fatigue limit, the crack data plotted in this review were based on an arbitrary value of fatigue strength at a given number of cycles of stress. The S-N curve at the value chosen is, however, still sloping downward for these materials. The data of Bennett and Baker (50) on 2024-T4, Fig. 4 and Bennett and Weinberg (54) on 2024-T4 and 6061-T6 aluminum alloys, Fig. 5, indicate that the $N_c/N_f$ ratio tends toward 100 per cent as the number of fatigue stress cycles required to fracture a specimen increases. This is another way of saying that the curves for fracture and cracking tend to become asymptotic as the number of stress cycles for fracture increases. The apparently anomalous behavior of the 7075-T6 alloy data is perhaps due to the large scatter encountered with these data. The results on 1050-0 aluminum of Hunter and Fricke (54), Fig. 8, though showing no crack curves do indicate convergence of the curves for first slip, slip saturation, and failure. In their data for Alclad 2024-T3 aluminum alloy the curves for first slip, first crack, and failure, also appear to converge at a very great number of cycles, but to show this would require

considerable extrapolation. The data of Hunter and Fricke for 2024-T3 and 7075-T6 alloys, Fig. 9 and 10, both indicate convergence of the crack and fracture lines for large numbers of cycles.

The preceding observations lead to the conclusion that, at least in nonferrous alloys of aluminum, any fatigue stressing resulting in a crack will ultimately result in fracture of the specimen if the alternating load remains constant. As pointed out by Head (54), there is a lack of experimental evidence as to whether the possession of a fatigue limit is essentially limited to some ferrous materials. It appears that any leveling off of the S-N relationship, which occurs at the order of one million cycles for these ferrous materials, is at a much greater value of N for nonferrous materials if in fact it exists at all. It is the general opinion, however, that the fatigue of ferrous and nonferrous metals above the fatigue limit, appears to be by the same basic mechanism. Forsyth (51) found that in an aluminum 1/2 per cent silver alloy, slip lines only were observed in a specimen which ran unbroken for $150 \times 10^6$ cycles. This, however, is no proof that cracking would not have initiated had the test been continued for a sufficiently long time.

The question of fatigue cracks forming in notched specimens when stressed at values below their fatigue 'limit' is indeed an interesting one. Unnotched steel specimens display a fatigue limit, but notched specimens generally behave more like nonferrous metals displaying a continuously downward sloping S-N curve for fracture. Moore (27) showed that filleted test specimens of steel in which a fatigue crack had been started or had spread to a definite length, showed a continuing spread of such a crack to failure under subsequent cycles of stress having a magnitude of 64 per cent of the fatigue limit of the virgin specimens, but such a crack in a test piece did not spread farther under cycles of stress having a magnitude of 50 per cent of the fatiguelimit of the virgin steel. This indication that even cracked specimens possess fatigue limits is of interest but does not answer the question at hand.

Of the given investigations reviewed in this paper which dealt with crack initiation in steel specimens with stress concentration, only two resulted in the detection of cracks below the fatigue limit of the notched specimens. It is a fact that in these two studies the materials used were of lower strength than in the other studies. Furthermore, in both of these studies by Lessells and Jacques (50) and Fenner et al. (51), the specimens were prepared by turning with contour lathe tools. Lessells and Jacques polished the notch root in the specimens of one steel but not in the other and got similar results from both. Fenner et al. tested both specimens annealed after machining and specimens not annealed and obtained similar test results. The theoretical stress concentration factor of the specimen form was approximately 4.3 for the rotating beam tests of Lessels and Jacques and at least 12 for the alternating tension-compression tests of Fenner et. al. The other studies on notched steel specimens in which no cracks were found below the fatigue limit were all on materials of relatively greater strength than the two above and in no case was the theoretical stress concentration factor greater than 3.1. In addition, in most of these cases, the notch root was polished after being formed by a lathe tool.

The results of MacGregor and Grossman (52) and Bennett and Weinberg (54) on aluminum alloys and Demer and Lazan (53) on a heat-resistant alloy indicate that the fracture and crack curves approach each other as the number of test cycles becomes very large although the ratios of $N_c/N_f$ for a stress ratio of 1.0 may only be from 0.5 to 0.7. The highest stress concentration factor that was used with these nonferrous alloys was 3.1. The specimens of Demer and Lazan were prepared by grinding the notch with contour wheels. For the other studies the notches were prepared by turning and polishing.

Thus two of the studies reviewed here disclose results in sharp disagreement with the other investigations. In these studies, although the fracture curves for the notched specimens showed a sharp fatigue limit, both Lessells and Jacques (50) and Fenner et al. (51)

found cracks at stress levels of only 40 - 60 per cent of that value. Both of these studies dealt with severely notched specimens of steel. There would appear to be three possible explanations for this occurrence:

1. This is the normal fatigue behavior with a relatively low strength steel when tested under conditions of very high stress concentration, or
2. Very minute microcracks were present due to the method of specimen preparation and were detected only after growing to a certain size, or
3. Cracks formed at these very low stress levels as a result of residual stresses resulting from the method of specimen preparation.

Until further investigations are made, designed to exert some control over the variables discussed above, the precise reason for the behavior of the materials in the studies of Lessels and Jacques, and Fenner, Owen, and Phillips apparently cannot be explained in a satisfactory manner.

### 3.7 Mode of Applied Stress

The majority of the investigations on cracking in fatigue specimens has been performed in rotating beam machines. A few studies have been carried out using reversed bending machines and only two of those reviewed here were performed under conditions of alternating axial tension-compression. Duce made his studies of the fatigue process on specimens stressed in reversed torsion.

Crack data for material of the same composition, with cracks detected in a similar manner, but with the material prepared in a different manner and with the specimens of a different form are shown in Fig. 31. This graph presents the data of Bennett and Baker (50) on 2024-T4 aluminum alloy sheet in reversed bending tests of sheet specimens at constant maximum deflection, and the data of Bennett and Weinberg (54) on 2024-T4 unnotched aluminum alloy rod tested in rotating bending at constant moment. Although the number of cycles at which cracking was observed to start is smaller for the rod specimens, the percentage of fracture cycles at which cracking was observed to start is approximately the same at the different stress levels. This, of course, means that the number of cycles between first cracking and fracture was greater in the case of the reversed bending tests than for the rotating bending case. The fact that the reversed bending tests were performed under conditions of constant maximum deflection would tend to decrease the rate of growth in this case when compared with the constant moment case.

Contrasting with the above results, Fig. 21 showing the results of tests on 7075-T6 aluminum alloy rod in rotating bending by Bennett and Weinberg (54) and Hunter and Fricke (54) show that the use of different techniques for crack detection and perhaps other factors can result in even a greater difference in values for the start of cracking and for the cycle ratio for cracking and fracture at various stress levels even though the tests were performed under otherwise similar conditions. It is clear that much further work remains to be done on the study of crack initiation on the same material as affected by the mode of stress, that is, direct, flexural, or torsional.

### 3.8 Speed of Testing

The speed of testing has not been considered important enough by many investigators whose work is reported in this review, even to be reported by them. It may only be one of the lesser factors affecting crack initiation and growth, but certainly none of the results reported to date may be interpreted so as to disclose an effect of this variable.

### 3.9 Temperature of Testing

Demer and Lazan (53) are apparently the only investigators who have reported crack data for tests at various temperatures on the same material using rotating beam specimens of the same form. In Fig. 32 are shown their data in summary form taken from Fig. 20.

Examination of the graphs of Figs. 20a, b, and c discloses the following observations. For comparable stress ratio values, cracking initiates earlier and thereis a smaller number of cycles between initial cracking and fracture at the elevated temperatures as compared with room temperature. Although the scatter in $N_c/N_f$ values is considerable, there is a tendency for this ratio to become larger as the test temperature is raised.

These results may seem surprising when it is considered that the effective stress concentration factor in a given form of notched specimen decreases with increasing testtemperature, see Demer and Lazan (53). The explanation for the apparent anomaly lies in the observation that the general shapes of the S-N curves are much flatter at the elevated temperatures than at room temperatures thus providing the results outlined above when compared on a stress ratio basis.

## SECTION IV. EXPERIMENTAL DATA ON THE ACTUAL RATE OF GROWTH OF FATIGUE CRACKS

### 4.1 General

Data have been presented and discussed previously in this review in regard to the number of cycles between the first evidence of cracking and final rupture. While this information is important, it supplies knowledge only of the average rate of crack growth from the point at which a fatigue crack was first detected to final failure and does not indicate how the actual rate of growth changes with length or depth of crack during the third stage of the fatigue process in a test specimen.

There have been some experimental investigations on fatigue in which the actual growth of specific cracks was followed and measured as a function of the number of cycles. The expermental data of many of these studies will be presented and then discussed. The number of investigations for which there are available data is so small that any separation of the studies, for example into those for unnotched and notched specimens, is undesirable.

### 4.2 Experimental Results

In an early study Moore (27) recorded the rate of crack growth at stresses below the fatigue limit for specimens in which a fatigue crack had been developed at a high stress. Fig. 33 shows his data for two specimens of each of two similar steels. The specimens were cut from heat-treated railroad car axles of 0.45 per cent carbon. They were tested in rotating cantilever beam fatigue machines under conditions of constant bending moment. The specimens contained a fillet giving a theoretical stress concentration factor of 1.45. A crack about 0.10 in. long was developed in each specimen at a stress above the fatigue limit and then each was subsequently tested at the stresses indicated on the curves. The results show that the rate of growth increases with the length of the crack. Furthermore, such cracks do not continue to spread under cycles of stress having magnitudes less than approximately 50 per cent of the fatigue limit of the virgin steel.

deForest (36) measured the growth of fatigue gracks in unnotched annealed specimens of SAE 1020 steel for three different surface finishes at each of three stresses in rotating beam machines under constant moment. As pointed out previously, he showed that although the point of crack initiation at a given stress varied with the specimen finish, yet the readings of peripheral crack length in inches versus the number of cycles for crack growth *all* fell on the same curve at each of the three stress levels regardless of surface finish. These data are shown in Fig. 34. The abscissa represents the number of cycles from an arbitrary starting crack length of 0.05 inch.

Peterson (36) gives data on crack growth in grooved specimens ($K_t$= 1.9) of normalized 0.45 per cent carbon steel in rotating bending under the condition of constant moment. In Fig. 35 are his data showing a measure of crack depth rather than peripheral crack length. He obtained these data from a series of contour lines on the finally fractured specimen resulting from periodic heat tinting during fatigue tests.

Hempel (39) in tests on smooth specimens of 0.05 per cent carbon obtained the results shown in Fig. 36 for rotating bending tests at constant bending moment. Data are shown in Fig. 36a, for peripheral crack length versus number of cycles from the start of the tests for two specimens tested at the same stress. Figure 36b shows the increase in depth of crack with number of cycles from the start of crack, and Fig. 36c presents the relative areas of the crack at different numbers of cycles from the start of the crack.

Bennett (46) made crack growth measurements at two stress levels for unnotched specimens of SAE X4130 steel in rotating beam tests at constant moment. The S-N fatigue curve and the number of cycles at which cracks were first seen in these specimens are shown in Fig. 3. Two of Bennett's measurements are shown in Fig. 37 where the crack length is given in degrees versus the number of cycles of growth. The specimens employed had a minimum diameter of 0.25 inch.

Lessells and Jacques (50) measured crack growth in sharply notched specimens ($K_t$= 4.3) of 0.18 and 0.21 per cent carbon steels. They found that cracks could be developed in these specimens at stress levels far below the endurance limit in rotating beam tests under constant moment. Data from their tests are shown in Fig. 38 for the two similar steels. Cracks were developed and showed evidence of growing at stresses of only 50 per cent of the endurance limit. The crack detection method was that of sectioning and etching after cyclic stress. Cracks were found in steel B at the low stress of 10,000 psi (FS = 25,800 psi) but owing to the difficulty of having to destroy each specimen by sectioning it was not determined whether cracks at such a low stress continued to spread. The crack growth appears to be nearly logarithmic at least at the lower stresses.

In the report of their investigation on aluminum alloys, Bennett and Baker (50) show three crack growth curves for 2024-T sheet specimens tested in reversed bending under constant maximum strain at a nominal stress of 30,000 psi. Crack measurements are given as the ratio of the crack length to the specimen width. These data are shown in Fig. 39.

MacGregor and Grossman (52) include in the report of their study curves of average radial crack depth versus number of cycles for sharply notched specimens ($K_t$=3.1) of three different materials tested at stresses resulting in approximate fatigue lives for the specimens of 450,000 cycles. The tests were in rotating bending under constant moment. Their data, shown in Fig. 40 for the two aluminum alloys and the alloy steel, fall in a band which approaches linearity at least in the lower range. Crack measurements are given as the average radial crack depth in inches.

It is true that the preceding experimental data on crack growth may not include all that have been published in the fatigue literature, but it is felt that it does encompass most of it. The surprising thing is that, considering all of the investigations concerned with the fatigue problem in the past 50 years, there has been so little attention devoted to the problem of crack growth and so few recent data obtained in regard to it. It appears that the subject has never been pursued with the zeal, determination, and persistency which its importance would seem to demand.

## SECTION V. DISCUSSION OF CRACK GROWTH DATA

The experimental data on the actual rate of crack growth presented in Figs. 33 through 40 show either the peripheral length of crack on the specimen surface versus the number of cycles, or the radial depth of crack versus number of cycles. These data were taken from unnotched, filleted, and sharply notched specimens. In some of the investigations only the number of cycles from an initial arbitrary size of crack were reported leaving in question the number of cycles from the beginning of the test to the start of the crack. There is considerable variation in the size of the initial discontinuity chosen for beginning measurement. Thus available data are few and the uniformity of test conditions is not great. Nevertheless, a discussion of the results appears desirable.

### 5.1 Length and Depth of Crack

Hempel (39) reported both crack length and crack depth data for the same material. Other investigators reported either one or the other. In general, the rate of crack growth expressed in either manner increases with length or depth of the crack. Attempts at conversions from one type of measurement to the other, however, are complicated by the following factors. As noted by Bennett and Weinberg (54) the cracks in notched specimens are much shallower in proportion to their length than in unnotched specimens for the rotating bending case. The magnitude of this effect is dependent upon the degree of stress concentration. In addition, as discussed by Peterson (50), in the case of an unnotched specimen a crack progresses across the section until rupture occurs with a segmental area bounded on one side by the shaft periphery. However, in specimens with stress concentration the crack tends to penetrate concentrically with a final rupture area enclosed by the cracked area and approximately circular or elliptical in form. The higher the stress level the more centrally located is the final rupture area.

### 5.2 Variation at Same Stress

Hempel (39) has shown crack curves for two specimens tested at the same stress, Fig. 36a. Superposition of these indicates that, although the initial portion of these curves is similar, there is dissimilarity in slope in the later portions of the curves. When cracks reach an appreciable magnitude, differences may be expected in their rate of growth depending upon the manner in which two or more shorter lengths of crack may combine to form a larger spreading crack.

### 5.3 Effect of Stress Level

The effect of stress level is shown by the curves of Moore, deForest, Peterson, Hempel, Bennett, and Lessells and Jacques, Figs. 33 through 38. In all cases the actual rate of growth increases with stress level in tests above the fatigue limit of the material.

Moore (27) in seeking an answer to the question whether cracks initiated above the fatigue limit could propagate at stress levels below the fatigue limit in steel specimens observed no growth when the stress was less than 50 per cent of the fatigue limit, see Fig. 33. Lessells and Jacques (50) found growth in sharply notched steel specimens tested continually at stresses of 50 per cent of the fatigue strength for a large number of cycles. As pointed out earlier in this paper, however, it has only been in steel specimens with extremely high stress concentration factors where cracks have been reported as found to initiate and grow at stresses below the fatigue limit. As Fig. 38 shows, the observed rate of growth at stresses in the neighborhood of 50 per cent of the fatigue limit is very small.

## 5.4 Manner of Testing

All of the available data on the actual rate of crack growth in metals during fatigue appears to have been obtained under the conditions of rotating bending or reversed bending. There are none reported here for the conditions of direct axial tension-compression or reversed torsion. The type of stress is, of course, the same in the axial case as in the bending case, but the stress gradient is not the same. It is certainly to be expected that the rate of crack growth in the two cases would be considerably different even for unnotched specimens, not only because of the initial stress gradient, but also due to the changes accompanying the progress of the crack through the test piece. There are also these differences between rotating bending and reversed bending. The case of torsion presents still other stress conditions.

Numerous investigators have observed changes in the stiffness of fatigue test specimens during the course of fatigue tests even before the detection of cracking. This has been attributed to changes in the dynamic modulus of elasticity. For stress levels at which the change in modulus is appreciable, differentiation should be made between fatigue tests performed at constant maximum stress and those performed at constant maximum strain. These two cases, along with the case of constant maximum moment, present three types of conditions under which fatigue tests may be performed. It is only reasonable to expect that both crack initiation and rate of crack growth will be different in each of these cases.

It is clear that more experimental data are needed to determine the effect of type of stress imposed as well as the condition under which the test is performed.

## 5.5 Empirical Formulas for Crack Growth

Bennett (46) noted that his crack growth curves, see Fig. 37, appeared to start from a finite value of crack length rather than from zero. He explained that the fact that small though numerous cracks frequently have been observed at stresses considerably in excess of the fatigue limit suggests that the large value of the initial crack length indicated in Fig. 37 is associated with stresses nearer the fatigue limit. He found that the crack length L could be expressed by the equation

$$\text{Log } (L - C) = \alpha N \qquad (1)$$

where C and $\alpha$ are constants, the latter dependent on stress, and N is the number of cycles of growth. He plotted (L - C) curves to a logarithmic scale versus number of cycles to a linear scale and obtained straight line relationships. Such a plot is shown in Fig. 41a for one of the curves of Fig. 37. Further, it was shown that when this was done for various nominal stress values, the slope of the crack growth curves was found to be a simple function of stress as indicated in Fig. 41b. The finite crack length for the apparent start of cracking at the stress level slightly above the knee of the S-N curve was found by Bennett to be approximately six degrees of circumferential length. For the 0.25 inch diameter specimen this corresponds to a length of approximately 0.013 inches. Bennett and Baker (50) did not employ the relationship shown in Equation 1 in their work on aluminum alloys. Neither was this used in the recent work by Bennett and Weinberg (54).

Lunchick (52) presented a theory of fatigue based on a statistical distribution of grain size. His theory recognized that the finite fatigue life is influenced by the rate of propagation of the microscopic cracks that are formed in the fatigue process. The rate at which the microscopic cracks are propagated to visible size was determined empirically with reasonable justification by past experimental data (viz., Moore (27), see Fig. 33), by assuming a linear relationship between the relative stress level and the logarithm of the number of cycles to failure from microscopic crack initiation. The factors of mean grain size, uniformity in grain size distribution, and stress-volume were considered in his expression for microscopic initiation but were not analyzed in regard to crack growth. Examination of the data for $(N_f - N_c)$ in Figs. 1 through 20 of this review also show the

general linear relationship between stress level and log $(N_f - N_c)$, but in some cases there is rather large scatter. Lunchick presented his theory to indicate the major factors involved and to show an analytical method of attacking the problem. His analytical approach was more detailed in reference to crack initiation than with crack growth. He did not support his conclusions with close experimental evidence.

## 5.6 Theoretical Expression for Crack Growth

Most of the fatigue theories assume that the major part of the fatigue life of a specimen is completed before the formation of a crack which once formed, grows rapidly to complete fracture. Some of the evidence presented in this review indicates that under certain conditions the crack is formed in the early stages of the test and then grows slowly for a large number of cycles. Head (53, 54) has proposed a model of a fatigue crack which has a rate of growth in satisfactory agreement with currently available data on the growth of fatigue cracks. The model and idealized representation of a crack for the growth theory are shown in Fig. 42. The representation consists of rigid-plastic elements A of length $a_o$, which yield at a stress $S_y$, and work harden linearly until fracture at strain $e_f$; elastic elements B, with modulus E; and shear elements C, with elastic shear modulus E/2. Head makes the following assumptions:

1. The medium is of infinite extent,
2. The applied stress remains constant as the crack grows,
3. The medium is homogeneous,
4. The crack is long compared with its width, and
5. The crack is growing under alternating tension-compression stresses.

If L is the crack length, S the applied stress, N the number of cycles, and $N_\infty$ the number of cycles to failure, he found that

$$L^{-1/2} = \frac{S^3}{(Sy-S)^2} \cdot \left[ \frac{1}{24\sqrt{2}\ Ea_o^{\ 1/2} e_f} \right] \rightarrow (N_\infty - N) \qquad (2)$$

This relationship predicts that a plot of $L^{-1/2}$ versus N should give a curve whose slope is a function of the yield stress of the material and the current level of alternating stress. However, L should be independent of the previous stress level.

The assumptions given above will be satisfied approximately provided that the crack is small in relation to the size of the specimen but large in comparison with the microstructure. It is clear that in a constant maximum moment bending test, the applied stress increases as the cracked area grows to appreciable magnitude. Conversely in a constant maximum strain test it would decrease. An additional point is that there should be only one fatigue crack present if the assumed conditions are to apply. This condition is approximately realized in steel specimens tested at stress levels near the fa-fatigue limits observed by Bennett (46). In some tests of aluminum alloys, see Head (54), it was observed that a large number of interacting cracks are formed. The stress level for these observations is not given. It has been observed elsewhere (unpublished observations of the Mechanics and Materials Department, University of Minnesota) that in aluminum alloys also, the number of cracks formed decreases at the lower stresses approaching the long time fatigue strength of the material. That the crack is long in comparison with its width is an assumption closely met by the fatigue cracks. The length of the first observed cracks relative to the microstructure of the material depends upon the grain size of the latter. In almost all cases there has been no information supplied by the crack growth investigators relative to this characteristic of their materials. Growth under alternating tension-compression stresses is, of course, a condition met by reversed direct stress tests and also by rotating bending and alternating bending tests.

## 5.7 Proof of Theory

The experimental data of Moore (27), deForest (36), Hempel (39), and Bennett (46) were all obtained from tests on steel in rotating bending at stresses near the fatigue limit. Head (54) used the data of all but Hempel to check his theory of crack growth replotting their data in the form of $L^{-1/2}$ versus number of cycles of crack growth as shown in Figs. 44 through 46. The data of Hempel have also been included here. Clearly the experimental points do show a strong tendency to lie on a straight line as predicted by the theory of Head. Part of the scatter in deForest's data may be due to the superposition of measurements on specimens with three different surface finishes.

Moore's data were given for growth at a low stress level for cracks developed above the fatigue limit. The data of the other investigators were for specimens tested at a given stress. The abscissas, except in the case of Hempel's data, are for the number of cycles of crack growth, not the number of cycles from the start of the test. To satisfy the straight line relationship the origin of N is arbitrary.

Head observes that if the relation between $L^{-1/2}$ and N is linear as suggested by the above data, then the measured crack growth curve can be extrapolated to earlier stages of the test, that is, before the crack was actually seen. Head made the extrapolation for one of the growth curves of Fig. 37, for S= 46,000 psi, and carried it back to the start of the test, an extrapolation of over two log cycles. This indicated that the crack could never have been shorter than $5 \times 10^{-4}$ inches. Head says that extrapolation of deForest's data in the same manner shows a minimum crack length of approximately $10^{-3}$ inches. Presumably these extrapolations were only approximated, for in the reports of the investigations by both Bennett and deForest it is difficult to determine the number of cycles at which the crack growth readings were started.

The minimum length values represent the size of crack which, if present at the beginning of the fatigue test, would grow to fracture the specimen in the observed number of cycles. Of course, if developed at some stage during the test, the crack would be correspondingly longer. Head points out, however, that due to the observed rate of growth, even if the crack were formed halfway through the test, it would need be only three or four times the minimum length.

These observations made by Head on the supporting data are interesting and perhaps should be investigated further. Table III shows the approximate length of the cracks at the beginning and end of the reported crack growth curves for the experimental data of Figs. 33 through 37. The circumferential lengths of the specimens employed are also given. It would appear from Table III that the experimental data satisfy the L-N relationship suggested by Head's derivation over a much greater range of crack lengths than the assumptions of his theory would predict, since the crack lengths were so long in relation to the specimen circumference at the end of the observations.

Some previously unpublished data obtained by Blatherwick (55) at the University of Minnesota from constant maximum strain tests in reversed bending on hollow specimens of SAE 1020 steel indicate that the L-N relationship discussed above is also satisfied to much higher values of $L^{-1/2}$, or much smaller crack lengths, than is indicated by any previously published data. His data are shown in Fig. 47. Blatherwick obtained crack growth curves starting at approximately 0.005 inch using a microscope for crack length measurements. Extrapolating his data for this one crack gave a minimum crack length at zero cycles of approximately $8 \times 10^{-4}$ inches which compares closely to corresponding values given above.

Head points out that if the L-N relationship obtained by his theory is actually valid, then the cracks must either be present in all materials initially or else they must initiate at a certain appreciable finite length which the data indicate to be of the order of two thousandths of an inch. Machlin (48, 49) and Shanley (52)

have theorized that fatigue is merely the growth of cracks present initially in the material. Head cites four arguments against this hypothesis. These are:

1. Data of deForest (36) indicate that the rate of growth of cracks is dependent upon stress level and independent of surface finish although the fatigue life is greatly changed by differences in surface finish.
2. Data of Moore (27), for the growth below the fatigue limit of cracks initially started above the fatigue limit, show that crack initiation and crack growth are two separate processes. The fatigue limit must first be exceeded to initiate a crack, which once initiated can grow at smaller values of stress.
3. There is no evidence that there invariably exist cracks of the order of $5 \times 10^{-4}$ inches long in all metals and alloys regardless of their preparation.
4. Bennett (46) found the number of fatigue cracks visible at the end of a fatigue test to be a function of the test stress. If there were always the same number of cracks present initially there should always be the same number present at fracture, but this is not the case. It therefore appears that the cracks form during the test.

Head's theory predicts that the factor giving the slope of the line for the plot of $L^{-1/2}$ versus N is:

$$\frac{dL^{-1/2}}{dN} = -\frac{S^3}{(Sy-S)^2} \cdot \left[\frac{1}{24\sqrt{2}\ Ea_o^{1/2} e_f}\right] \qquad (3)$$

Making certain assumptions and using the data of Bennett (46), Head obtained a theoretical value for this slope which agreed reasonably well with the experimental value.

A recent note by McClintock and Ryan (54) reports some tests designed to determine whether the slope is dependent on the stress level and independent of past history as indicated above. They reasoned that according to Head's theory:

$$\frac{dL^{-1/2}}{dN} \cdot \frac{(Sy-S)^2}{S^3} = -\frac{1}{24\ \sqrt{2}\ Ea_o^{1/2} e_f} = K \qquad (4)$$

Then, assuming no appreciable change in E, the value of this K should be constant. That is, the slope of the curves for $L^{-1/2}$ versus N should be dependent only on the stress level of the test for any given material. They planned tests to check this hypothesis by making crack growth studies on specimens subjected to varying levels of stress. They used 1/4 inch cold rolled B1112 steel with specimens having a minimum diameter of 0.145 in. with a 1 in. longitudinal radius of curvature. The work was done in rotary bending at 6000 rpm and an initial stress of 80,000 psi. These investigators measured crack growth at this initial stress stopping the tests frequently for microscopic measurement at 30X. The specimens were subsequently run at lower stress levels to minimize work hardening of the specimen as a whole during crack growth. Data were obtained at each stress level for L as a function of N. Their results were not in a form readily reproducible here.

McClintock and Ryan found that, except for a brief "incubation period" after changes in stress, the slopes of the curves of $L^{-1/2}$ versus N were fairly constant for any stress level and reasonably independent of stress history. They determined that in almost all cases the uncertainty interval for the factor K of Equation 4 was within a factor of 1.5 times the value $-2.5 \times 10^{-9}$ in.$^{3/2}$ lb. Thus they noted that Head's theory seems to explain most of the effect of stress level on the rate of crack growth. However, they found that the magnitude of K is not satisfactory since a theoretical value determined by them was between $-0.22 \times 10^{-7}$ and $-2.2 \times 10^{-7}$ in.$^{3/2}$ lb.

McClintock and Ryan propose examining some of the assumptions of Head's theory suggesting that the width of the plastic region may not be constant as the crack proceeds and that the shear elements should perhaps have plastic, as well as elastic properties. They point out, in addition, that provision should be made for carrying a compression load across the crack. They observe that Head's theory predicts that under static loading of a work hardening material, a crack will propagate to failure when the mean stress reaches the yield point, which is not observed in tensile tests.

In spite of its shortcomings, Head's theory is the best one suggested to date for dealing with the actual rate of growth of fatigue cracks. It satisfies experimental data quite closely and points the way for future investigations on the subject. As Head points out, the pressing need at the present time is for more accurate information on the exact interval during the fatigue process when the crack forms.

## SECTION VI. SUMMARY AND CONCLUSIONS

There are some experimental data available in the literature on fatigue which are concerned with the initiation and growth of fatigue cracks. These have been obtained on a variety of materials from pure metals to high strength alloys, using diversified crack detection methods, in fatigue tests conducted in many cases under dissimilar test conditions. These have been reviewed and analyzed in this paper. An attempt has been made to consider the various factors involved and, where possible, to determine their effects.

### 6.1 General Factors

Analysis of the results of the studies reviewed here reveals several significant facts which are listed below.

1. There are usually three recognizable stages in the fatigue process in ductile metals, namely:
   a. An initial stage of overall deformation and work hardening subsequently followed by slip,
   b. An intermediate stage in which the slip lines thicken and intensify into slip bands usually in the direction of greatest shear stress. This finally results in rupture of the crystal lattice and the appearance of submicroscopic cracks, and
   c. The final stage involving coalescence of the submicroscopic cracks to form visible spreading cracks resulting finally in fracture.
2. The lengths of the three stages are dependent upon many factors. Of primary importance among these are the:
   a. Nature of the test material,
   b. Character of the specimen,
   c. Stress level of the test, and
   d. Manner of testing.

### 6.2 Specific Behavior

A convenient method for comparing the crack and fracture fatigue data for materials of widely different strengths is to make the comparison on the basis of the ratio of test stress or strain to the fatigue strength or fatigue strain at an arbitrarily chosen number of cycles. For materials or specimen forms displaying a sharp fatigue limit, this value may be used for the arbitrary fatigue strength. The comparisons which follow are all made on this stress ratio basis.

In many cases the observations of this review are based on rather limited data obtained by various investigators under different test conditions. Therefore the conclusions below are not to be regarded as definitely established behaviors. The experimental

Peterson, R. E., "Interpretation of Service Fractures," -"Handbook of Experimental Stress Analysis," John Wiley & Sons, pp. 593-635, New York, 1950.

Peterson, R. E., "Stress Concentration Design Factors," John Wiley & Sons, Inc., New York, 1953.

Russell, H. W. and Welcker, W. A., "Damage and Overstress in the Fatigue of Ferrous Materials," Proc. Am. Soc. Test. Mat., Vol. 36, Part II, pp. 118-135, discussion pp. 135-138 (1936).

Shanley, F. R., "A Theory of Fatigue Based on Unbonding During Reversed Slip," The Rand Corporation, Santa Monica, California, 1952.

Sinclair, G. M. and Dolan, T. J., "Some Effects of Austenitic Grain Size and Metallurgical Structure on the Mechanical Properties of Steel," Proc. Am. Soc. Test. Mat., Vol. 50, pp. 507-616 (1950).

Sinclair, G. M. and Dolan, T. J., "Use of a Recrystallization Method to Study the Nature of Damage in Fatigue of Metals," Technical Report No. 21 of the Behavior of Materials Under Repeated Stress, Contract N6ori-71, T. O. 4, February 1951. Dept. of Th. and Appl. Mech., University of Illinois, February 1952.

Timoshenko, S. and Dietz, W., "Stress Concentration Produced by Holes and Fillets," Trans. Am. Soc. Mech. Eng., Vol. 27, pp. 210-220, (1925).

Vitovec, F. H., "The Effect of Specimen Surface as a Discontinuity in Fatigue Phenomena," Wright Air Development Center Technical Report 53-167, September 1953.

TABLE I

FACTORS RELATING TO FATIGUE CRACK INITIATION AND PROPAGATION

- Definition of "crack initiation"
- Definition of "failure"
- Detection method employed
- Test material
  - Crystal structure
  - State of purity
  - Number of phases
  - Grain size
  - Homogeneity
  - Strength level
  - Thermal treatment
- Specimen characteristics
  - Form
  - Size
  - Surface finish
  - Residual stresses
- Mode of Fatigue Stressing Employed
  - Alternating tension-compression
  - Reversed flexure
  - Rotating bending
  - Reversed torsion
  - Combined stress tests
- Manner of Testing
  - Constant stress amplitude
  - Constant strain amplitude
  - Constant load or moment amplitude
- Stress level of test
- Speed of test
- Temperature of test

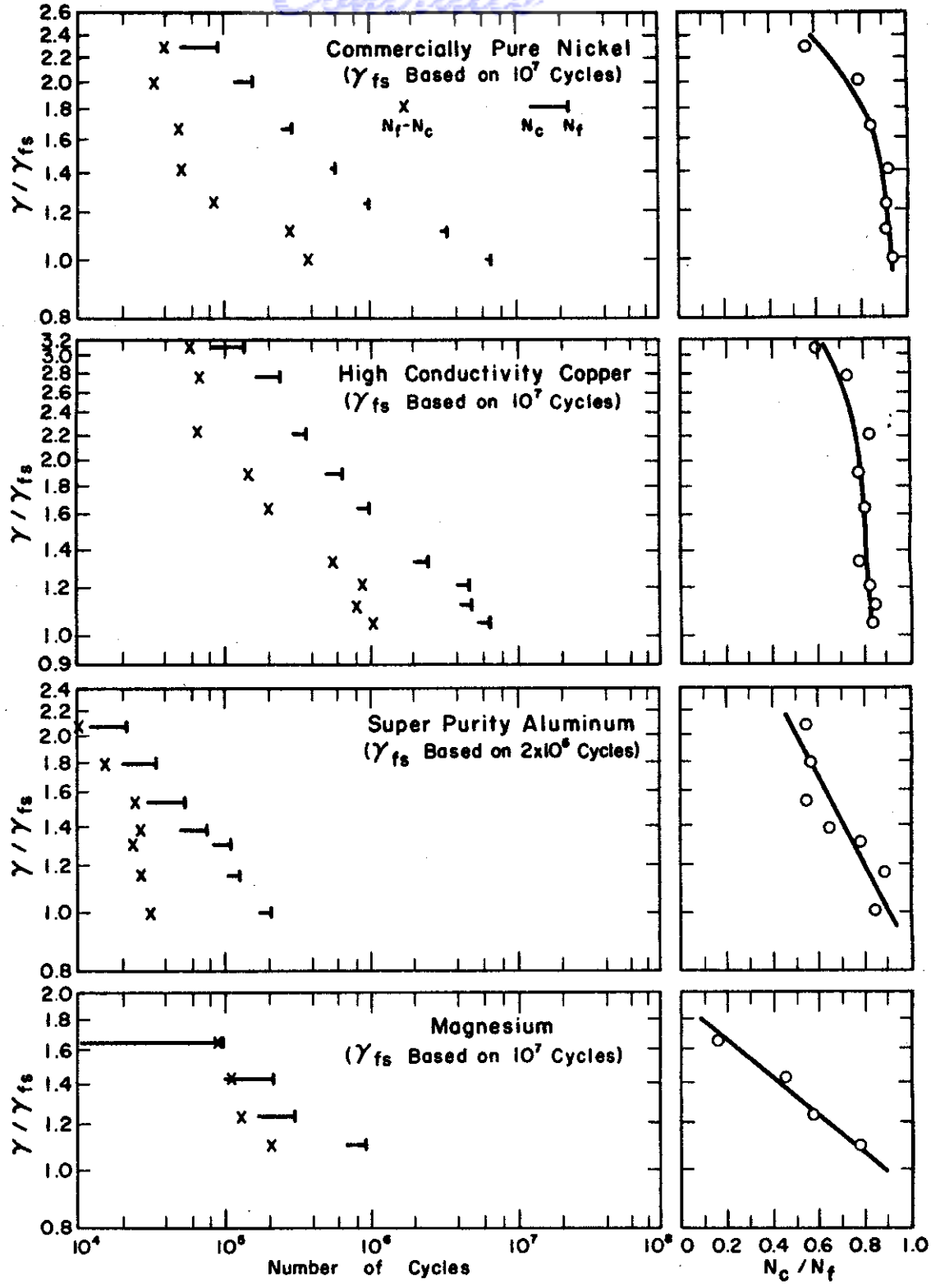


Fig. 6.--Duce (50). Unnotched 0.06 in. Diameter Specimens of Four Pure Metals Tested in Reversed Torsion With Constant Maximum Strain. Crack Detection by Damping and Elasticity Measurements.

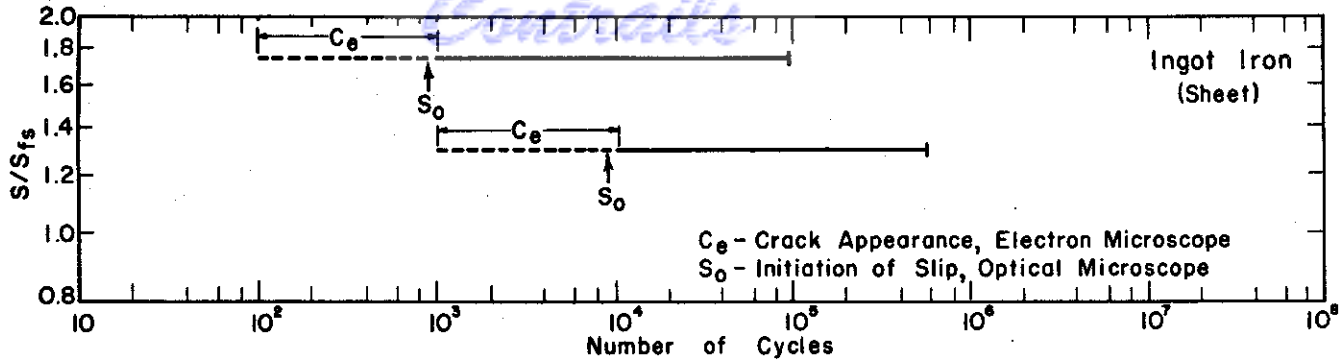


Fig. 7.--Love (52). Unnotched Sheet Bending Specimens of 3/16 in. Minimum Width Ingot Iron Tested in Reversed Bending With Constant Maximum Moment. Crack Detection by Electron Microscope.

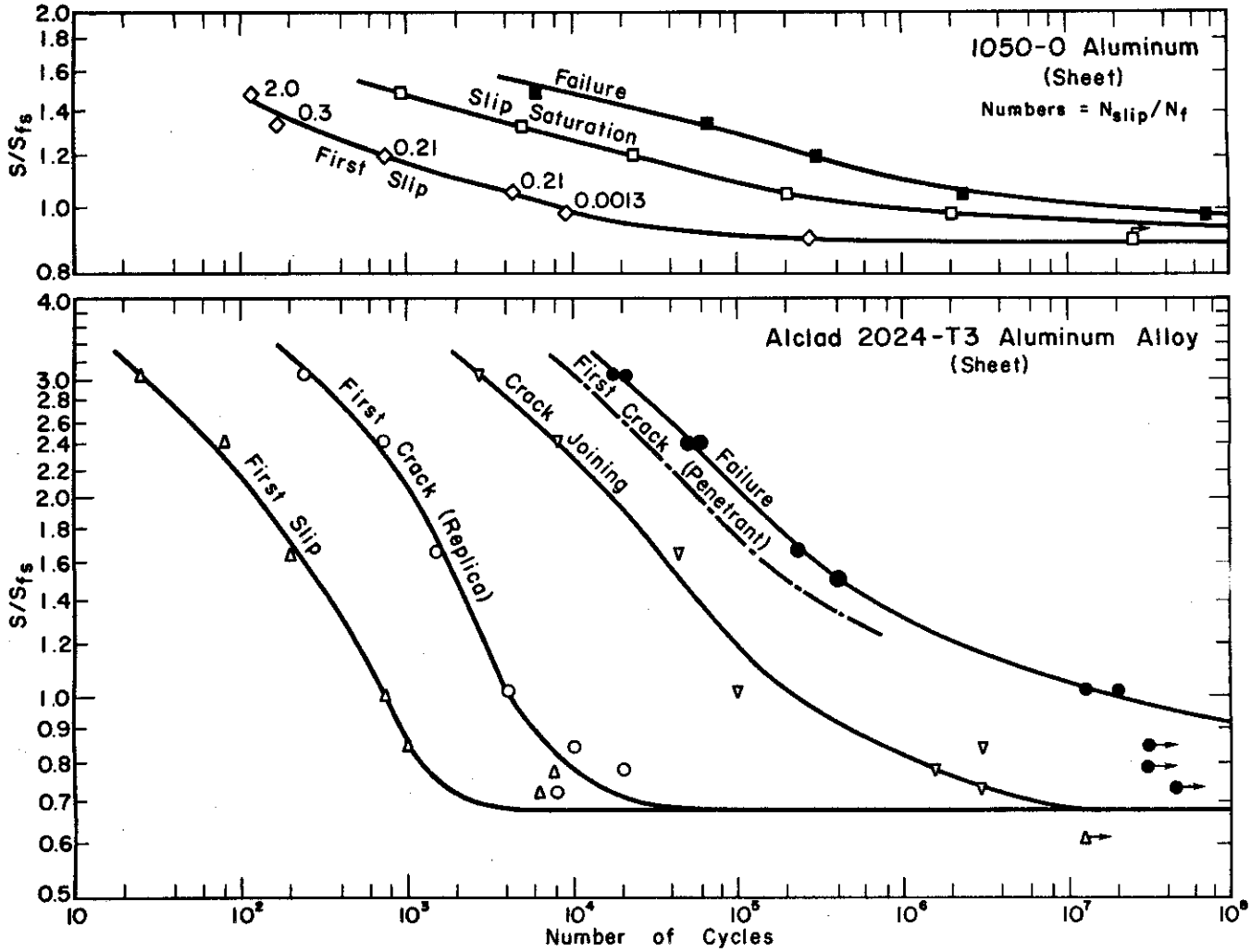


Fig. 8.--Hunter and Fricke (54). Unnotched Sheet Specimens of 1050-0 Aluminum and Alclad 2024-T3 Alloy Tested in Reversed Bending With Constant Maximum Deflection. Crack Detection by Electron Microscope, Plastic Replica - Optical Microscope, and Dye Penetrant Methods.

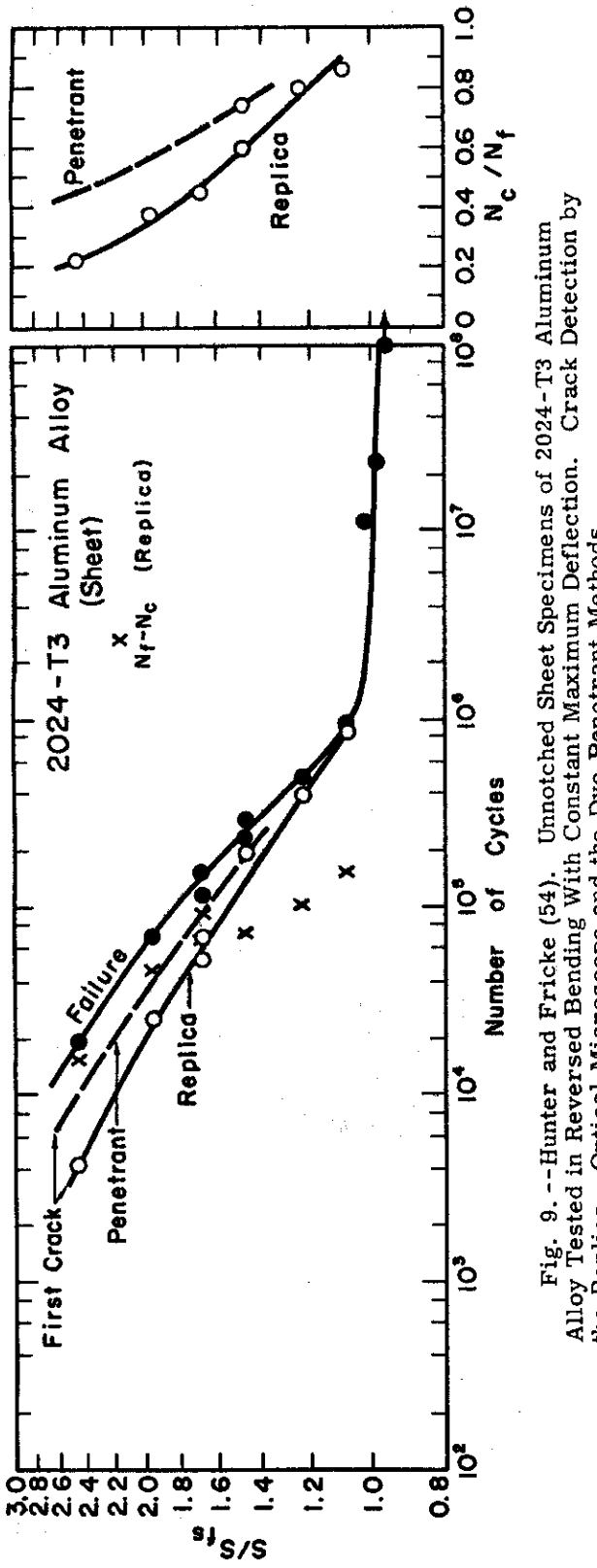


Fig. 9.--Hunter and Fricke (54). Unnotched Sheet Specimens of 2024-T3 Aluminum Alloy Tested in Reversed Bending With Constant Maximum Deflection. Crack Detection by the Replica - Optical Microscope and the Dye Penetrant Methods.

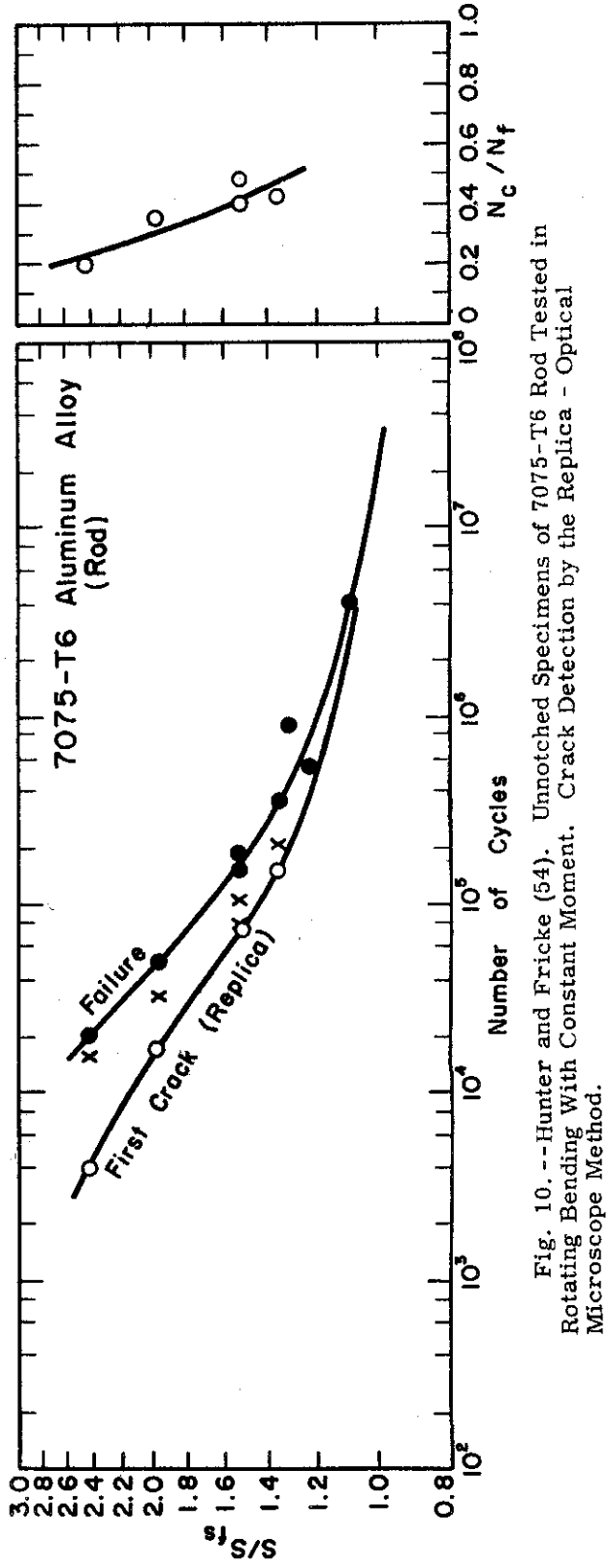


Fig. 10.--Hunter and Fricke (54). Unnotched Specimens of 7075-T6 Rod Tested in Rotating Bending With Constant Moment. Crack Detection by the Replica - Optical Microscope Method.

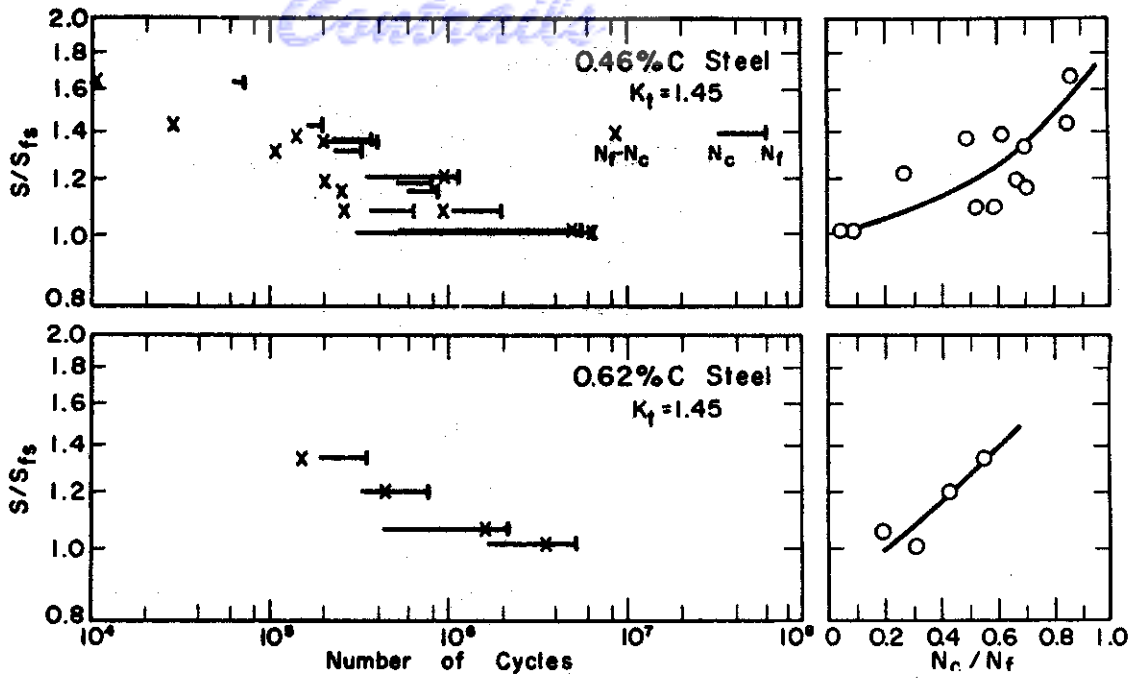


Fig. 11.--Moore (27). One Inch Diameter Specimens With 3/16 in. Radius Fillet, Cut From Heat Treated Steel R. R. Car Axles, Tested as Rotating Cantilever Beams With Constant Moment. Crack Detection by Oil-Whiting Test and Low (10 X) Power Microscope.

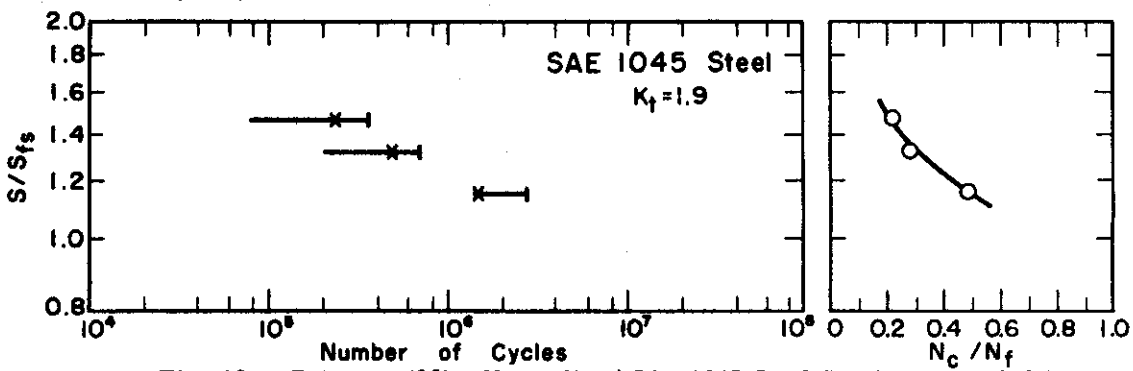


Fig. 12.--Peterson (36). Normalized SAE 1045 Steel Specimens, 0.812 in. Diameter, Containing Semicircular Circumferential Groove 1/16 in. Radius, 1/16 in. Deep, Tested in Rotating Bending With Constant Moment. Crack Detection by Heat Tinting.

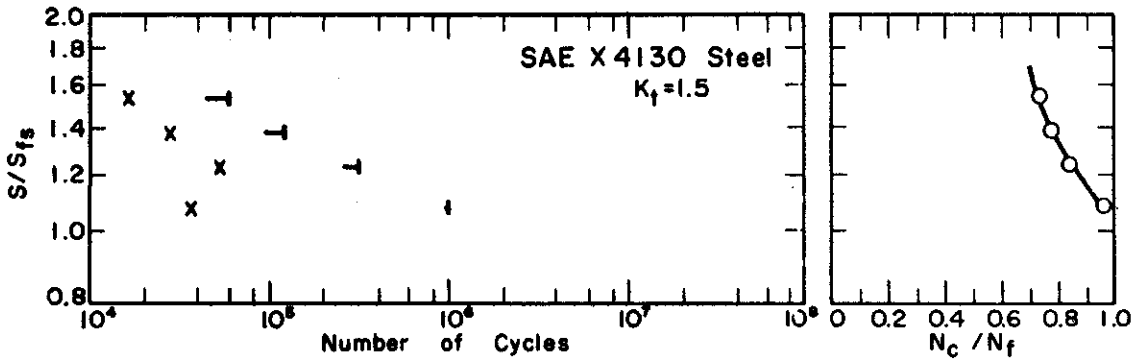


Fig. 13.--Bennett (46). Normalized SAE X4130 Specimens, 0.35 in. Diameter, Containing Semicircular Circumferential Groove 0.05 in. Deep, Tested in Rotating Bending With Constant Moment. Crack Detection by Deflection Method Followed by Examination Under Optical Microscope.

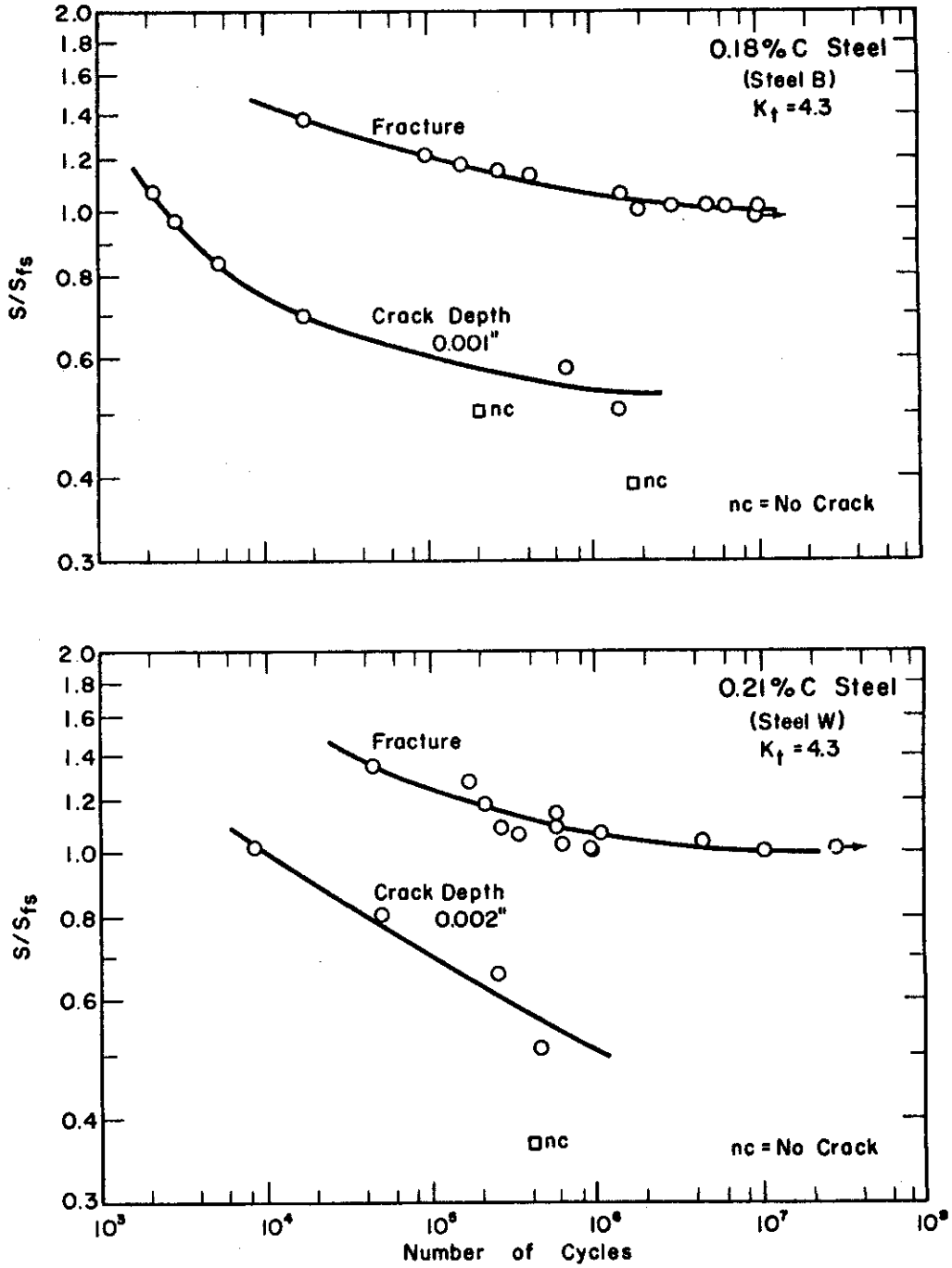


Fig. 14.--Lessells and Jacques (50). One-Half Inch Diameter Specimens, Containing a 45° Circumferential V-Notch 0.05 in. Deep With 0.005 in. Root Radius, of Semi-Killed, Hot-Rolled Ship Steels Tested in Rotating Bending With Constant Moment. Crack Detection by Longitudinal Sectioning, Polishing, Etching, and Examination With Optical Microscope.

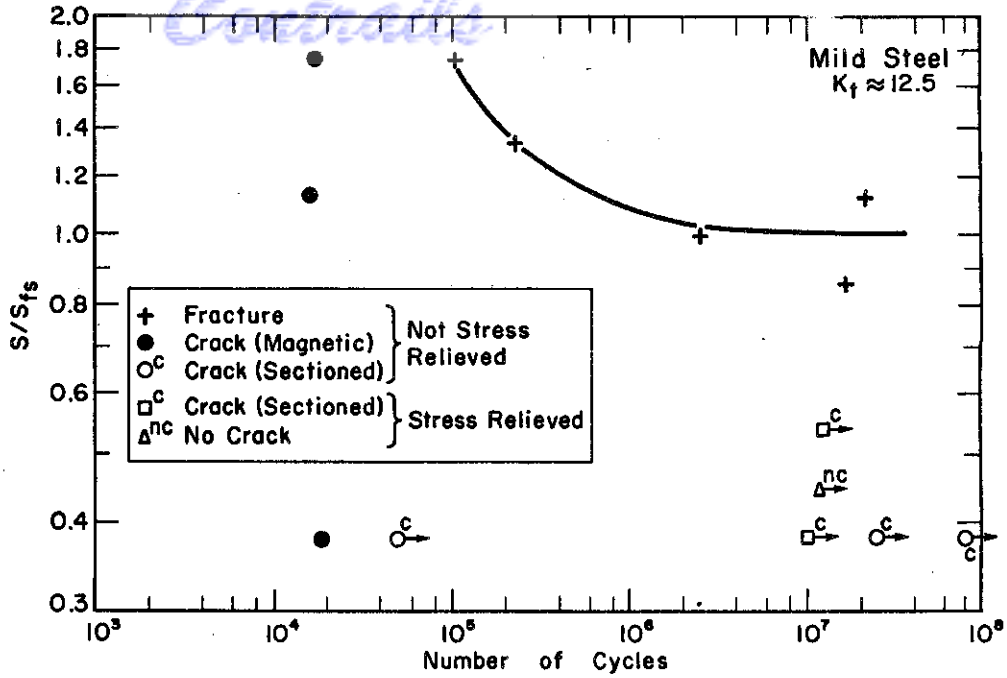


Fig. 15.--Fenner, Owen, and Phillips (51). Normalized Mild Steel Specimens, 1.7 in. Diameter, With a Circumferential V-Notch 0.2 in. Deep of 55° Included Angle With Root Radius of 0.002 in., Tested in Alternating Tension-Compression With Constant Maximum Force. Crack Detection by a Portable Magnetic Crack Detector in Conjunction With Longitudinal Sectioning and Examination by Optical Microscope.

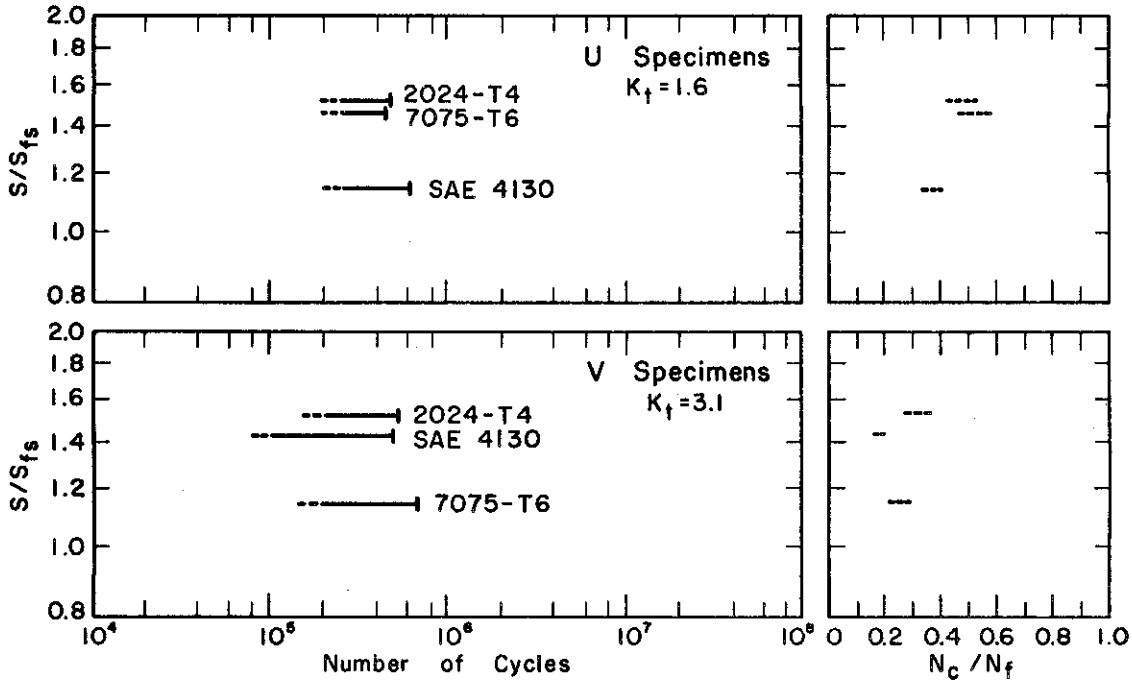


Fig. 16.--MacGregor and Grossman (52). Specimens 0.480 in. Diameter With Either a U-Notch, 1/16 in. Deep With a 1/16 in. Radius, or a 45° V-Notch, 1/16 in. Deep With a 0.010 in. Root Radius, of an Alloy Steel and Two Aluminum Alloys Tested in Rotating Bending With Constant Moment. Crack Detection by Slow Bend Test and Fracture Examination or Longitudinal Sectioning and Examination Under Optical Microscope.

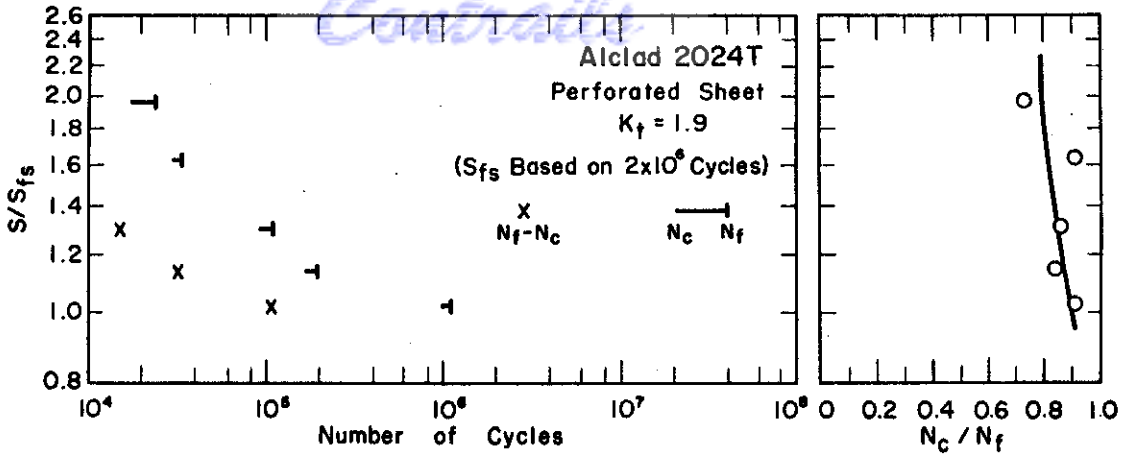


Fig. 17. --Foster (47). Flat Strip Specimens of Alclad 2024-T Aluminum Alloy Sheet, 0.2 in. Thick and 1-1/2 in. Wide With Perforated 1/4 in. Diameter Hole, Tested in Reversed Bending. Crack Detection by Fracture Wire Technique.

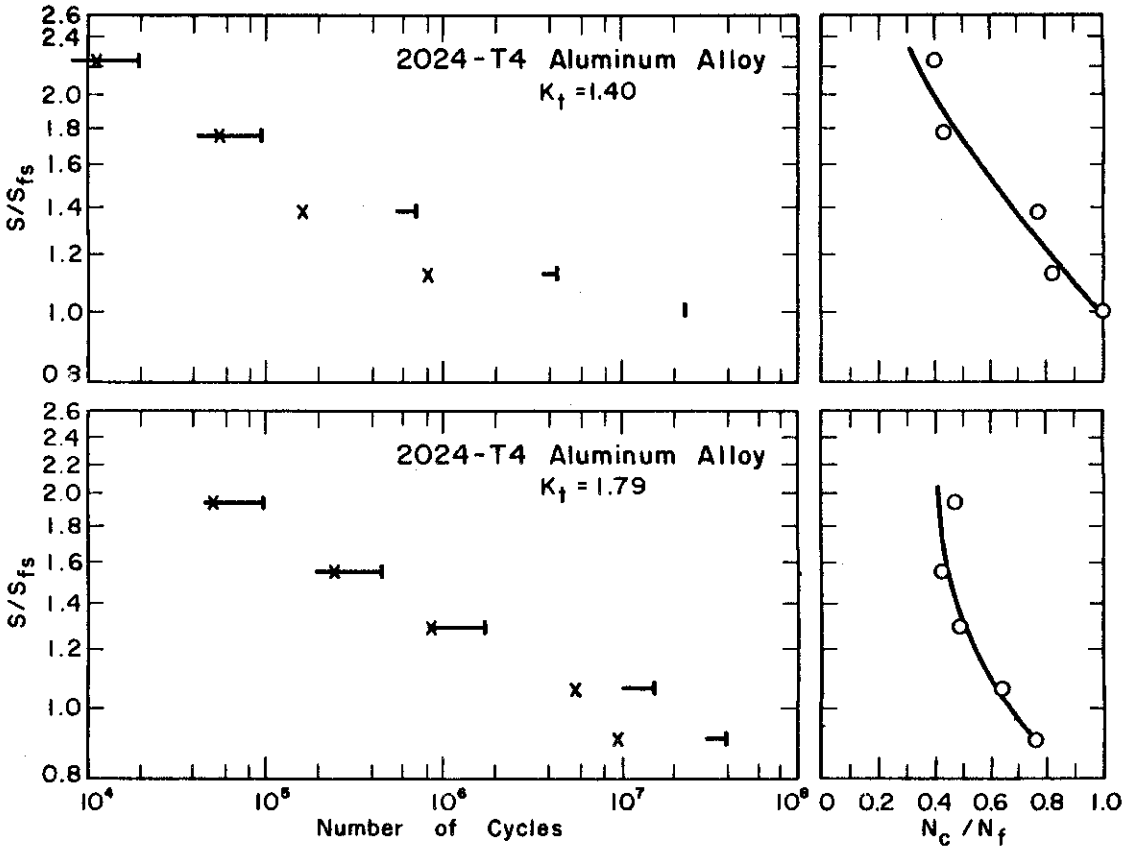


Fig. 18. --Bennett and Weinberg (54). Cylindrical Specimens 0.030 in. Diameter, of 2024-T4 Aluminum Alloy, With a Fillet Radius of 1/16 in. ($K_t$ = 1.40), or a Radius of 0.025 in. ($K_t$ = 1.79), Tested in Rotating Bending With Constant Moment. Crack Detection by Deflection Method and Examination by Optical Microscope.

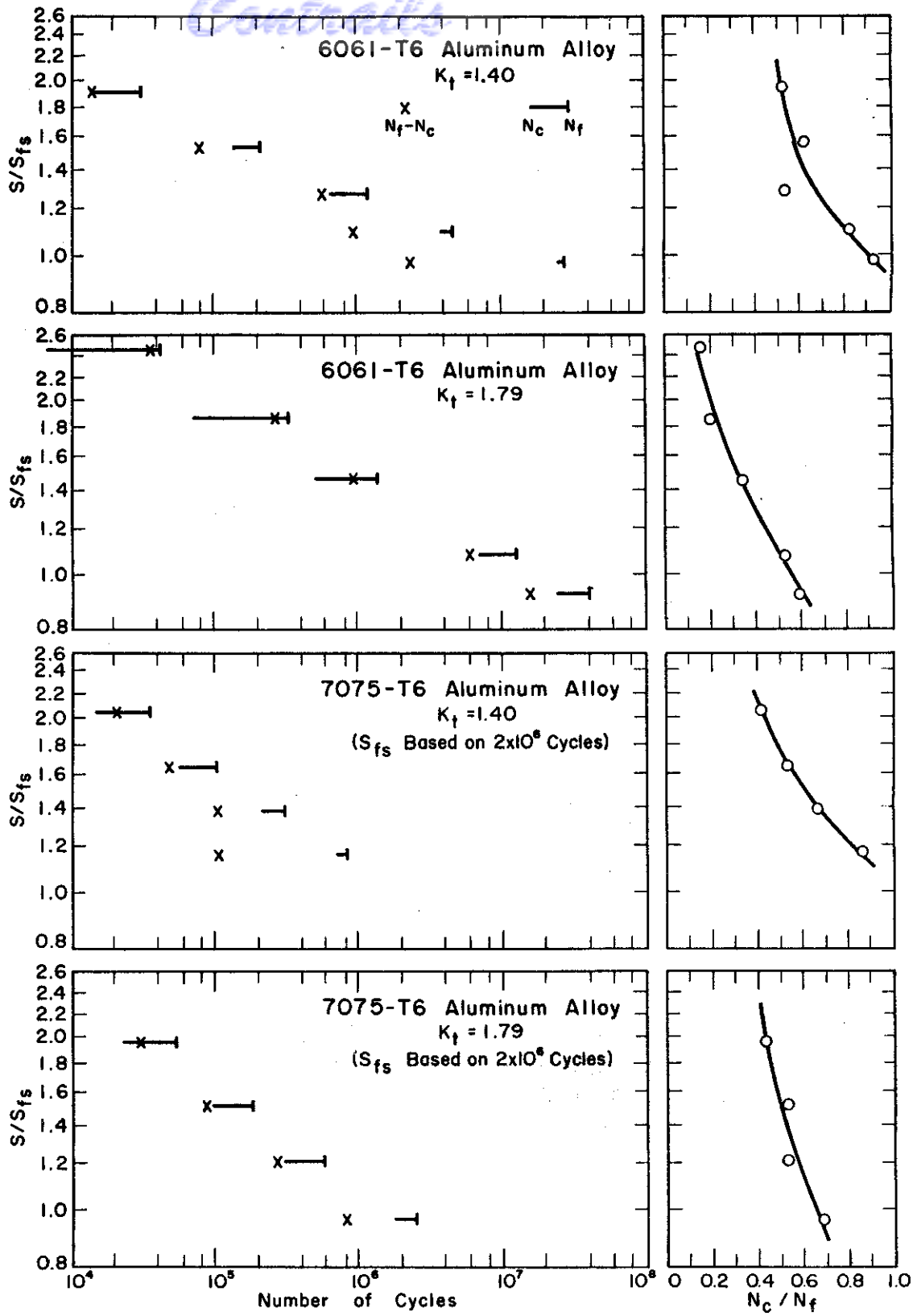


Fig. 19.--Bennett and Weinberg (54). Cylindrical Specimens, 0.30 in. Diameter, of 6061-T6 and 7075-T6 Aluminum Alloys, With a Fillet Radius of 1/16 in. ($K_t$ = 1.40), or a Radius of 0.025 in. ($K_t$ = 1.79), Tested in Rotating Bending With Constant Moment. Crack Detection by Deflection Method and Examination by Optical Microscope.

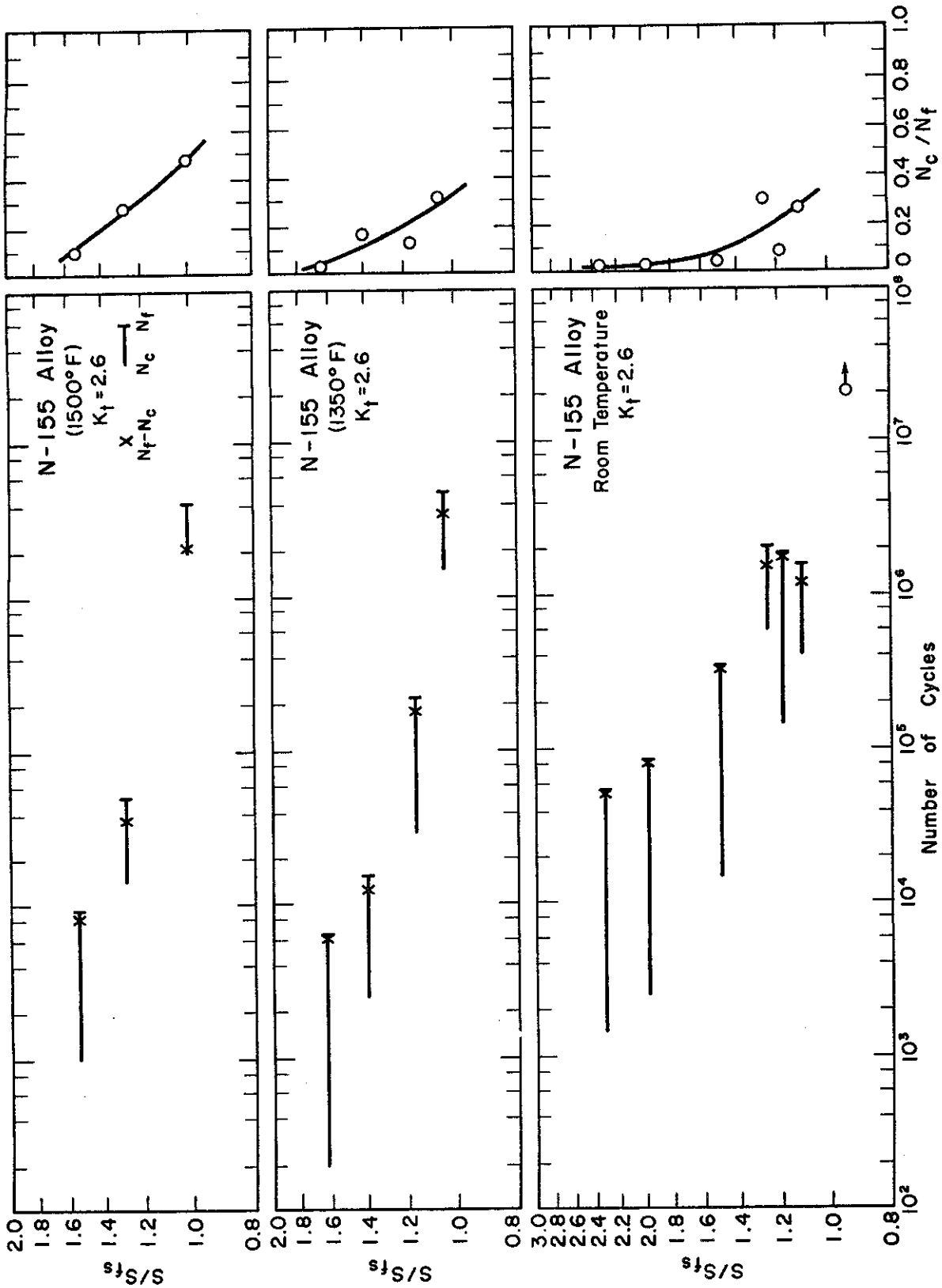


Fig. 20.--Demer and Lazan (53). Cylindrical Specimens, 0.55 in. Diameter, With a 45° V-Notch, 0.122 in. Deep With a 0.010 in. Root Radius, of the Heat Resistant Alloy N-155, Tested at Three Temperature Levels as Rotating Cantilever Beams With Constant Moment. Crack Detection by a Deflection Method.

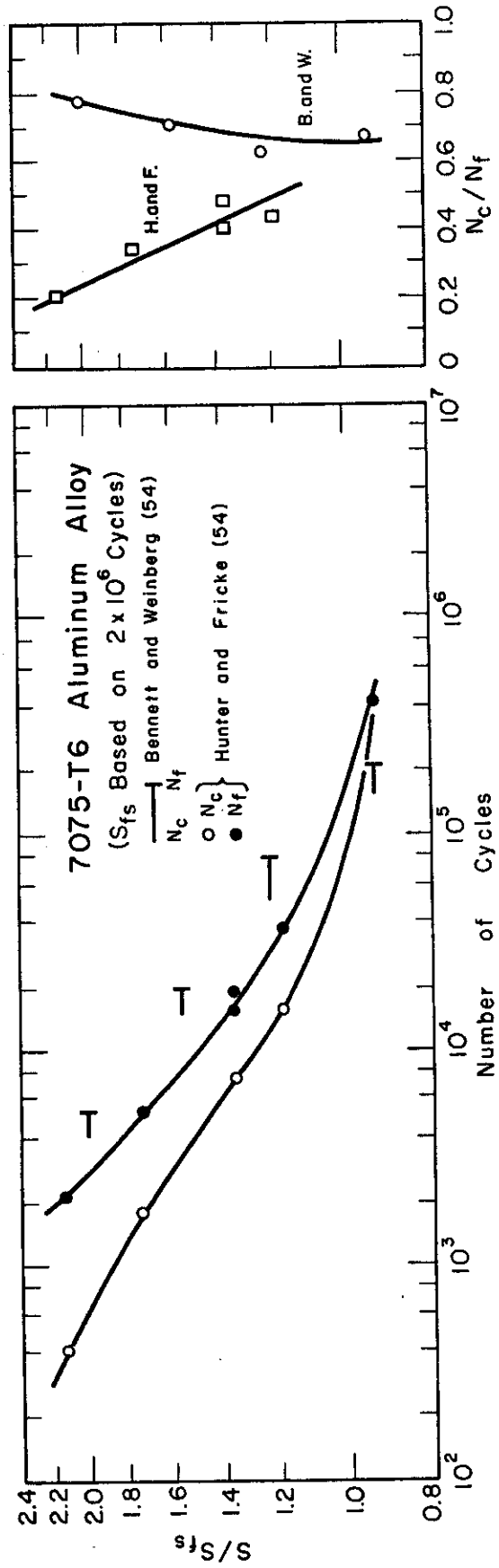


Fig. 21.--Comparison of Crack and Fracture Data Obtained on the Same Material in Rotating Bending with Constant Moment by Bennett and Weinberg (54) Using Deflection Techniques and Optical Microscope, and Hunter and Fricke (54) Employing the Plastic Replica-Optical Microscope Method.

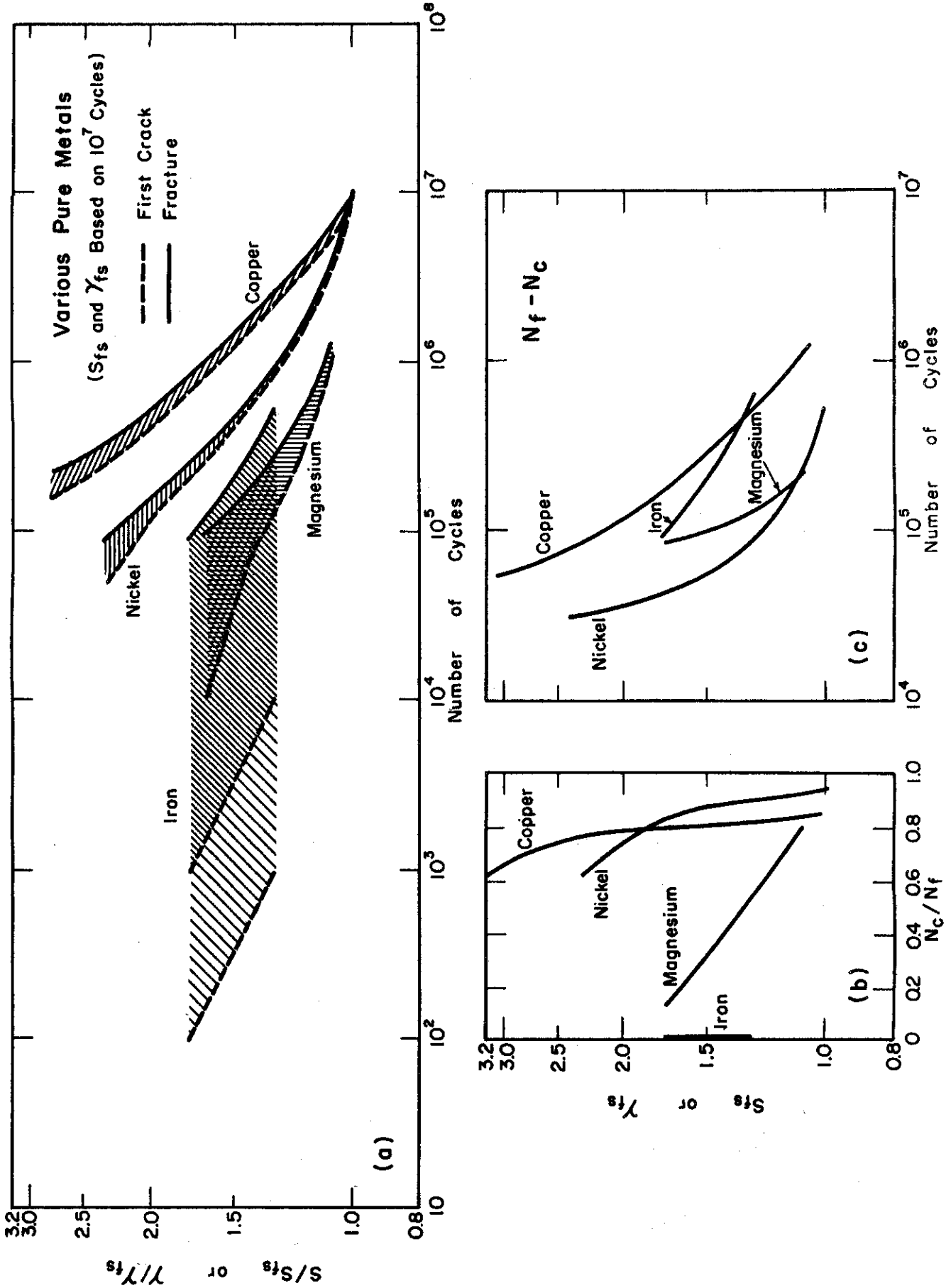


Fig. 22--Comparison of Crack and Fracture Data for Pure Metals. Data from Love (52) for Ingot Iron and Duce (50) for Nickel, Copper, and Magnesium. Crack Detection by Electron Microscope and Damping Methods.

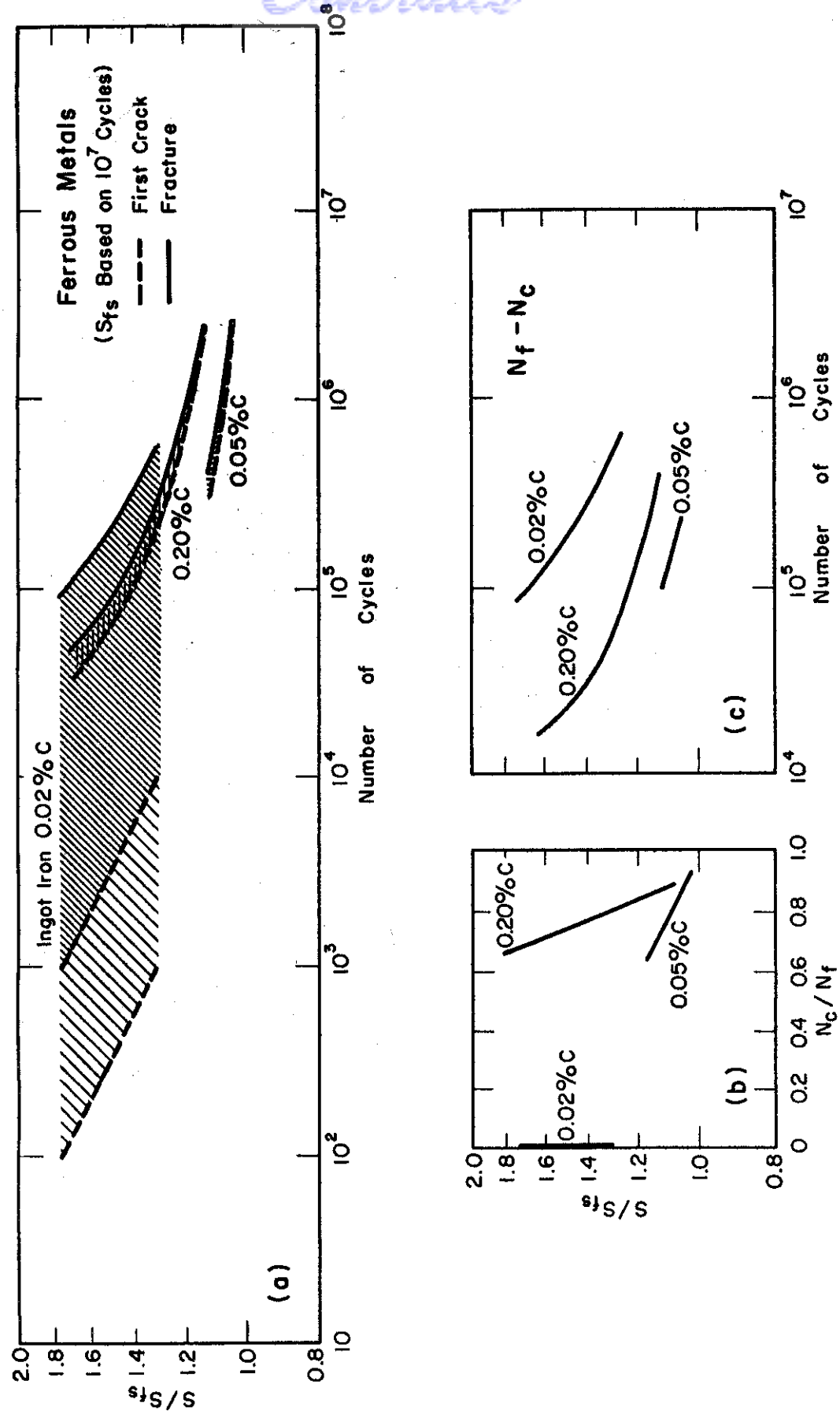


Fig. 23.--Comparison of Crack and Fracture Data for Materials of Varying Carbon Content. Data from Love (52) on Ingot Iron (0.02% C.), Hempel (39) on 0.05% C. Steel, and deForest (36) on SAE 1020 Steel. Crack Detection by Electron Microscope (Love) and Magnaflux Methods.

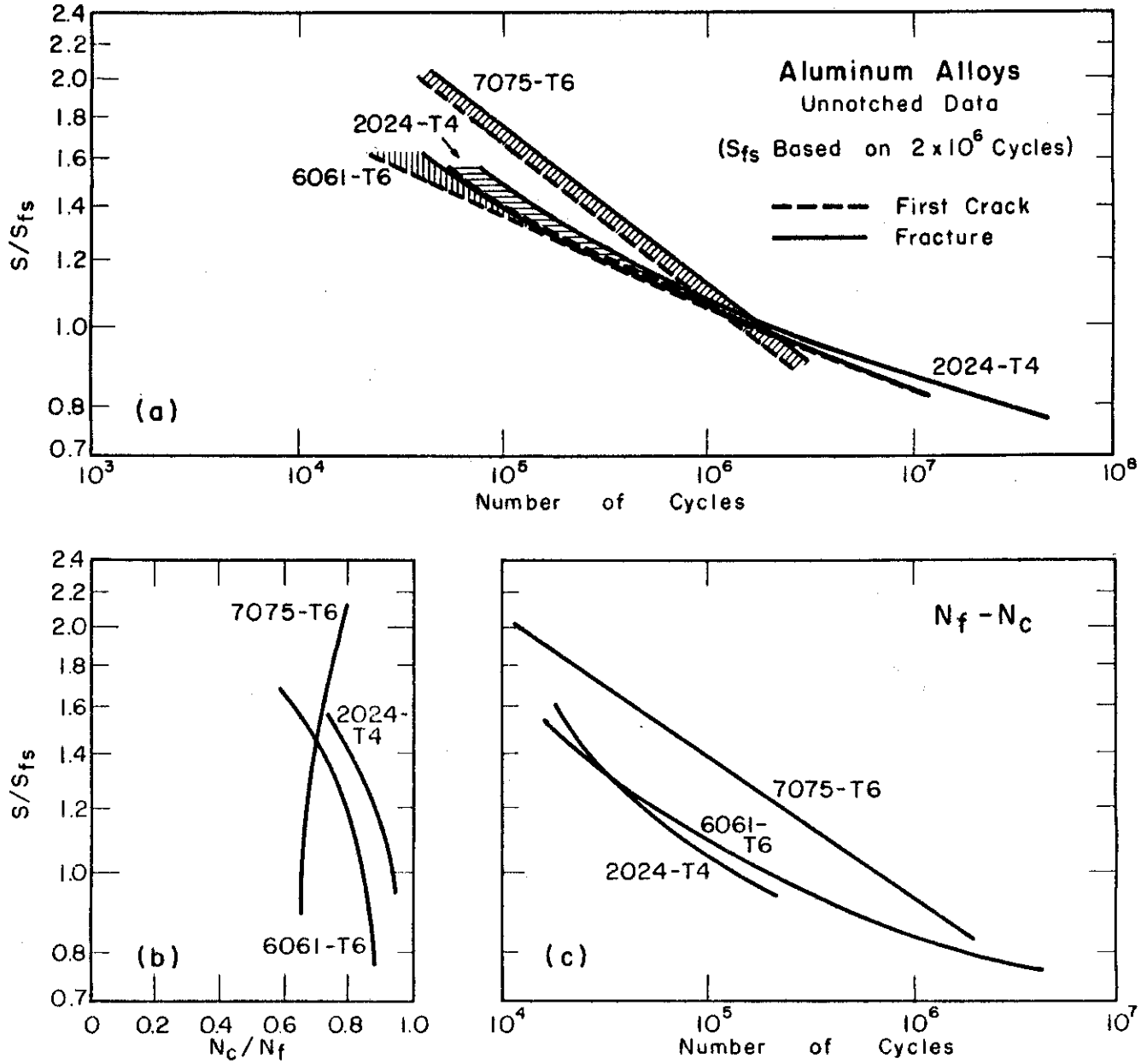


Fig. 24. --Comparison of Crack and Fracture Data for Three Aluminum Alloys. Data from Bennett and Weinberg (54).

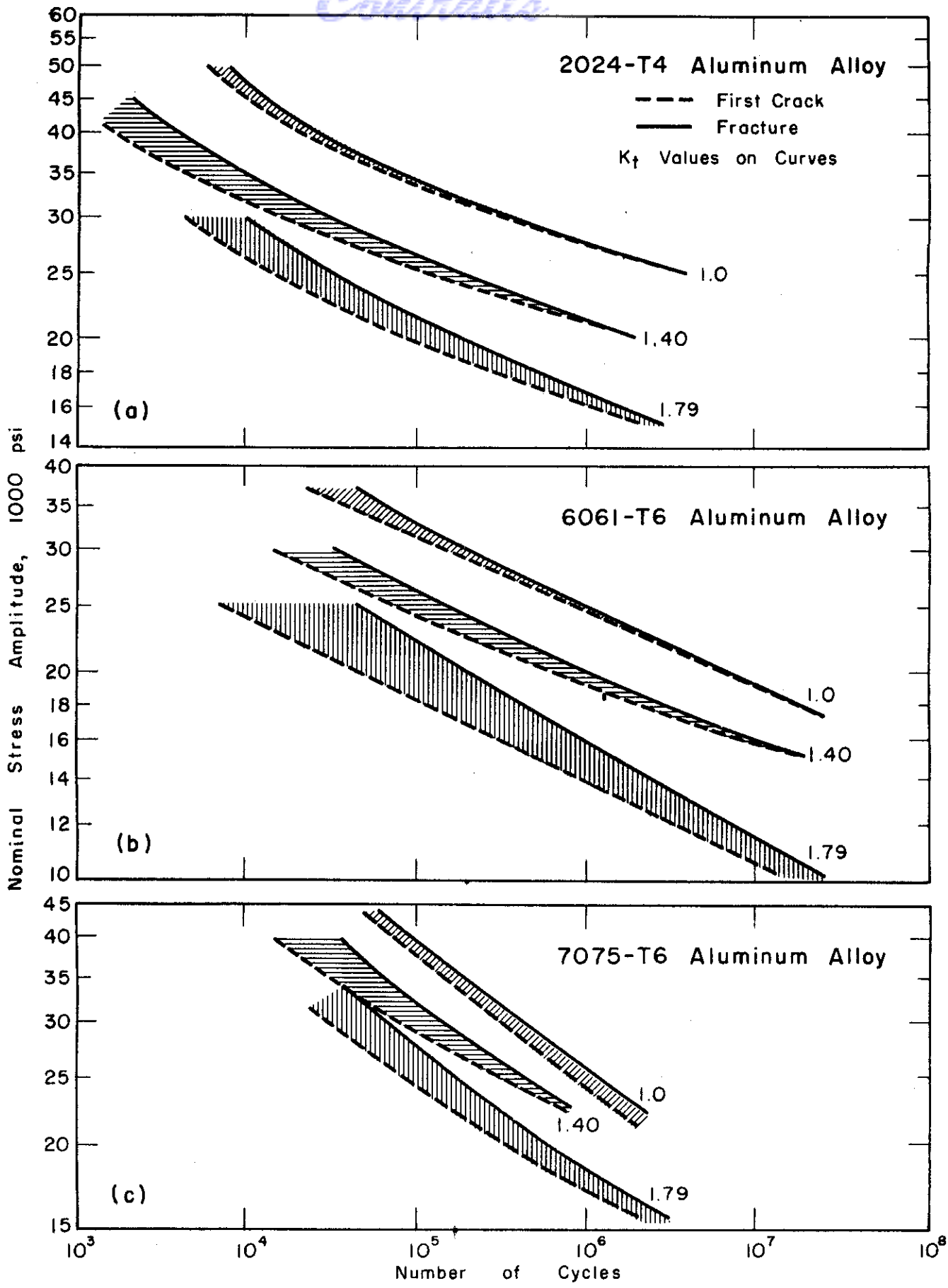


Fig. 25. -- Effect of Specimen Form on Cracking and Fracture for Three Aluminum Alloys. Data from Bennett and Weinberg (54).

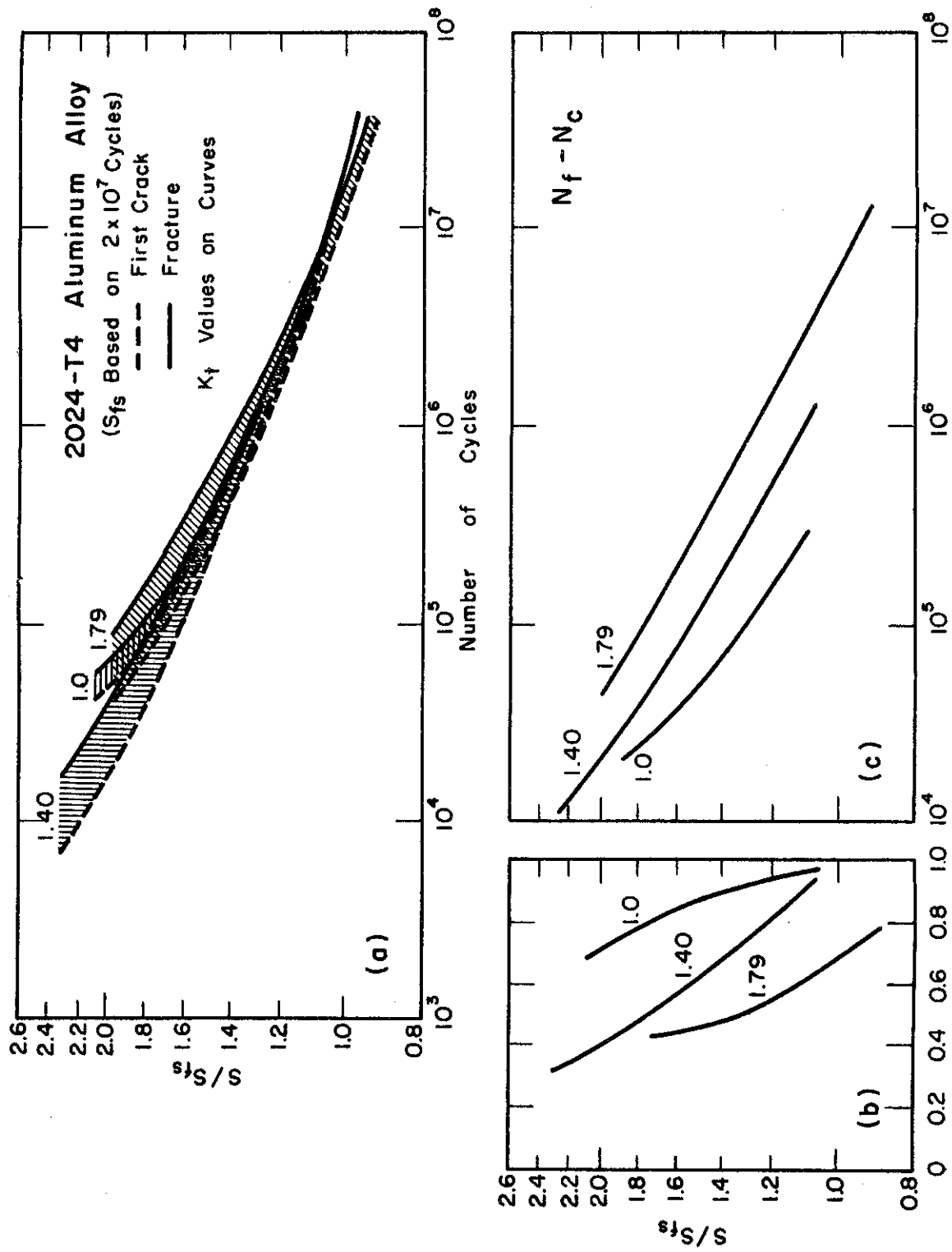


Fig. 26.--Crack and Fracture Data for 2024-T4 Aluminum Alloy in Three Specimen Forms. Data from Bennett and Weinberg (54).

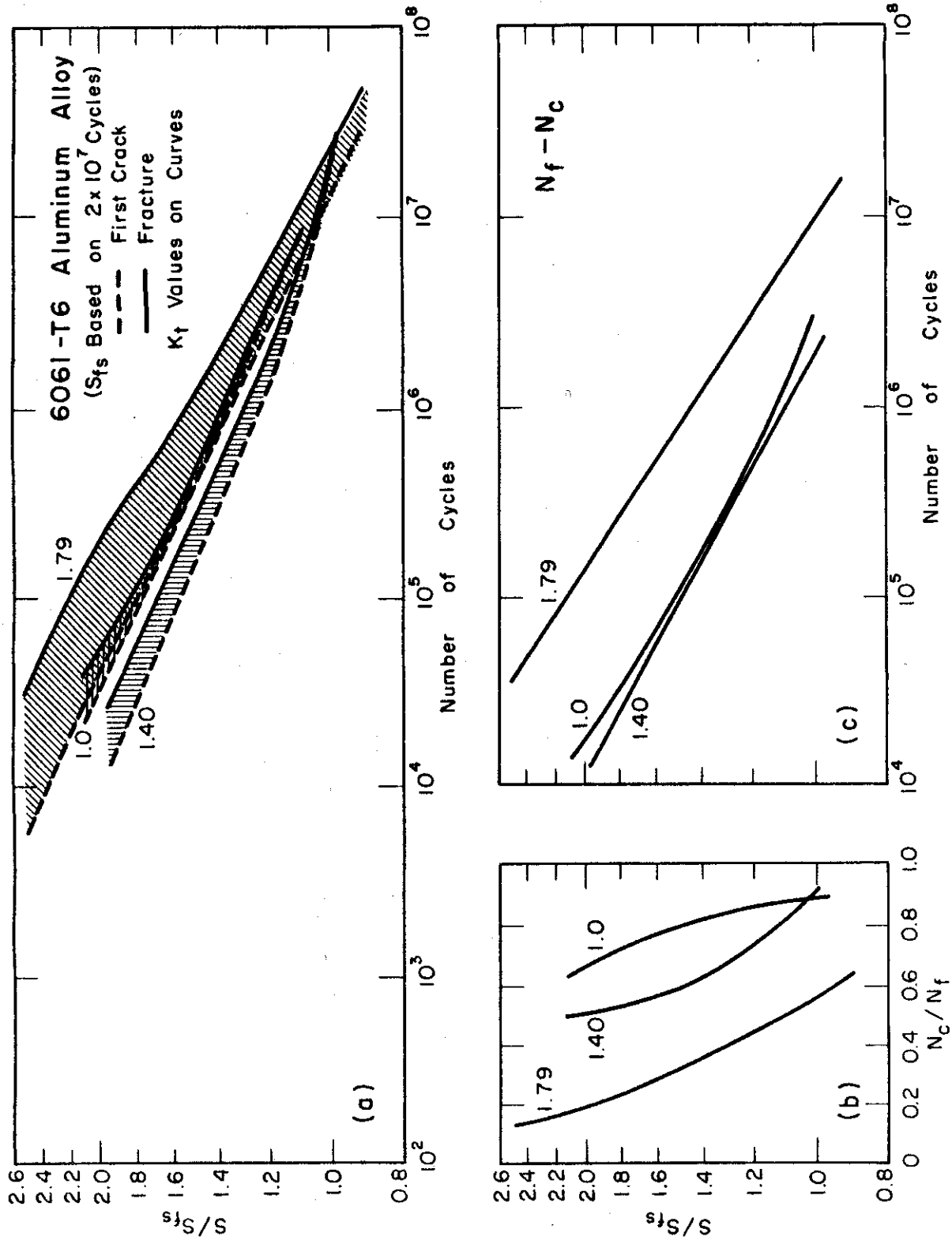


Fig. 27.--Crack and Fracture Data for 6061-T6 Aluminum Alloy in Three Specimen Forms. Data from Bennett and Weinberg (54).

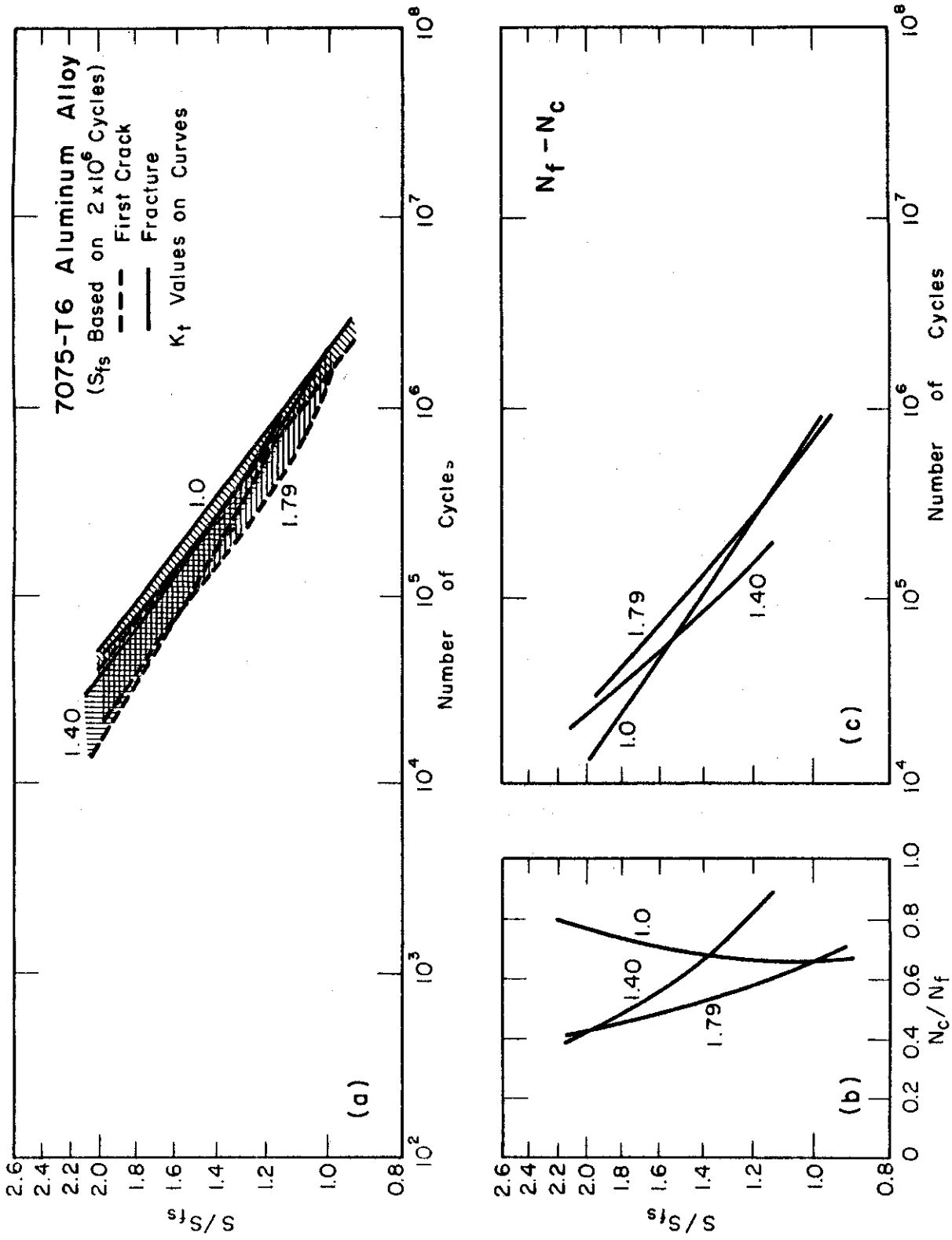


Fig. 28.--Crack and Fracture Data for 7075-T6 Aluminum Alloy in Three Specimen Forms. Data from Bennett and Weinberg (54).

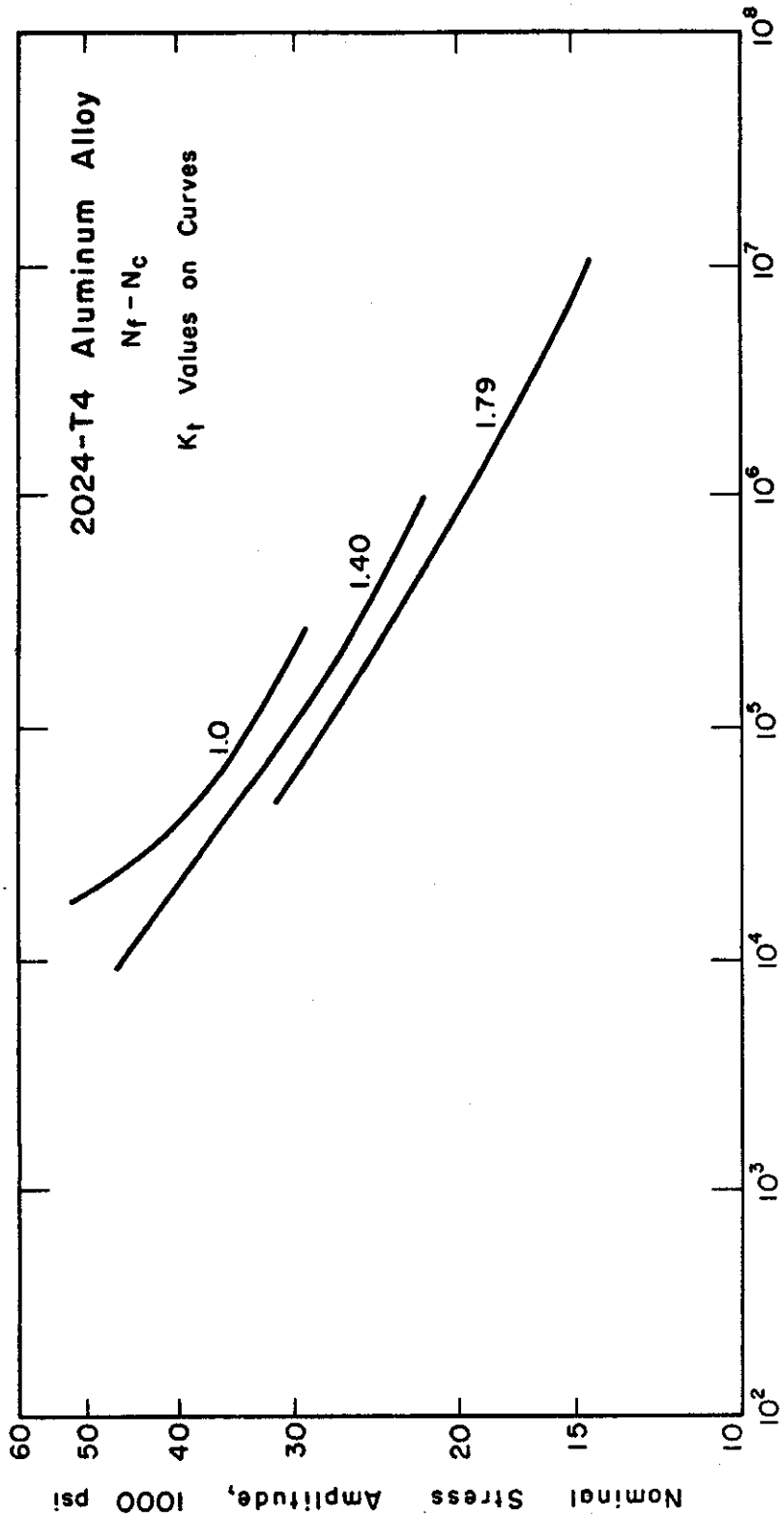


Fig. 29.--Comparison of Crack Growth Data on Basis of Nominal Stress for 2024-T4 Aluminum Alloy in Three Specimen Forms. Data from Bennett and Weinberg (54).

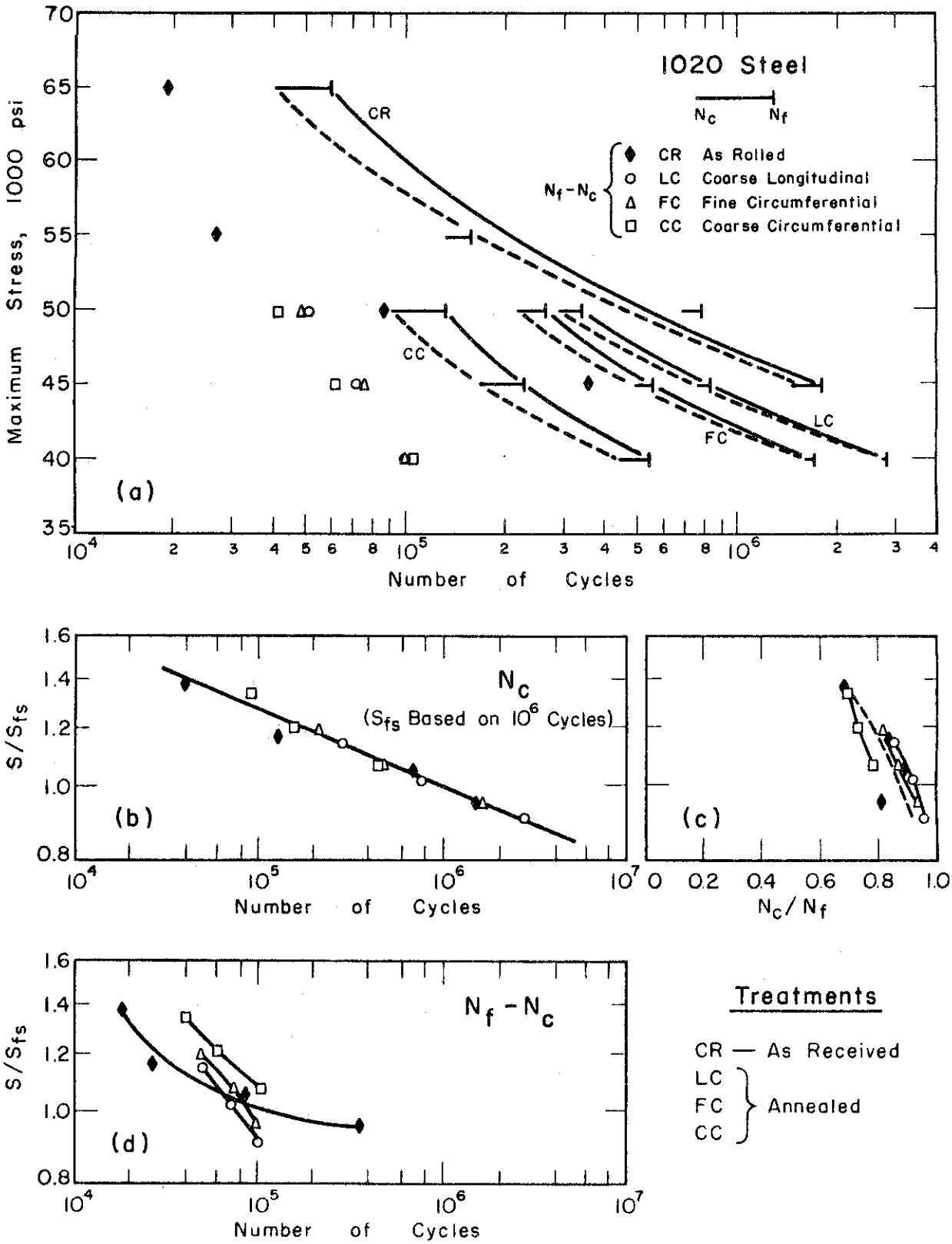


Fig. 30. --Effect of Surface Finish on Crack and Fracture Data for SAE 1020 Steel. Data from deForest (36).

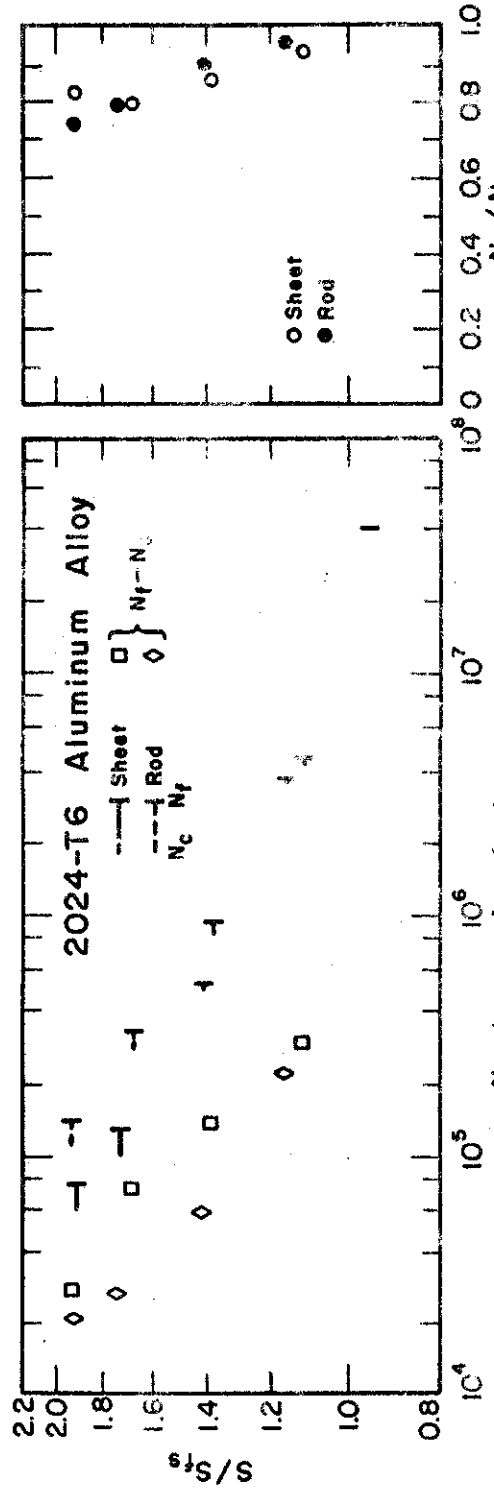


Fig. 31.--Comparison of Crack and Fracture Data on 2024-T4 Aluminum Alloy in Reversed Bending with Constant Maximum Deflection, Bennett and Baker (50), and in Rotating Bending with Constant Moment, Bennett and Weinberg(54).

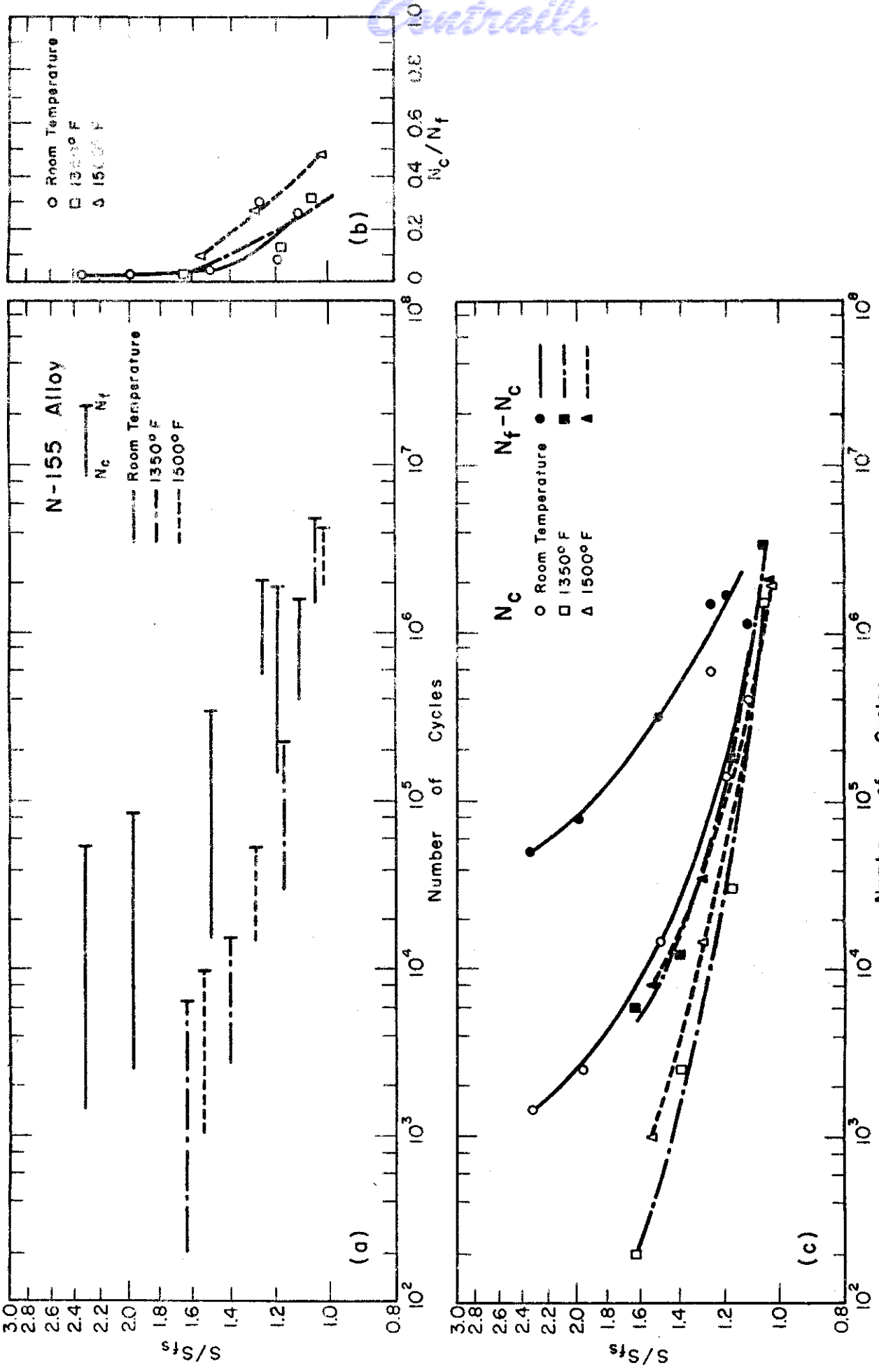


Fig. 32.--Effect of Temperature on Crack and Fracture Data for Notched Specimens of a Heat-Resistant Alloy Tested in Rotating Bending Under Constant Moment. Data from Demer and Lazan (53).

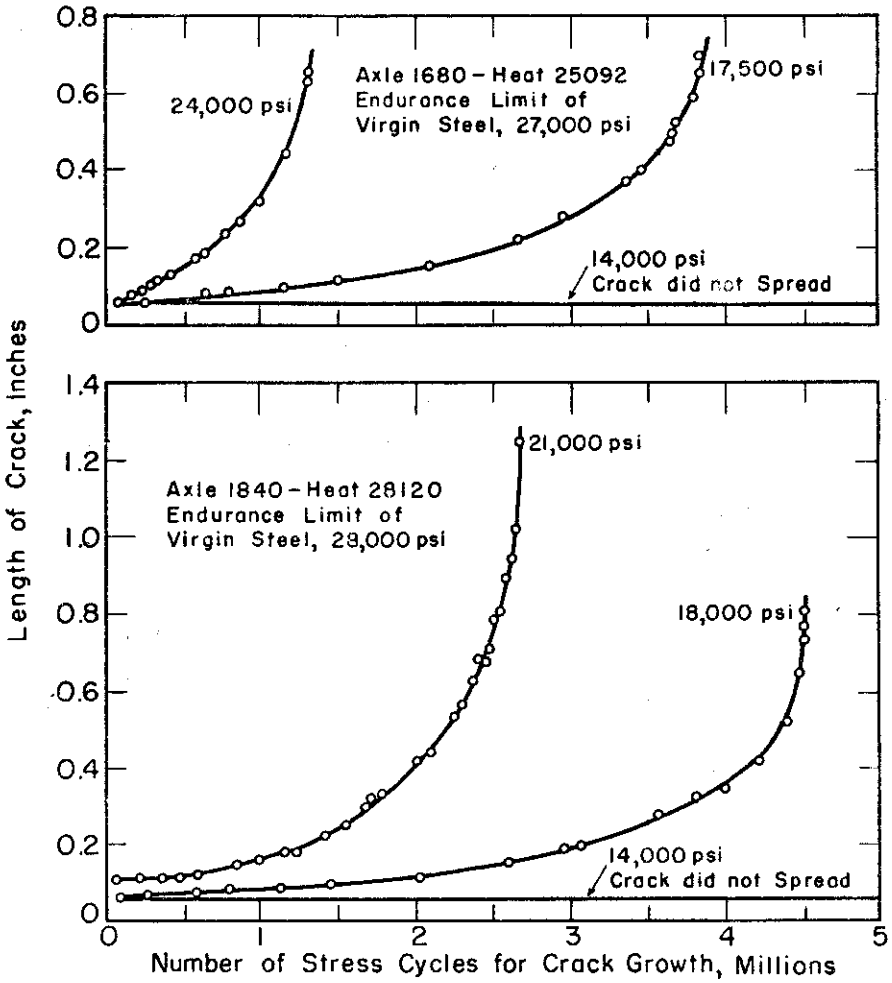


Fig. 33. --Crack Growth at Subsequent Low Stress of Cracks Started Under High Stress in Filleted Specimens of 0.45 per cent Carbon Steel. Data from Moore (27).

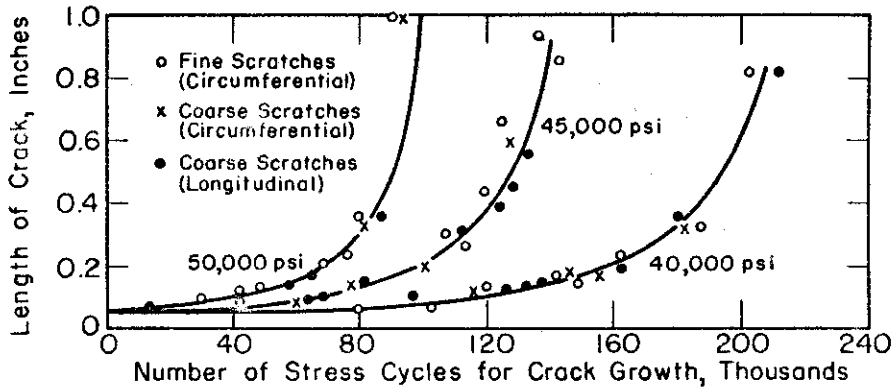


Fig. 34. --Propagation of Fatigue Cracks from 0.05 in. long to Fracture in Specimens of SAE 1020 Steel with Various Surface Finishes. Data from deForest (36).

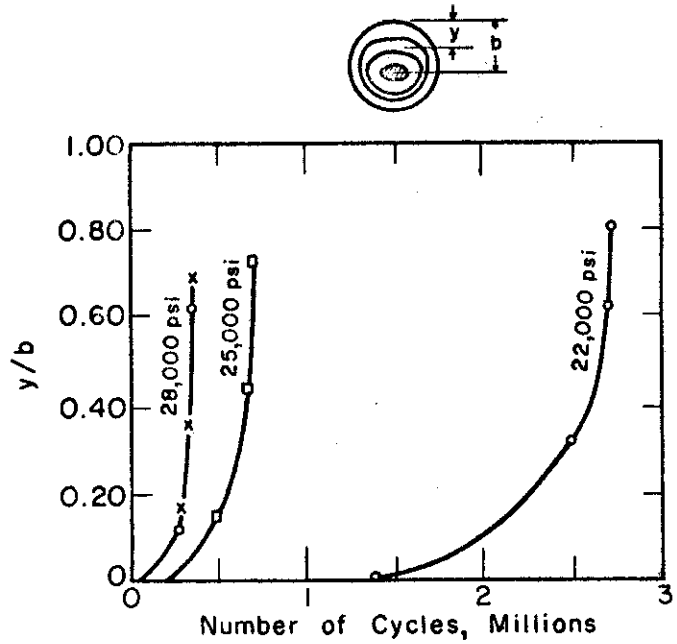


Fig. 35. --Penetration of Fatigue Cracks in Grooved Specimens of Normalized 0.45 per cent Carbon Steel. Data from Peterson (36).

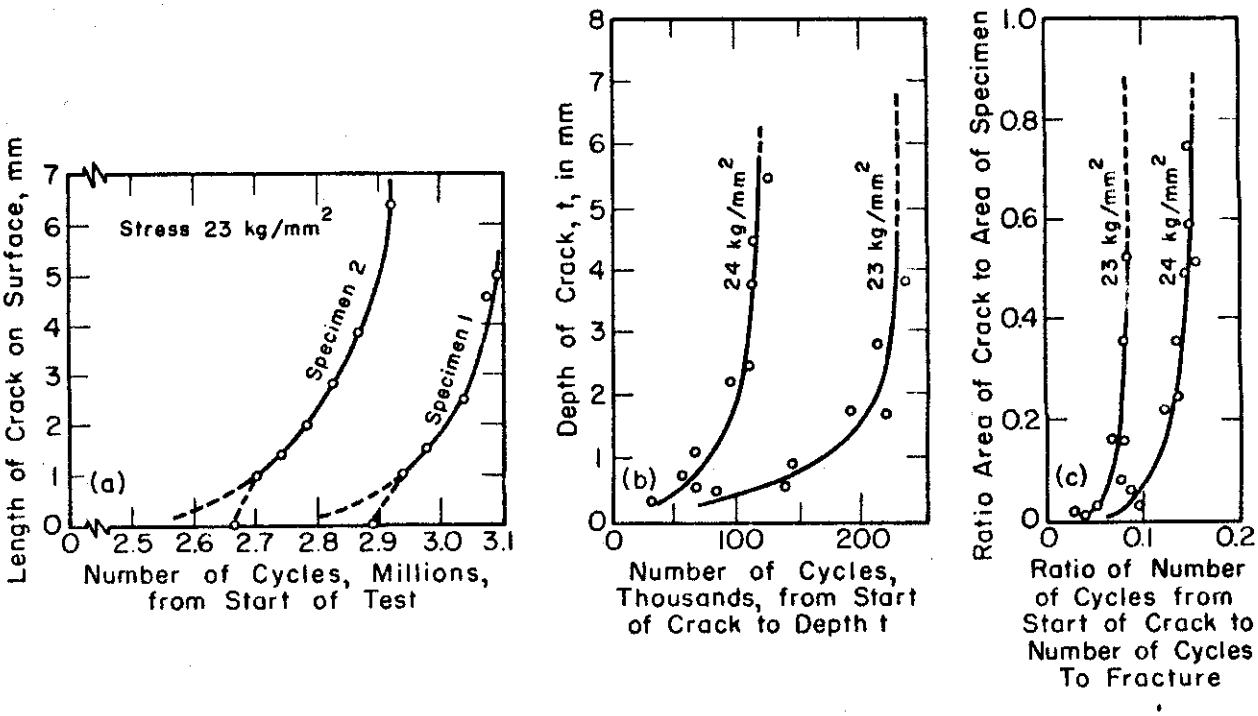


Fig. 36. --Crack Growth in Smooth Specimens of 0.05 per cent Carbon Steel. Data from Hempel (39).

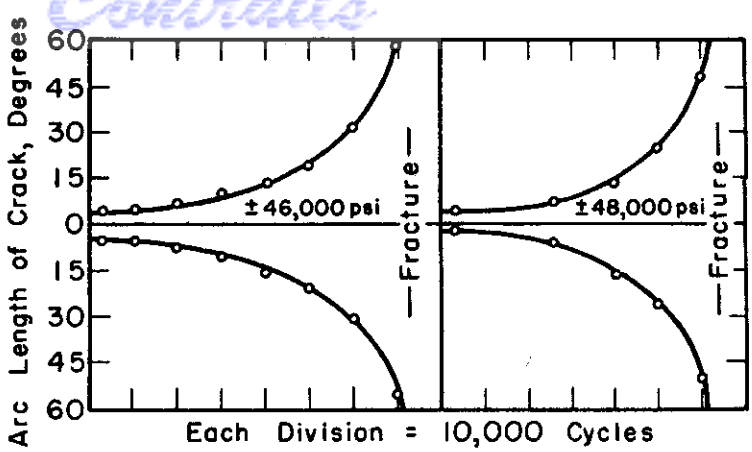


Fig. 37. --Crack Growth at Two Stress Levels for Smooth Specimens of SAE X4130 Steel. Minimum Specimen Diameter, 0.25 in. Data from Bennett (46).

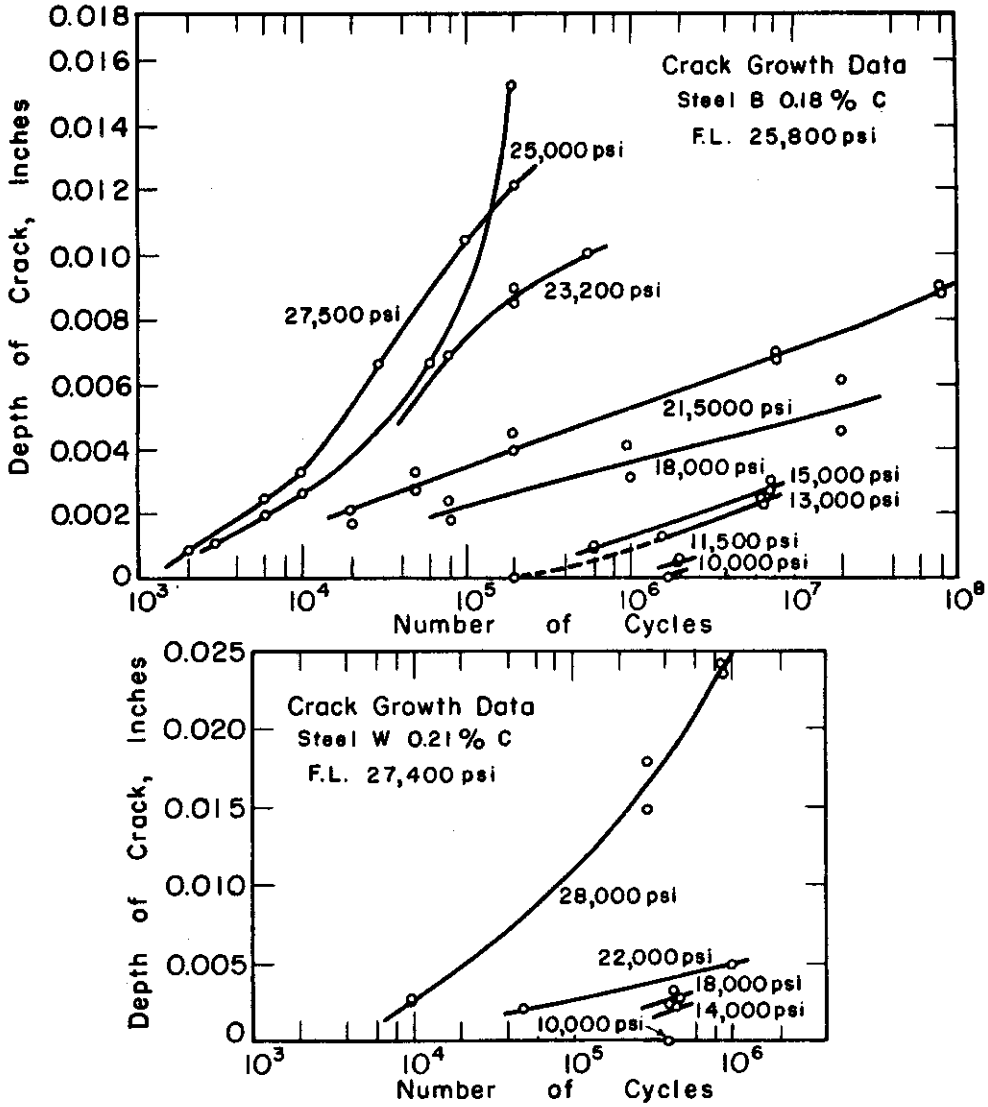


Fig. 38. --Crack Growth in Severely Notched Specimens of Steel Measured at Various Stress Levels. Data from Lessells and Jacques (50).

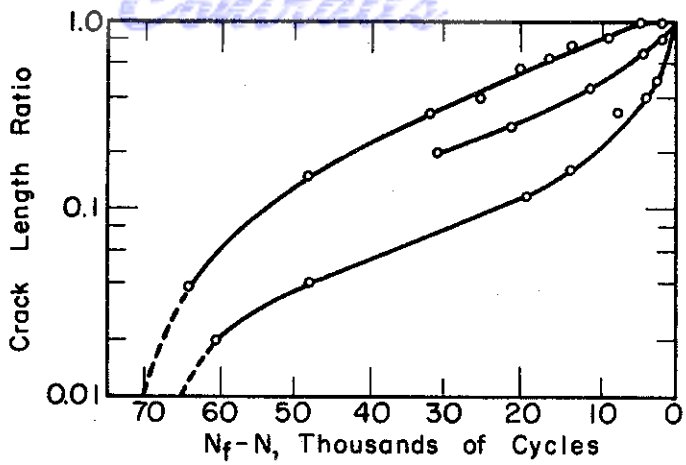


Fig. 39. --Crack Growth Curves for Sheet Specimens of 2024-T Aluminum Alloy Tested at a Nominal Stress Amplitude of 30,000 psi. Crack Length Ratio is the Crack Length Divided by the Specimen Width. Data from Bennett and Baker (50).

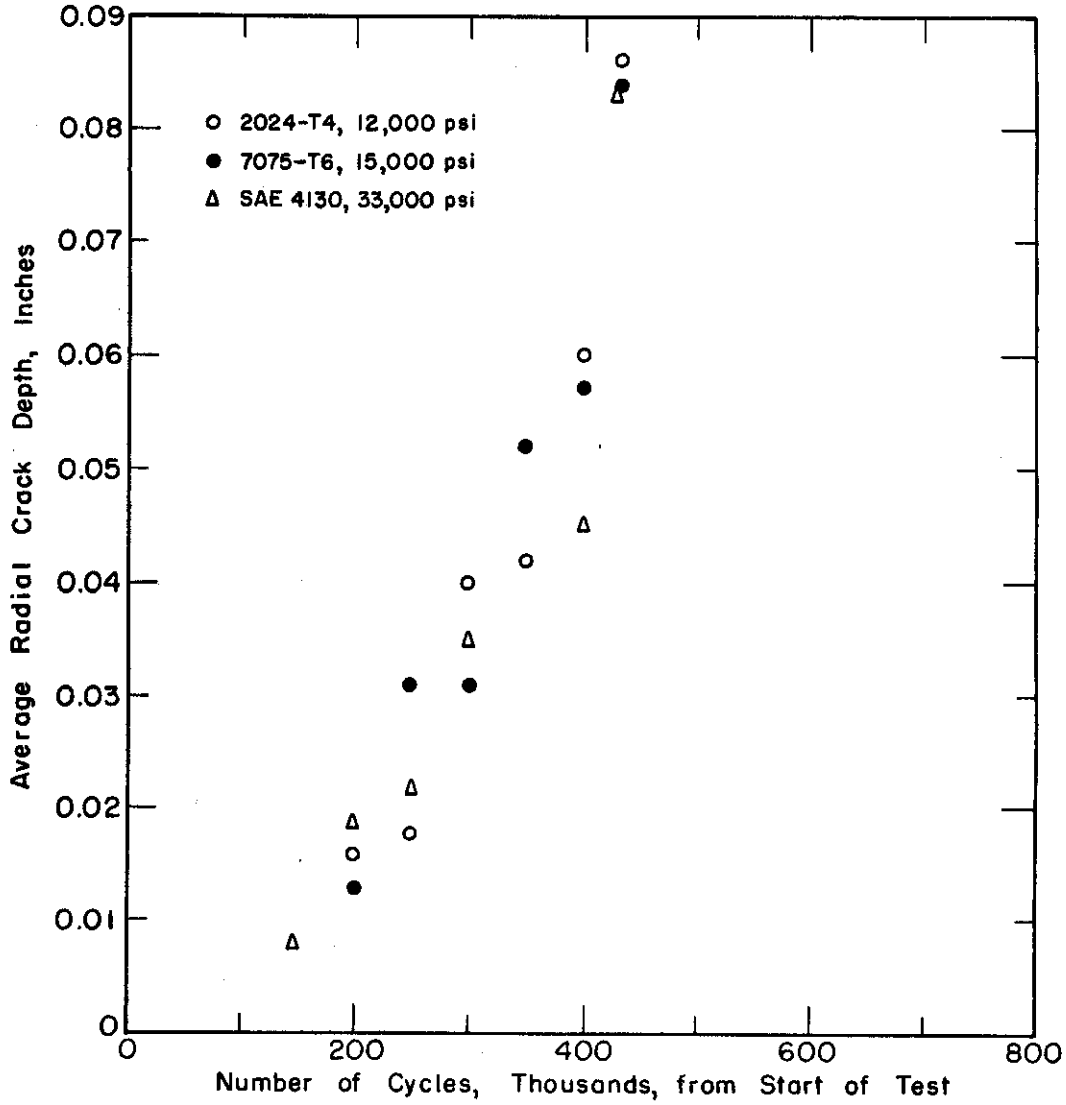


Fig. 40. --Average Radial Crack Depth for Different Numbers of Cycles. Approximate Fatigue Life, 450,000 Cycles at Respective Stress Levels. V-Shaped Notch, 1/16 in. Deep with a 0.01 in. Radius. Data from MacGregor and Grossman (52).

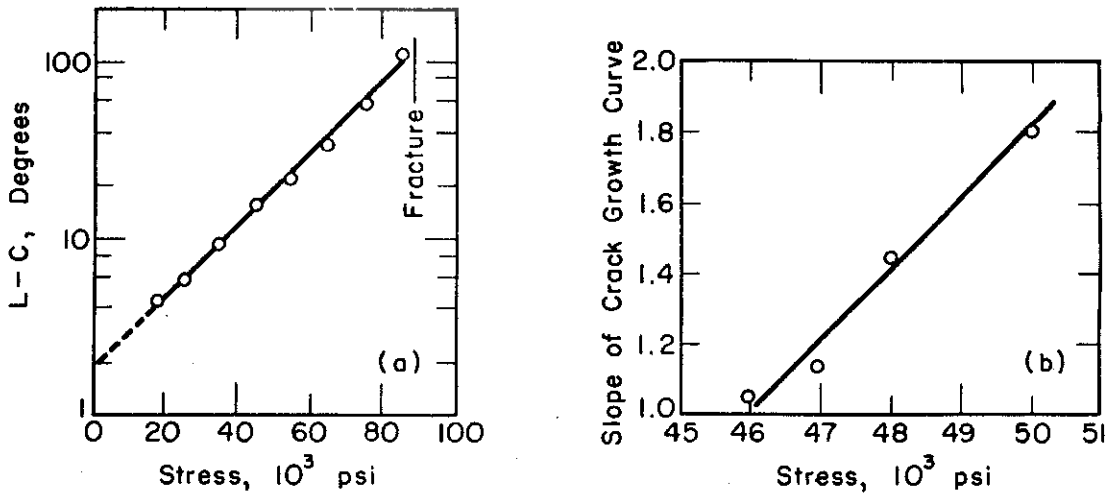


Fig. 41. --(a) Semi-Logarithmic Plot of Crack Growth Curve; Ordinate is Crack Length Minus a Constant. (b) Influence of Stress on Rate of Crack Growth. Data of Bennett (46) on SAE X4130 Steel.

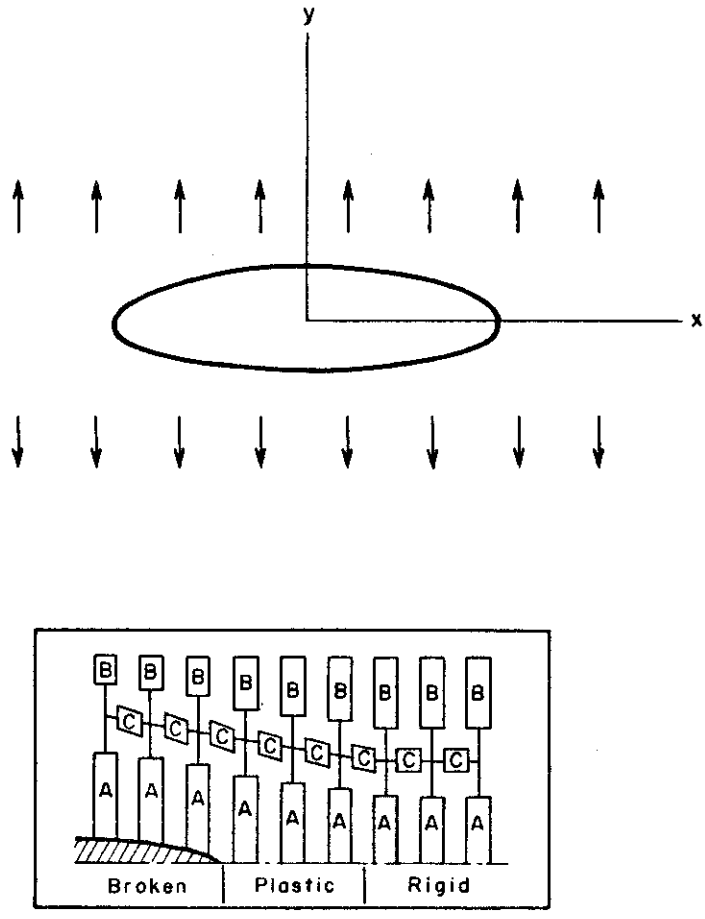


Fig. 42. --Crack Model and Idealized Representation of a Crack According to Head (53, 54).

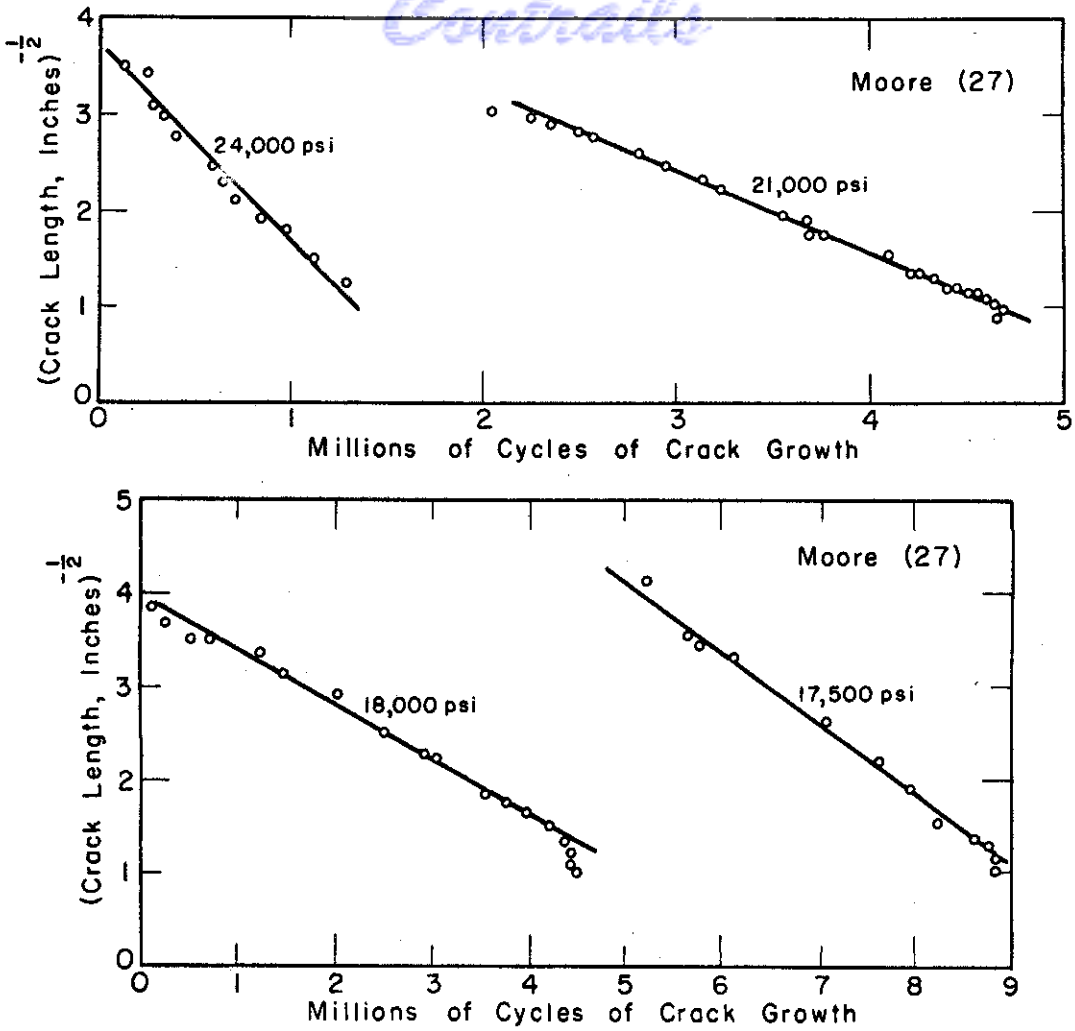


Fig. 43. --Crack Growth Curves of Moore (27). Data of Fig. 33 Plotted in the Manner of Head (53, 54).

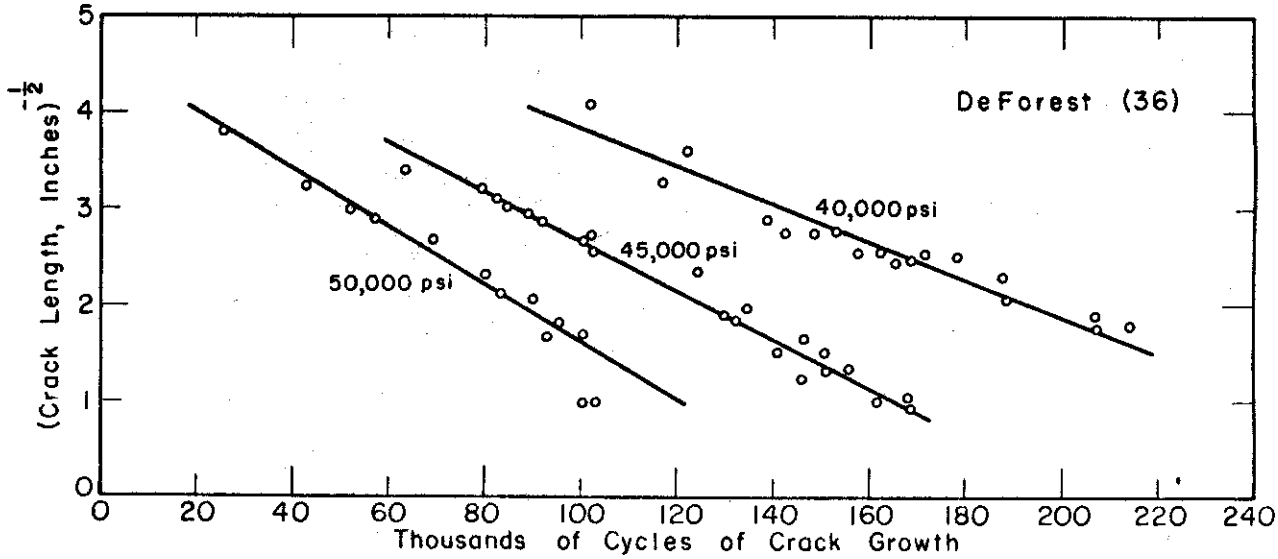


Fig. 44. --Crack Growth Curves of deForest (36). Data from Fig. 34 Plotted in the Manner of Head (53, 54).

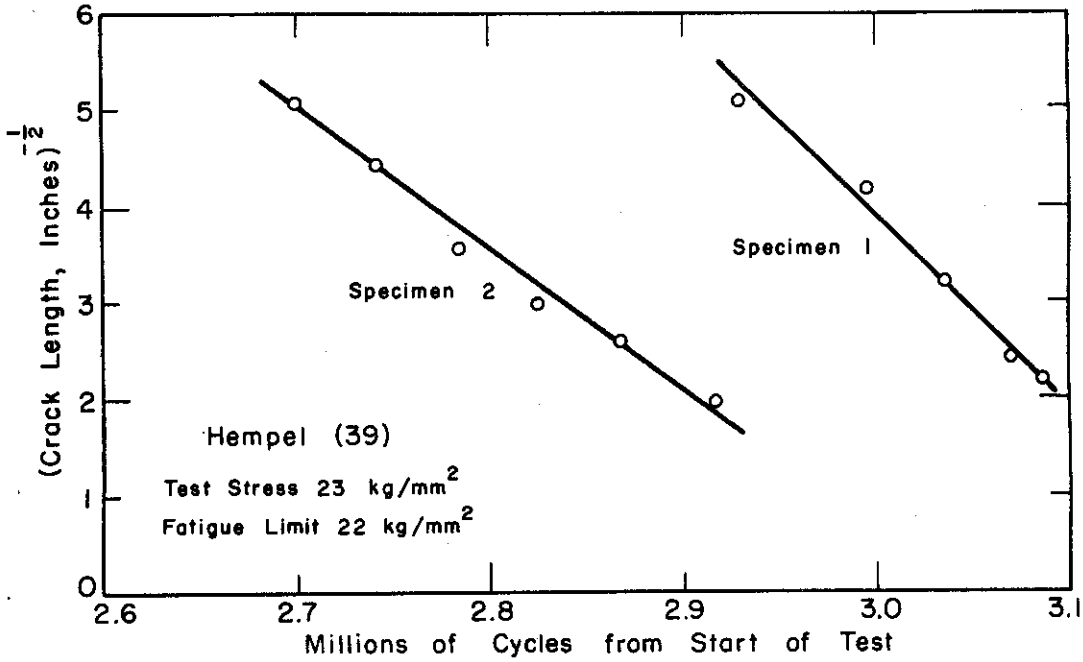


Fig. 45.--Crack Growth Curves of Hempel (39). Data from Fig. 36a Plotted in the Manner of Head (53, 54).

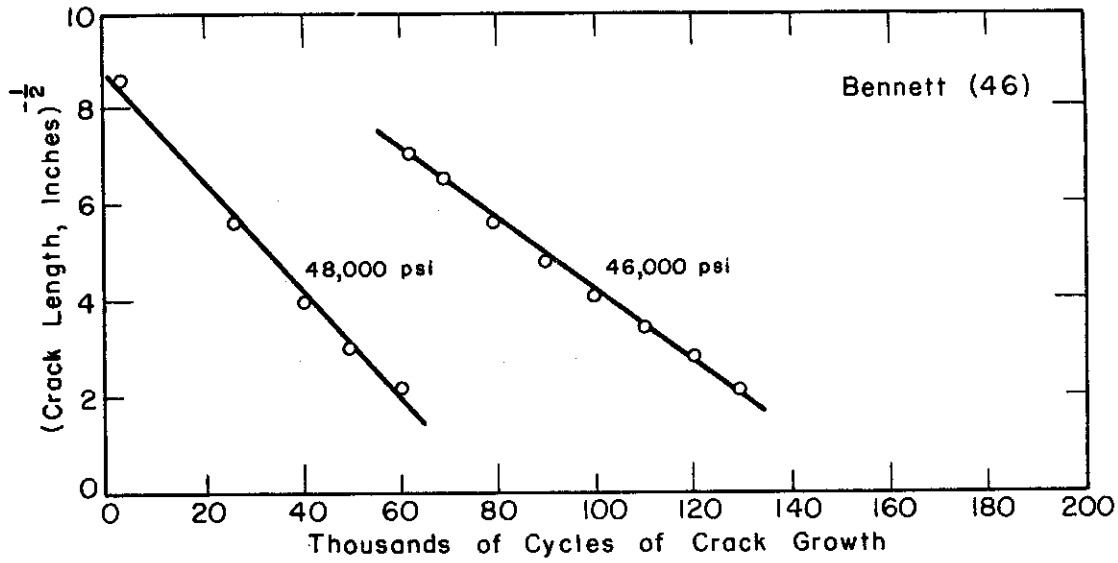


Fig. 46.--Crack Growth Curves of Bennett (46). Data from Fig. 37 Plotted in the Manner of Head (53, 54).

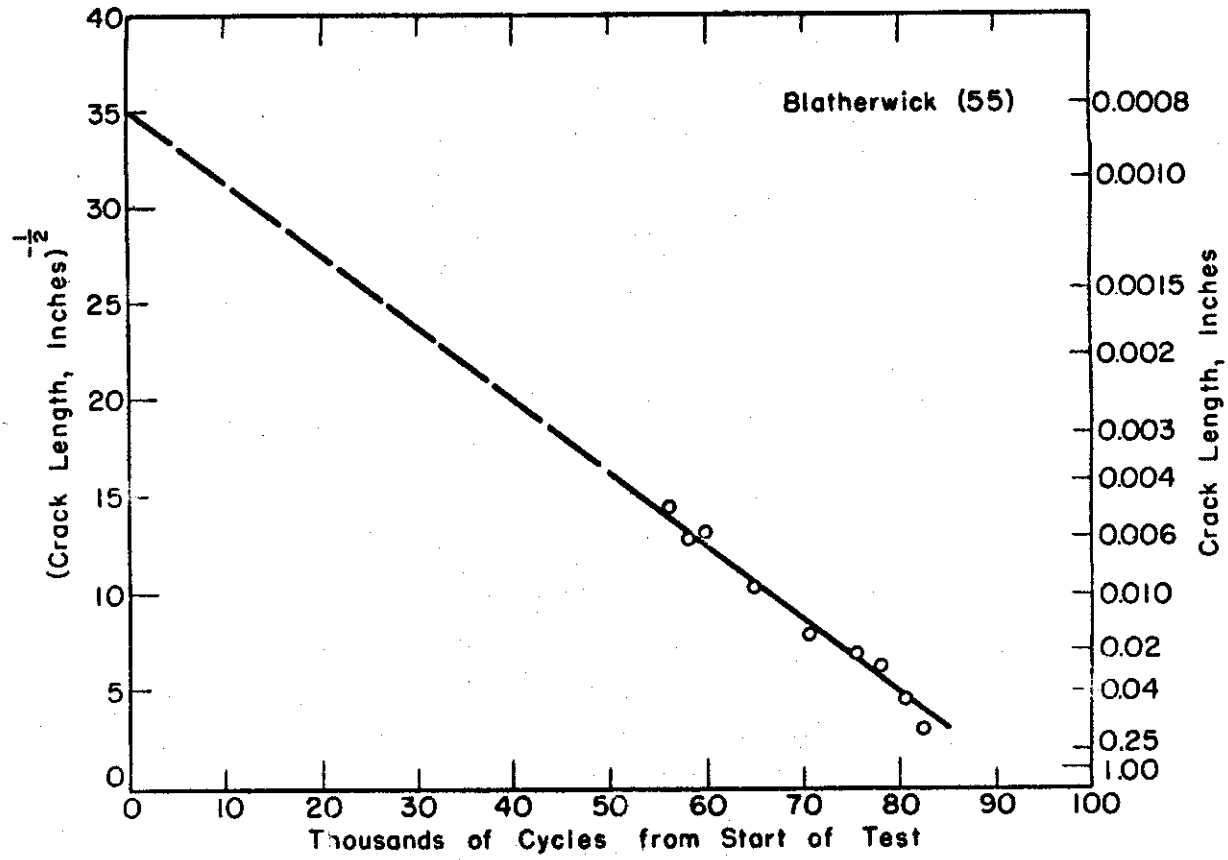


Fig. 47. --Crack Growth Curve of Blatherwick (55) Obtained in a Reversed Bending Test on a Hollow Specimen of SAE 1020 Steel Tested Under Constant Maximum Strain of 1650 Micro-Inches per Inch. Plotted in the Manner of Head (53, 54).